DETECTION OF THROMBI USING A Tc-99m LABELLED ANTIFIBRIN MONOCLONAL ANTIBODY (MoAb)

experiments in vitro and in animals

MARTIN   N.J.M.   WASSER

DETECTION OF THROMBI USING A Tc-99m LABELLED ANTIFIBRIN MONOCLONAL ANTIBODY (MoAb)

experiments in vitro and in animals

PROEFSCHRIFT

TER VERKRIJGING VAN DE GRAAD VAN DOCTOR AAN
DE RIJKSUNIVERSITEIT TE LEIDEN, OP GEZAG VAN
DE RECTOR MAGNIFICUS DR. J.J.M. BEENAKKER,
HOOGLERAAR IN DE FACULTEIT DER WISKUNDE EN
NATUURWETENSCHAPPEN, VOLGENS BESLUIT VAN
HET COLLEGE VAN DEKANEN TE VERDEDIGEN OP
DINSDAG 12 DECEMBER 1989 TE KLOKKE 14.15 UUR.

DOOR

MARTINUS NORBERTUS JOHANNES MARIA WASSER

GEBOREN TE EINDHOVEN IN 1958

Promotiecommissie:

Promotor: Prof. dr. E.K.J. Pauwels

Co-promotor: Dr. W. Nieuwenhuizen (Gaubius Instituut TNO)

Referent: Prof. dr. P. Brakman

Overige leden: Prof. dr. A.E. van Voorthuisen
                                    Prof. dr R. Willemze

A drug is that substance which, when injected into a rat, will produce a scientific report

Arthur Bloch, Medical Murphology, Murphy's law book II

Aan mijn ouders,

mijn eerste opleiders

STELLINGEN

1) "Humanisering" van muize-monoclonale antilichamen ter vermindering van de immunogeniciteit in vivo heeft voor scintigrafische toepassing het nadeel dat de halveringstijd in de circulatie sterk wordt verlengd.
LoBuglio et al., Proc Natl Acad Sci USA, 1989; 86: 4220-4224

2) Koppeling van een fibrine- of thrombocyt-specifiek monoclonaal antilichaam aan een thrombolyticum lijkt een aantrekkelijke methode om de effektiviteit van de huidige generatie thrombolytica te verhogen.

3) De stelling dat transfusie van "vers" bloed bij coronary bypass-operaties het postoperatieve bloedverlies kan beperken berust op een achterhaalde mythe.
Wasser et al., Br J Haematol 1989; 72: 81-84

4) Een anafylactische reaktie bij bariumonderzoek van de dikke darm is een zeer zeldzame, maar reële complicatie.
Wasser et al., Neth J Med 1989; 35: 147-150

5) Indien bij echografisch onderzoek van een patient met een stomp buiktrauma aan nieren en retroperitoneum geen afwijkingen worden gevonden, kan intraveneuze pyelografie (IVP) achterwege blijven.

6) Primaire gastroscopie bij patienten met dyspeptische klachten toont overeenkomsten met het schieten met een kanon op een mug.

7) Onderzoek aan pas-overledenen (z.g. "neomort" of "newly dead") is ethisch gezien een zeer dubieuze interpretatie van het begrip "ex-vivo" experiment.
Coller et al., Ann Int Med 1988; 109: 635-638

8) Het bestaan van een commercieel televisiestation lijkt op dat van een koorddanser: het is de kunst op de kabel te komen én te blijven.

9) Het feit dat sommige, zich supporters noemende, toeschouwers van voetbalwedstrijden spelers bekogelen met (al dan niet explosieve) voorwerpen, wekt de indruk dat niet het publiek de doelgroep is van de spelers, maar dat de spelers de doelgroep vormen van het publiek.

10) He who would climb the ladder should begin at the bottom.
    Japans gezegde (vrij van invoerrechten)

Leiden, 12 december 1989
Martin Wasser

CONTENTS

LIST OF ABBREVIATIONS

BSA	: bovine serum albumin
DMF	: N,N-dimethylformamide
DTPA	: diethylene triamine pentaacetic acid
DVT	: deep venous thrombosis
EIA	: enzyme immunoassay
FITC	: fluorescein isothiocyanate
FPA	: fibrinopeptide A
FPB	: fibrinopeptide B
FPLC	: fast protein liquid chromatography
GAM-FITC	: FITC labelled goat antimouse antibody
GAM-Fab/PO	: peroxidase-labelled goat antimouse-Fab antibody
Gly-Pro-Arg-Pro	: H-glycyl-L-prolyl-L-arginyl-L-proline
HAT - medium	: hypoxanthine-aminopterin-thymidine medium
HPLC	: high pressure liquid chromatography
HSA	: human serum albumin
MoAb	: monoclonal antibody
PBS	: phosphate buffered saline
RAM	: rabbit antimouse antibody
SEM	: scanning electron microscopy
SDS-PAGE	: sodium dodecyl sulphate polyacrylamide gel electrophoresis
SPDP	: N-succimidyl 3-(2-pyridyldithio) propionate
TCA	: trichloroacetic acid
TEM	: transmission electron microscopy
TMB	: 3,3'5,5'-tetramethylbenzidine
t-PA	: tissue-type plasminogen activator

CHAPTER I

GENERAL INTRODUCTION

deep venous thrombosis (DVT)

I.1 Epidemiologic considerations

Venous thrombosis is a frequently encountered clinical entity in medical practice and occurs most frequently in the deep veins of the lower extremities. It is estimated that clinical diagnosis of deep venous thrombosis (DVT) of the legs is made yearly in 1 in 1000 of the population at large [1]. Surgery is a well known risk-factor for the development of DVT. Roughly 30% of surgical patients over 40 years of age develop DVT, if no adequate prophylactic measurements are taken [2]. In patients older than 60 years and in patients with certain other risk-factors e.g. malignancies, this frequency is increased to more than 50%. The majority of these cases of postoperative thrombosis originates in the deep veins of the calfs [3-5], and ascends to the veins of the upper leg in 20% of these cases [4,6]. Occasionally, a thrombus originates primarily in the popliteal, femoral or iliac veins [7]. In 6.7% of patients, a bilateral DVT can be observed [8]. Patients suffering from deep venous thrombosis (DVT) are at high risk for the development of pulmonary embolism. The frequency of fatal pulmonary embolism in the postoperative period has been reported as 0.7-1.4% [6,8,9] and it has been shown that leg DVT accounts for some 85-95% of pulmonary embolization [10-12]. Some investigators concluded that there is no danger of embolization when thrombosis is confined to the calf veins [13,14]. Postmortem and venographic studies, however, have shown the opposite [15,16] and this issue remains controversial.
Another, although less serious but still invalidating, complication of deep

venous thrombosis is the development of the so-called postphlebitic syndrome - the sequelae of varicose veins, persistent pain or swelling of the legs due to destruction of the venous valves. For these reasons, it is necessary to recognize the condition of DVT at an early stage and to start anticoagulant (or possibly thrombolytic) therapy as soon as possible. However, because of its hemorrhagic side effects, anticoagulant therapy is not without risk (estimated mortality rate 0.6% [17]) and it should be limited to patients in whom the diagnosis is certain.

I.2 Pathophysiologic considerations

Thrombosis is the result of activation of an intravascular clotting process that blocks the vascular volume either partly or completely. The extent and rate of formation of the flow obstruction determines the amount of resulting tissue injury. Thrombi may vary in composition, depending on the part of the vascular system from which they originate.

a. white thrombi ("platelet thrombi")

> Thrombi formed at sites with high flow rate and high pressure (on intimal lesions of arteries) are composed primarily of platelets and have a variable amount of superimposed fibrin clot.

b. red thrombi ("coagulation thrombi")

> Thrombi formed in areas of low pressure and low flow rate (veins) are primarily composed of a fibrin-red cell coagulum. This type of thrombi is also common in atonic atria with their associated stasis.

c. mixed thrombi

> Most thrombi have properties of both red and white thrombi and are of a mixed type. They have a white head and a red tail, i.e where blood flow has slowed down

A common feature of all thrombi is the presence of a fibrin network. Fibrin plays an essential role in the regulation of haemostasis in vivo. Activation of the clotting process, resulting in fibrin formation, activates an oppposing cascade, the fibrinolytic process, aimed at the degradation of the formed fibrin. The equilibrium between the two opposing processes coagulation and fibrinolysis is the so-called haemostatic balance (Fig. I.1).
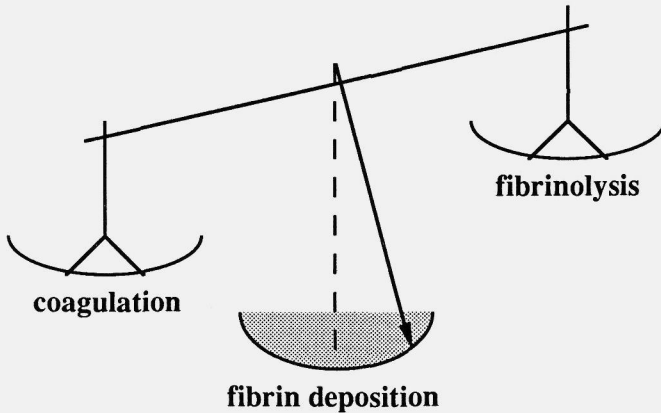
Fig. I.1 *Balance between coagulation and fibrinolysis*

These two opposing systems do not operate independently, but are interrelated via complicated feedback mechanisms, through which they influence each other. Furthermore, both systems are within themselves controlled by built-in feedback mechanisms. Disturbance of the haemostatic balance will either result in bleeding (in case of hypo-coagulation or hyper-fibrinolysis) or in thrombosis (in case of hyper-coagulation or hypo-fibrinolysis). A global overview of the complicated interrelation between coagulation and fibrinolysis is given in Figure I.2.
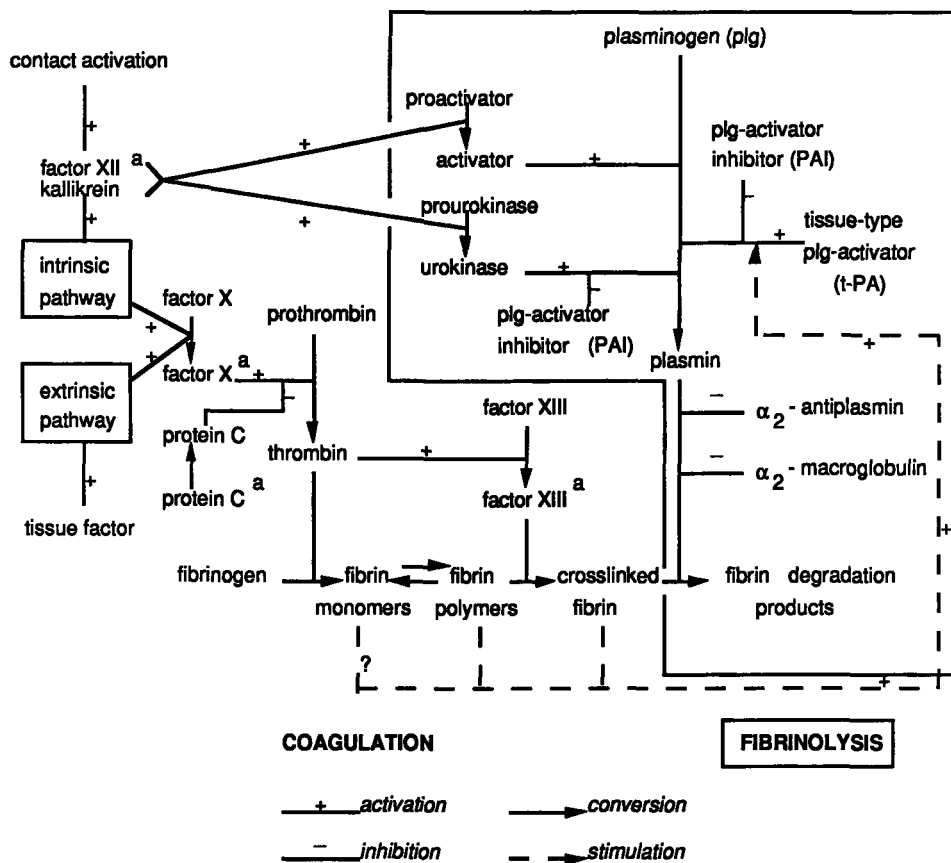
Fig. I.2 *Relation between coagulation and fibrinolysis*

Considering the haemostatic balance, thrombosis must be regarded as a dynamic process. On the one hand, stimulation of the coagulation cascade results in formation of fibrin, while on the other hand, concomittant activation of the fibrinolysis cascade leads to degradation of the formed fibrin.

I.3 Fibrin, formation and degradation

Formation

The final step in the coagulation cascade is the conversion of fibrinogen into fibrin by the action of thrombin. Fibrinogen, present in plasma, is a symmetrical glycoprotein with a molecular weight of approximately 340 kD (containing approximately 3000 amino acids). It consists of 6 chains: two Aα, two Bβ and two γ-chains (Fig. I.3) [20].

Fig. I.3   *Schematic representation of the fibrinogen molecule; FPA = fibrinopeptide A, FPB = fibrinopeptide B*

The classical Hall-Slayter model (based on electronmicroscopic observations) depicts fibrinogen as a trinodular structure (Fig. I.4) [18,19]. Three functional domains can be distinguished in the fibrinogen molecule i.e. two distal D-domains and one central E domain which contains the fibrinopeptides A and B [20].

475 Å

< 15 Å

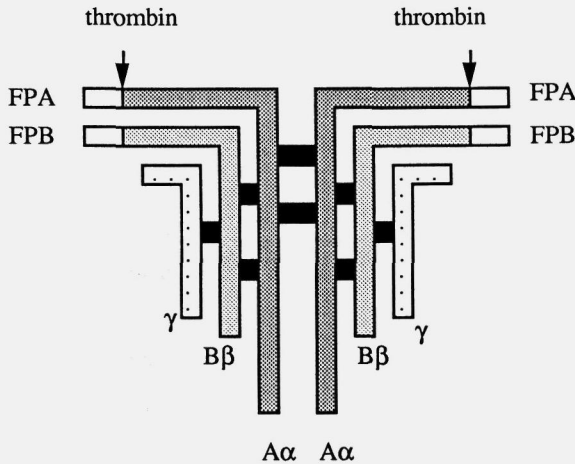65 Å   50 Å   65 Å

D   E   D
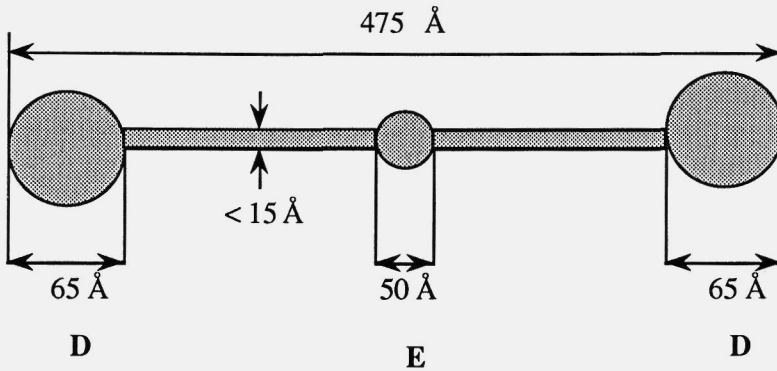
Fig. I. 4 *Trinodular model of Hall and Slayter of fibrinogen*

By the action of thrombin, the fibrinopeptides A and B (MW 1800 D each, containing 16 and 14 amino acids, respectively) are split off and so-called fibrin-monomers are formed. Beyond a certain critical concentration, these fibrin-monomers polymerise and form a fibrin gel. The formed fibrin is then stabilized by crosslinking of the fibrin monomers in the gel by activated coagulation factor XIII (Fig. I.2).

Degradation

Activation of the fibrinolysis system results in the formation of plasmin and the subsequent degradation of fibrin by the formed plasmin. This degradation is a multi-step process, by which fragments of fibrin are cleaved off by the proteolytic action of plasmin.

Plasmin, however, is not specific for fibrin and can also degrade fibrinogen. This degradation is analogous to that of fibrin and can serve as a model for fibrin degradation. Fibrinogen degradation proceeds via a family of early

(large) degradation products called X and Y, to late (smaller) degradation products designated as D and E (Fig. I.5)
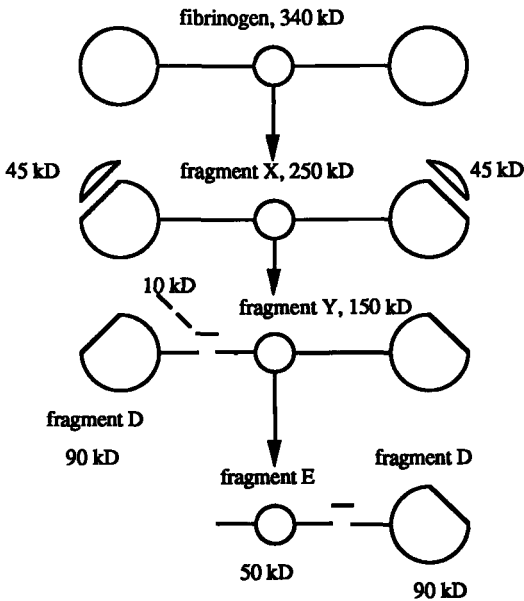
Fig. I.5 *Schematic representation of plasmin degradation of fibrinogen (after Doolittle [20])*

By analogy, non-crosslinked fibrin can be degraded to fragments X, Y, D and E. These products, however, lack the fibrinopeptides A and B. Plasmin digestion of crosslinked fibrin yields, amongst other products, fragment E and the crosslinked products X-oligomer and D-dimer.

The degradation products of fibrin are soluble in plasma. Thus, by converting the insoluble fibrin deposits into soluble degradation products, plasmin dissolves the fibrin network of a thrombus and restores the bloodflow.

I.4 Diagnosis of deep venous thrombosis - general remarks

Relying solely on clinical signs and symptoms for the diagnosis of deep venous thrombosis has become obsolete. It is now generally accepted that only about half of the patients who receive the clinical diagnosis of DVT have objective evidence of venous thrombosis [21-24]. Many other clinical conditions may give rise to the "typical" signs of DVT: a red, warm, swollen and painful leg, positive Homan sign (painful dorsiflexion of foot), subfebrile temperature. Clinical conditions mimicking the signs of DVT include cellulitis, superficial phlebitis, muscle tear, Baker's cyst, haematoma, lymphangitis, erythema nodosum, torsion of knee or ankle joint, inguinal abscess [14]).

To overcome the problems of false diagnosis and treatment, many objective diagnostic procedures have been developed for the diagnosis of DVT.

I.5 Overview of objective diagnostic tests for DVT

Objective tests for detection of thrombosis can be divided into two groups: imaging and non-imaging techniques

IMAGING TECHNIQUES

1. Contrast venography

Among the tests available, contrast venography is considered the gold standard [25,26] and it is found to be safe to withhold therapy from patients with a negative venography [27]. Nevertheless, the procedure has several disadvantages, some of which are due to the use of contrast media: the risk of inducing new thrombi by destruction of the endothelial lining of the vessel; injection of the contrast medium may be painful and there is a risk of allergic reactions to the contrast medium [28]. Although the recent development of low-osmolar contrast media has reduced the risk of vascular complications, other

disadvantages have remained: the problems in execution and interpretation of the test; the difficulty in visualizing ileofemoral venous segments; examination of only the side suspected of being clinically involved and therefore possibly missing bilateral femoral or ileofemoral occlusions.

2. Real-time ultrasonography

This modality is a safe, inexpensive and easy to perform diagnostic procedure for the detection of deep venous thrombosis. It has a high sensitivity and specificity for the detection of proximal DVT (29-36), but is relatively insensitive for the detection of calf vein thrombi (36).

3. Radionuclide bloodpool venography

In the legs, veins of the deep system lack smooth muscle and may act as distensible blood reservoirs. After radiolabelling of the vascular compartment, imaging of the legs will therefore preferentially reveal the deep venous system. The object of bloodpool venography is the detection of obstructed blood flow in the deep veins.

Bloodpool labelling may be achieved with Tc-99m human serum albumin (Tc-99m-HSA) or Tc-99m labelled red blood cells (Tc-99m-RBC). Tc-99m-HSA is inferior to Tc-99m-RBC, since it tends to leak from the vascular space, leading to an elevated background activity and lower target-to-background ratios [36].

The overall concordance rate of Tc-99m-RBC venography compared to contrast venography is 89% [37], with a sensitivity of 73% for ileofemoral venous occlusion [38].

4. Scintigraphy with Tc-99m labelled albumin aggregates

Upon injection in a dorsal foot vein, Tc-99m-macroaggregates (MAA) not only provide information on blood flow in the deep veins of the legs, but also tend to

aggregate in an evolving thrombus, thereby localizing it as a hotspot. Moreover, perfusion scintigrams can be obtained following injection of Tc-99m-MAA to examine whether pulmonary embolization has occurred. However, the sensitivity of Tc-99m-MAA venography is reported to be 73-77% for proximal venous occlusion [49,40].

5. Iodine-123-fibrinogen scintigraphy

This method requires an active uptake of fibrinogen by thrombi and it takes more than 24 hours after injection of the labelled fibrinogen to localize in the clot [41]. Denardo et al. [41] found an overall correlation of 91% with contrast venography. However, false negative results may be obtained in heparinized patients or in patients with established thrombosis (i.e. no active uptake of fibrinogen [41]. Moreover, the radionuclide Iodine-123 is expensive and requires protection of the thyroid gland.

Finally, the use of fibrinogen purified from pooled plasma includes the (small) risk of transmission of hepatitis and AIDS.

6. Scintigraphy with Indium-111 labelled platelets

Although good results have been reported on scintigraphy with In-111 labelled autologous platelets [42,43], this technique has never gained widespread application. Its major drawback is the time and technical skill required for separation and labelling of functionally active platelets.

7. Others

Several other non-invasive tests have been developed, mostly using radiopharmaceuticals: Tc-99m-plasmin [44,45], I-131-streptokinase [46], radioiodinated fibrin fragments [47], In-111-labelled tissue-type plasminogen activator [48], I-131-labelled thrombospondin [49], radiolabelled monoclonal

antibody to platelets [50,51]. However, none of these techniques has gained widespread application due to lack of sensitivity and/or specificity, or to the fact that they have not yet been thoroughly evaluated for accuracy.

NON-IMAGING TECHNIQUES

1. Iodine-125-fibrinogen uptake test

After injection of Iodine-125 labelled fibrinogen, active uptake of the fibrinogen by a thrombus causes an accumulation of radioactivity at the site of the thrombus. This can be measured with a scintillation counter. The fibrinogen uptake test is a useful screening test in the follow-up of patients at risk, e.g. surgical patients [10,52]. It is not to be used as the sole test in the diagnosis of symptomatic deep venous thrombosis, since it does not provide accurate information on the ileofemoral area (specificity 50-70%, [53]). This is of particular relevance in patients undergoing hip surgery, who are at high risk for the development of ileofemoral thrombosis [54]. The sensitivity and specificity for calf vein thrombosis is 97% and 96% respectively [53]. However, false negative results may be obtained in heparinized patients and in patients with thrombi that are not actively extending [55]. False positive results may be caused by hematomas, inflammatory processes or wounds [53]. Other disadvantages are: necessary protection of the thyroid gland, the long time required to complete the study, and the (small) risk of transmission of hepatitis and aids.

2. Impedance plethysmography

With this method, changes in electric resistance due to changes in blood volume (caused by in- and deflation of a cuff) are measured by electrodes, applied to the calf. In patients with thrombosis of the proximal veins, the difference in electric resistance at in- and deflated cuff is reduced.
It has been shown by Huisman et al [14] that serial impedance plethysmography

is a safe and effective non-invasive tool in the diagnosis of leg venous thrombosis in outpatients. It has a high sensitivity and specificity for proximal vein thrombosis, but a low sensitivity for calf vein thrombosis [52].

However, they concluded that thrombosis confined to the calf veins is of little significance for the immediate risk of embolization. Nevertheless, there is always a possibility of proximal progression of venous occlusion and subsequent embolization. Moreover, patients with distal thrombosis may still develop the post-thrombotic syndrome, which may be prevented by adequate and early anticoagulant therapy [56]. Impedance plethysmography does not discriminate between old and recent thrombi - it only detects thrombi that produce obstruction to venous outflow and it does not discriminate between thrombotic and non-thrombotic causes of flow obstruction.

3. Doppler ultrasound

This is a safe, easy-to-perform non-invasive diagnostic procedure, which, in skilled hands, has a high sensitivity for proximal deep vein thrombosis, but is less sensitive (50%) for detection of calf-vein thrombosis [57-59]. False negative results may occur due to non-occlusive thrombi and thrombi in branches of the major veins.

False positive results may be caused by haematomas, edema or inadequate positioning of the doppler transducer.

CONCLUSION

At present, contrast venography is the gold standard with which other tests are compared. Of the non-invasive tests, impedance plethysmography, doppler ultrasound, ultrasonography and the 125-I-fibrinogen uptake test have been evaluated most extensively.

The results of these evaluations are summarized in Table I.1.

Table I.1   **Sensitivity and specificity for symptomatic proximal leg vein thrombosis (as compared with contrast venography)**

	sensitivity	specificity	ref
Impedance plethysmography	87-100%	92-100%	64-72
Real-time ultrasonography	94-100%	88-100%	29-35
Doppler ultrasound	31- 94%	41- 94%	57-63
I-125-fibrinogen uptake	34- 40%	50- 70%	54,73,74

Impedance plethysmography and real-time ultrasonography have proven to be highly sensitive and specific for the detection of thrombi in the proximal leg veins, but provide no accurate information on the calf veins, from which most of the thrombi originate.

I.6 Aim of the study

Most of the above mentioned diagnostic procedures detect thrombi indirectly by measuring their effects i.e. obstruction of blood flow. However, obstruction of blood flow is not necessarily caused by thrombosis, but may also be due to other abnormalities such as hematomas, tumors, aneurysms or Baker's cysts. Methods based on detection of a thrombus itself will not suffer from this problem.

Since fibrin is an important constituent of thrombi, a method for the specific detection of fibrin deposits may be a powerful tool in the detection of venous thrombosis. Antibodies, which are specific for fibrin and which do not react with circulating fibrinogen are good candidates for this approach. Polyclonal

antibodies will almost inevitably crossreact with fibrinogen in plasma, since fibrin and fibrinogen have a 98% identical covalent structure. Monoclonal antibody technology offers the opportunity to obtain highly fibrin-specific targeting agents. Therefore, a study was initiated to investigate the possibility of immunoscintigraphic detection of thrombi using an antifibrin monoclonal antibody, and fragments of the latter. The antifibrin antibody and its fragments were labelled with the radionuclide Tc-99m, which has excellent characteristics for imaging with a gamma camera. This thesis describes the characterization of the antifibrin antibody and its fragments (chapters II and III), the assessment of quality of labelling with Tc-99m (chapter IV), and results of experiments in vitro (chapter V) and in animals (chapter VI), which show the potential of immunoscintigraphic detection of thrombi.

I.7 References

1. Kierkegaard A. Incidence of acute deep vein thrombosis in two districts. Acta Chir Scan 1980, 146: 267-270.

2. Linde DL van der. Het voorkomen van postoperatieve diepe veneuze thrombose. Thesis, Nijmegen, 1975.

3. Kakkar VV, Flanc C, Howe CT, Clarke MB. Natural history of postoperative deep vein thrombosis. Lancet 1969, II: 230-232

4. Nicolaides AN, Kakkar VV, Field ES, Fish P. Venous stasis and deep vein thrombosis. Br J Surg 1972, 59: 713-717.

5. Bolton JP, Hoffman VJ. Incidence of early postoperative iliofemoral thrombosis. Br Med J 1973, 1: 247-249.

6. International Multicenter Trial. Prevention of fatal post-operative pulmonary embolism by low doses of heparin. Lancet II: 45-51

7. Hartsuck JM, Greenfield LJ. Postoperative thromboembolism. A clinical study with 125I-fibrinogen and pulmonary scanning. Arch Surg 1973, 107: 733-739.

8. International Multicenter Trial. Prevention of fatal post-operative pulmonary embolism by low doses of heparin. Lancet 1977, I: 567-569.

9. Kiil J, Kiil J, Axelsen F, Andersen D. Prophylaxis against postoperative pulmonary embolism and deep vein thrombosis by low dose heparin. Lancet 1978, I: 1115-1116.

10. Sherry S. The problem of thromboembolic disease. Semin Nucl Med 1977, 7: 205-211.

11. Sasahara AA, Cella G, Palla A. Detection of deep vein thrombosis in the diagnosis of pulmonary embolism. J Nucl Med All Sci 1986, 30: 57-61.

12. Sevitt S, Gallagher Ng. Venous thrombosis and pulmonary embolism: a clinico-pathological study in injured and burned patients. Brit J Surg 1961, 55: 475-483.

13. Moser KM, LeMoine JR. Is embolic risk conditioned by location of deep venous thrombosis? Ann Intern Med 1981, 94: 439-444.

14. Huisman MV, Buller HR, Ten Cate JW, Vreeken J. Serial impedance plethysmography for suspected deep venous thrombosis in outpatients. N Engl J Med 1986, 314: 823-828.

15. Havig O. Deep vein thrombosis and pulmonary embolism: an autopsy study with multiple regression analysis of possible risk factors. Acta Chir Scand (suppl.) 1977, 478: 1-120.

16. Moreno-Cabral R, Leistner RL, Nordyke RA. Importance of calf vein thrombophlebitis. Surgery 1976, 80: 735-742.

17. Nelson PH, Moser KM, Stoner C. Risk of complications during heparin therapy. West J Med 1982, 136: 189-197.

18. Hall CE, Slayter HS. The fibrinogen molecule, its size, shape and mode of polymerization. J Biophys Biochem Cytol 1959, 5: 11-17.

19. Hall CE. Visualization of individual macromolecules with the electron microscope. Proc Natl Acad Sci 1956, 42: 801-806.

20. Doolittle RF. Annu Rev Biochem 1984; 53:195-229.

21. Cranley JJ, Canos AJ, Sull WJ. The diagnosis of deep venous thrombosis. Fallibility of clinical signs and symptoms. Arch Surg 1976, 111: 34-36.

22. O'Donnell TF, Abbott WM, Athansoulis CA, Millan VG, Callow AD Diagnosis of deep vein thrombosis in the out-patient by venography. Surg Gyn Obst 1980, 150: 69-74.

23. Hirsh J, Gallus AS. Diagnosis of venous thromboembolism: limitations and applications. In: Madden JL, Hume M (eds.). Venous Thromboembolism: Prevention and Treatment. 1976: pp 183-213.

24. Haeger K. Problems of acute deep venous thrombosis I. The interpretation of signs and symptoms. Angiology 1969, 20: 219-223.

25. Lea Thomas M,. Phlebography. Arch Surg 1972, 104: 141-151.

26. Rabinov K, Paulin S. Roentgen diagnosis of venous thrombosis in the leg. Arch Surg 1972, 104: 134-144.

27. Hull R, Hirsh J, Sackett DL. Clinical validity of a negative venogram in patients with clinically suspected venous thrombosis. Circulation 1981, 64: 622-625.

28. Bettman MA, Paulin S. Leg phlebography: the incidence, nature and modification of undesirable side effects. Radiology 1977, 122: 101-104.

29. Raghavendra BN, Rosen RJ, Lam S et al. Deep venous thrombosis: detection by high-resolution real-time ultrasonography. Radiology 1984, 152: 789-793.

30. Vogel P, Laing FC, Jeffrey RB, Wing VW. Deep venous thrombosis of the lower extremity: US evaluation. Radiology 1985, 163: 747-751.

31. Flanagan LD, Cranley JJ,. Real-time B-mode ultrasound imaging in the diagnosis of venous diseases of the extremities. Diagnostic techniques and assessment procedures in vascular surgery. London: Grune and Stratton, 1985.

32. Danzat MM, Laroche JP, Charras C, et al. Real-time B-mode ultrasonography for better specificity in the noninvasive diagnosis of deep venous thrombosis. J Ultrasound Med 1986, 5: 625-631.

33. Sullivan ED, Peter DJ, Cranley JJ. Real-time B-mode versus ultrasound. J Vasc Surg 1984, 1: 465-471.

34. Aitken AGF, Godden DJ. Real-time ultrasound diagnosis of deep venous

thrombosis: A comparison with venography. Clinical Radiol 1987, 38: 309-313.

35. Appelman PTM, Sluzewski M, Lampmann LEH. Ultrasonography in diagnosis of deep venous thrombosis: US findings. Radiology 1987, 163: 743-746.

36. Srivastava SC, Chervu RL. Radionuclide labeled red blood cells: current status and future prospects. Semin Nucl Med 1984, 10: 68-82.

37. Lisbona R, Stern J, Derbekyan V. 99mTc red blood cell venography in deep vein thrombosis of the leg: a correlation with contrast venography. Radiology 1982, 143: 771-773.

38. Singer I, Royal HD, Uren RF. Radionuclide plethysmography and Tc-99m red blood cell venography in venous thrombosis: comparison with contrast venography. Radiology 1984, 150: 213-217.

39. Bentley PG. Radionuclide venography in management of proximal venous occlusion: comparison with X-ray contrast phlebography. Br J Radiol 1979, 52: 289-300.

40. Webber MM. Labeled albumin aggregates for detection of clots. Semin Nucl Med 1977, 3: 253-261.

41. DeNardo SJ, Bogren HG, DeNardo GL. Detection of thrombophlebitis in the lower extremities: a regional comparison of I-123-fibrinogen scintigraphy and contrast venography. Am J Radiol 1985, 145: 1045-1052.

42. Knight LC, Primeau JL, Siegel BA, Welch MJ. Comparison of In-111 labeled platelets and iodinated fibrinogen for the detection of deep vein thrombosis. J Nucl Med 1978, 19: 891-894.

43. Moser KM, Spragg RG, Bender F, Konopka R, Hartman MT, Fedullo P. Study of factors that may condition scintigraphic detection of venous thrombi and pulmonary emboli with Indium-111 labeled platelets. J Nucl Med 1980, 21: 1051-1058.

44. Overgaard K. Thromboscintigraphy with 99mTc-plasmin; a new diagnostic method of deep venous thrombosis of the legs. Nucl Med

Commun 1984, 5: 101-107.

45. Dahlborn M et al. Gamma camera detection of Tc-99m plasmin in diagnosis of deep vein thrombosis. Eur J Nucl Med 1984, 9: 499-501.

46. Goodman LR, Goodman C, Greenspan RH. Failure to visualise experimentally produced emboli and thrombi using I-131 streptokinase. Invest Radiol 1973, 8: 377-383.

47. Knight LC, Olexa SA, Malmud LS. Specific uptake of radioiodinated E_1 by venous thrombi in pigs. J Clin Invest 1983, 72: 2007-2013.

48. Hnatowich DJ, Virz F, Doherty PW. Indium-111 labelled tissue plasminogen activator. Eur J Nucl Med 1987, 13: 467-473.

49. Perlman SB, Folts JD, Hammes RJ, Besorzi MC, Mosher DF The accumulation of a platelet protein, thrombospondin at the site of arterial thrombus formation: preliminary report. Eur J Nucl Med 1987, 12: 492-495.

50. Som P, Oster ZH, Zamora PO, Yamamoto K, Sacker DF, Brill AB, Newell KD, Rhodes BA. Radioimmunoimaging of experimental thrombi in dogs using Tc-99m labeled monoclonal antibody fragments reactive with human platelets. J Nucl Med 1986, 2 : 1315-1320.

51. Peters AM, Lavender JP, Needham SG, Louth I, Snook D, Epenetos AA, Lumley P, Keery RJ, Hogg N. Imaging thrombus with radiolabelled monoclonal antibody to platelets. Brit Med J 1986, 293: 1525-1527.

52. Hull RD, Raskob GE, Leclec JR, Jay RM, Hirsh J. The diagnosis of venous thrombosis in symptomatic patients. In: Poller L (ed.). Recent advances in blood coagulation IV. Churchill Livingstone, London, 1985: pp 35-63.

53. Kakkar VV. Fibrinogen uptake test for detection of deep venous thrombosis: a review of current practice. Semin Nucl Med 1977, 7: 229-244.

54. Harris WH, Salzman EW, Athanasoulis Ch, Waltman A, Baum S, DeSanctis RW, Potsaid MS, Sise H. Comparison of I-125 fibrinogen count scanning with phlebography for detection of venous thrombi after elective hip surgery. N Engl J Med 1975, 292: 665-667.

55. Quereshi GD, Fratkin MJ, Robert PS. Advances in the diagnosis of venous thrombosis. Prog Clin Pathol 1977, 7: 317-336.

56. Watz R, Savidge GF. Rapid thrombolysis and preservation of valvular venous function in high deep vein thrombosis. Acta Med Scand 1979, 205: 293-298.

57. Sigel B, Felix GL, Popky GL. Diagnosis of lower limb venous thrombosis by Doppler ultrasonic technique. Arch Surg 1972, 104: 174-179

58. Johnson WC. Evaluation of newer techniques for the diagnosis of venous thrombosis. J Surg Res 1974, 16: 473-481.

59. Evans DS. The early diagnosis of deep vein thrombosis by ultrasound. Br J Surg 1970, 57: 726-729.

60. Milne RM, Griffiths JMT, Gunn AA. Postoperative deep venous thrombosis. Lancet 1971, II: 445-447.

61. Yao JST, Gourmos C, Hobbs JT. Detection of proximal vein thrombosis by Doppler ultrasonic flow detection method. Lancet 1972, I: 1-4.

62. Strandness DE Jr, Sumner DS. Ultrasonic velocity detector in the diagnosis of thrombophlebitis. Arch Surg 1972, 104: 180-183.

63. Yao JST, Henkin RE, Bergan JJ. Venous thromboembolic disease: evaluation of new methodology in treatment. Arch Surg 1974, 109: 664-669.

64. Hull R, Van Aken WG, Hirsh J. Impedance plethysmography using the occlusive cuff technique in the diagnosis of venous thrombosis. Circulation 1976, 53: 696-700.

65. Toy PTCY, Schrier SL. Occlusive impedance plethysmography. A non-invasive method of diagnosis of deep-vein thrombosis. West J Med 1978, 129: 89-93.

66. Flanigan DP, Goodreau JJ, Buruham SJ, Bergan JJ, Yao JST. Vascular-laboratory diagnosis of clinically suspected acute deep-vein thrombosis. Lancet 1978, II: 331-334.

67. Hull R, Hirsh J, Powers P. Impedance plethysmography. The relationship between venous filling and sensitivity and specificity for proximal-vein

thrombosis. Circulation 1978, 64: 622-625.

68. Gross WS, Burney RE. Therapeutic and economic implications of emergency department evaluation for venous thrombosis. J Am Coll Emerg Phys 1979, 8: 110-113.

69. Cooperman M, Martin EW Jr,Satiani B, Clarke M, Evans WE. Detection of venous thrombosis by impedance plethysmography. Am J Surg 1978, 137: 252-254.

70. Wheeler HB, Anderson FA Jr,. Can non-invasive tests be used as the basis for treatment of deep-vein thrombosis? In: Bernstein EF (ed.). Non-invasive diagnostic techniques in vascular disease. Mosby, St. Louis, 1981, pp 545-559.

71. Hull R, Hirsh J, Sackett DL, Stoddard G. Cost effectiveness of clinical diagnosis, venography and non-invasive testing in patients with symptomatic deep-vein thrombosis. N Engl J Med 1981, 304: 1561-1567.

72. Peters SHA, Jonker JJC, de Boer AC, den Ottolander GJH. Home diagnosis of deep venous thrombosis with impedance plethysmography. Thromb Hemost 1982, 48: 297-300.

73. Mavor GE, Walker MG, Dhall DP, Mahaffy RG, Duthie JS, Gaddie J, Reid GF. Peripheral venous scanning with I-125 tagged fibrinogen. Lancet 1972, I: 661-663.

74. Kerrigan GNW, Buchanan MR, Cade JF. Investigation of the mechanism of false positive I-125 labelled fibrinogen scans. Br J Haematol 1974, 26: 469-473.

CHAPTER II

PRODUCTION AND CHARACTERIZATION OF ANTIFIBRIN MONOCLONAL ANTIBODY Y22

As stated in the introduction, fibrin is an important constituent of thrombi. Therefore, a method for the specific detection of fibrin deposits may be a useful tool in the diagnosis of venous thrombosis.

Efforts to raise polyclonal antibodies to fibrin have generally yielded antibodies that also react with fibrinogen in plasma [1]. This is not surprising, since fibrinogen and fibrin are 98% identical to one another in primary structure. Monoclonal antibodies, however, offer the possibility of obtaining highly specific targeting agents, which may surmount the problem of crossreactivity with fibrinogen.

This chapter, after a brief general introduction to monoclonal antibody production, describes the production of an antifibrin monoclonal antibody, its antigenic determinants and its binding to artificial thrombi as assessed by immunofluorescence microscopy.

II.1 GENERAL INTRODUCTION TO MONOCLONAL ANTIBODIES

Since their introduction by Köhler and Milstein [2], monoclonal antibodies (MoAb's) have found widespread application in vitro for immunochemical characterization and quantitation of antigens. Because of their specific targeting properties they are also increasingly used in nuclear medicine for the immunoscintigraphic detection of primary and metastatic tumor sites [3].

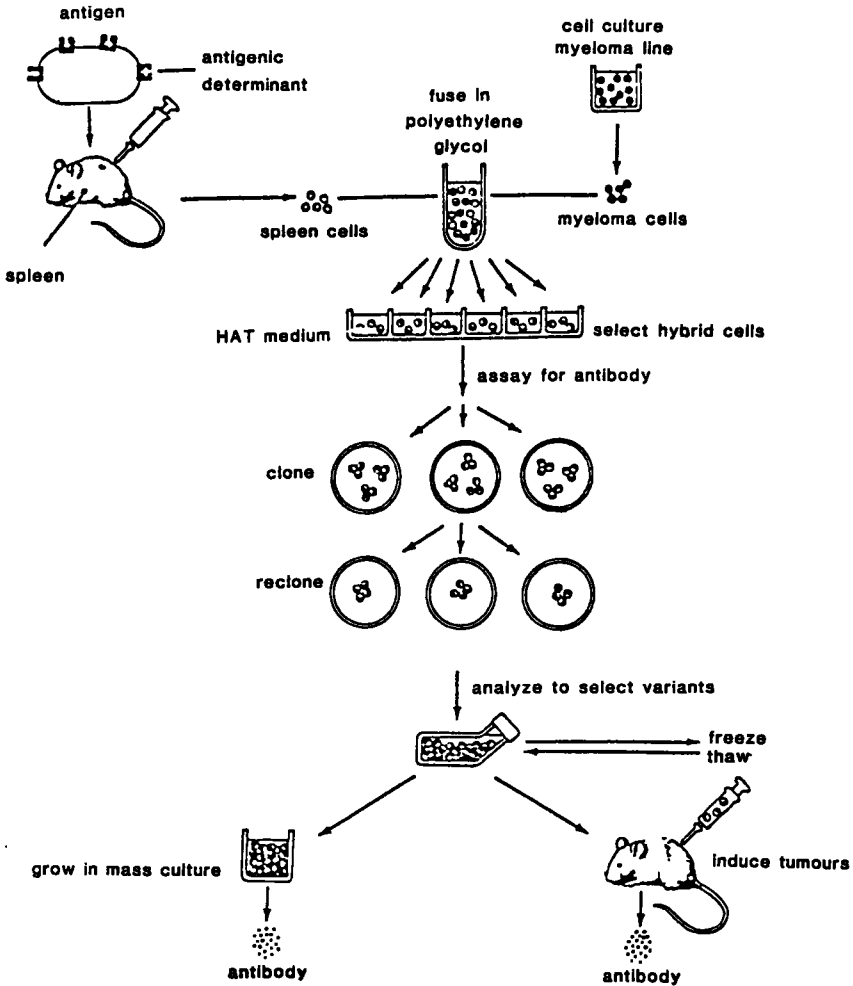Figure II.1 shows the principle of mouse monoclonal antibody production.

Fig. II.1   *Production and selection of monoclonal antibodies (adapted from Sci Am 1980; 243: 66-74)*

After immunization of mice with an immunogen, splenic lymphocytes of the mice are fused with a myeloma cell line that lacks the capacity to produce antibodies. The resulting hybridoma cells are selected by their ability to propagate in hypoxanthine-aminopterin-thymidine (HAT) containing medium. Unfused lymphocytes and myeloma cells do not grow in the HAT medium. The hybridoma cells are cloned and the clones generating antibodies to the selected

antigenic determinant are identified using a screening assay. After selection of the desired antibody secreting clones, the hybridomas can be maintained in mass culture in which the supernatant serves as a dilute source of antibodies. To obtain higher concentrations of antibodies, the clones can be grown intraperitoneally in mice to produce MoAb-rich ascites fluid.

Hybridomas usually produce IgG (of IgG1 or IgG2a isotype) and occasionally IgM antibodies. IgG antibodies consist of two long and two short amino acid chains, referred to as heavy (H) and light (L) chains. The chains are linked together by disulfide bridges. The IgG isotypes differ structurally in the number of disulfide bridges linking the heavy chains together. The constant region is the same for all IgG's of the same isotype and can activate various components of the immune system. It includes the Fc-fragment, so called because of its tendency to crystallize in vitro. The variable regions in the two antigen-binding Fab-fragments determine the antigen-specificity of the antibody. IgG antibodies can be degraded to F(ab)2-fragments, Fab-fragments and Fc-fragments by enzymatic cleavage e.g. with pepsin or papain (Fig. II.2).
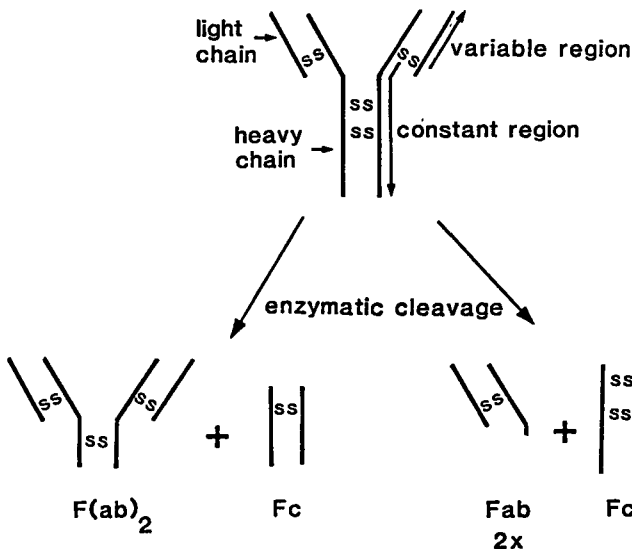

Fig. II.2   *Fragmentation of IgG monoclonal antibodies*

II.2 ANTI-FIBRIN MONOCLONAL ANTIBODY Y22

Introduction

For immunoscintigraphic detection of thrombi with MoAb's, fibrin specificity of the latter is a prerequisite. The levels of circulating fibrinogen are so high (approximately 2 mg/ml), that almost any crossreactivity of the MoAb with fibrinogen will saturate all free antibody injected into the circulation. In order to have fibrin-specificity, antifibrin MoAb's should be directed against an epitope that is not available in fibrinogen, but becomes exposed in fibrin due to conformational changes in the fibrinogen molecule when it is converted to fibrin by the action of thrombin.

Hui et al. [4] produced fibrin-specific monoclonal antibodies by immunizing mice with a synthetic peptide containing the amino acids of the N-terminal end of the beta-chain of fibrin. This antigenic site appears to be blocked in the intact fibrinogen molecule and is de-blocked upon release of the fibrinopeptide B. Kudryk et al. [5] immunized mice with thrombin-digested NDSK (N-terminal disulfide knot, a fibrinogen fragment obtained after cyanogen bromide digestion). They also obtained antibodies against the N-terminal end of the beta-chain of fibrin. Both the Hui and the Kudryk antifibrin MoAb's have been radiolabelled and used for immunoscintigraphic detection of thrombi with promising results [6,7].

Scheefers-Borchel et al. [8] produced antibodies against a synthetic hexapeptide containing the amino acids of the N-terminal region of the alpha-chain of fibrin. This antibody was used in an assay for the detection of soluble fibrin in plasma.

We used an alternative approach for the production of our antifibrin antibody. The rationale behind this approach was the following. It has been found that fibrinogen degradation products (e.g. fragment Y) share some properties with fibrin, such as the capacity to accelerate the activation of plasminogen by tissue-type plasminogen activator [9]. Intact fibrinogen does not have that capacity.

Three-dimensional structures within fibrinogen degradation products and fibrin may be important for these properties and may be recognized by monoclonal antibodies. For that reason we included possible reactivity with fibrin in our protocol to screen hybridomas resulting from fusions of mouse myeloma cells with spleen cells of mice immunized with fibrinogen fragment Y. We came across a MoAb with a much higher affinity for fibrin than for fibrinogen in our screening protocol with an enzyme immunoassay (EIA). This MoAb (designated as Y22) was further characterized and appeared to react also with preformed clots in vitro.

Materials

Balb/c mice were obtained from the Centraal Proefdieren Bedrijf TNO, Zeist, The Netherlands; Freund's adjuvant from Difco, Amsterdam, the Netherlands; Polyethylene glycol 4000 from Baker Chemical Co., Deventer, the Netherlands; 96-well cell culture plates from Costar, Cambridge, Mass. U.S.A. Protein A-Sepharose CL-4B was obtained from Pharmacia, Uppsala, Sweden. Antisera against mouse immunoglobulin chains were gifts from Dr. Radl (Institute for Experimental Geron tology TNO, Rijswijk, the Netherlands). Microtiter plates (Immulon) were purchased from Greiner, Alphen a/d Rijn, the Netherlands. Rabbit antimouse Ig (7S) was obtained from Nordic, Tilburg, the Netherlands; 3, 3', 5, 5'-tetramethylbenzidine (TMB) from Aldrich Chemical Co., Milwaukee, U.S.A. N-succimidyl 3-(2-pyridyl-dithio) propionate (SPDP) from Pharmacia, Uppsala, Sweden; bovine thrombin from Leo, Ballerup, Denmark. Goat-antimouse Ig, conjugated with fluorescein isothiocyanate (FITC) was obtained from Tago Inc., Burlingame, U.S.A. A control MoAb (anti-FITC IgG1) was kindly provided by Dr. J.J. Haaijman Medical Biological Laboratory TNO, Rijswijk, the Netherlands. The synthetic peptide H-Glycyl-L-Prolyl-L-Arginyl-L-Proline (Gly-Pro-Arg-Pro) was kindly provided by Dr. G. van Dedem at Diosynth, Oss, The Netherlands.

Methods

Purified proteins

Fibrinogen was purified as described by Van Ruijven et al [10]. Plasmin-generated fibrin(ogen) degradation products were prepared and purified as described by Nieuwenhuizen et al. for fragment X [11] and Y [12] and by Van Ruijven et al [13] for fragment E, D-dimer and D-cate. Fibrinogen Aα, Bβ and γ-chains were separated after reduction and subsequent carboxymethylation of fibrinogen and purified as described by Doolittle et al [14]. Fibrin monomers were prepared and purified as described by Haverkate et al. [15] and stored in 20 mM acetic acid at -20`C. Occasionally, soluble fibrin was generated by treatment of plasma or fibrinogen solutions with thrombin (2 NIH units/ml) in the presence of 15 mM Gly-Pro-Arg-Pro to prevent polymerization (16).

Production of monoclonal antibody Y22

Female Balb/c mice were immunized by intraperitoneal injection of 25 µg purified fibrinogen fragment Y in complete Freund's adjuvant and then at three-week intervals with 25 µg of fragment Y in incomplete Freund's adjuvant. An intravenous injection of 10 µg of fragment Y in phosphate-buffered saline (PBS) was given three days before fusion. Spleen cells of the immunized mice were fused with P3 x Ag 8653 cells in 40% polyethylene glycol 4000 as described before [17]. Growth and selection media were as described by Köhler and Milstein [2]. The cell suspension was diluted and divided over 96-well microtiter plates. Wells with growing cells were screened for antibody production by double-sandwich enzyme immunoassay (EIA) as described below. Reactive antibody producing cell lines were subcloned twice by limiting dilution (0.5 cells per well). One hybridoma was selected, producing the monoclonal antibody designated as Y22. The Y22 hybridoma cells were injected into the peritoneal cavity of Balb/c mice to produce Y22 containing ascites fluid.

Purification and subclass assessment

Y22 was purified from ascites fluid by adsorption to protein A-Sepharose CL-4B and subsequent elution with citrate buffer pH 5.0 according to Ey et al. [18]. Subclass was assessed by immunoelectrophoresis as described by Radl [19].

Double-sandwich Enzyme Immuno Assay (EIA)

Immune reactivity of Y22 was determined using the double-sandwich EIA as described by Koppert et al. [20]. Wells of microtiter plates were coated with rabbit antimouse Ig (7S) in a concentration of 10 µg/ml in PBS (120 µl/well). After incubation for 16 hours at 4°C, the plates were washed three times with PBS containing 0.05% Tween 20 (PBS/Tween). Hybridoma supernatant (for screening) or purified Y22 (for immunoreactivity; concentration 2 µg/ml in PBS/Tween) was added (100 µl/well) and incubated for 30 minutes at room temperature. After three washings with PBS/Tween, 100 µl portions of human fibrin monomer or fibrinogen solutions in PBS/Tween were pipetted into the wells and incubated for 30 minutes. Monomers were diluted in 0.02 M acetic acid to a concentration of 0.1 mg/ml. Further dilutions were made in PBS/Tween (pH 7.4). Occasionally fibrin was used, generated (by thrombin treatment) in plasma or in fibrinogen solution, and kept in solution by Gly-Pro-Arg-Pro in PBS/Tween (pH 7.4). Finally, a horseradish peroxidase conjugate of IgG's from pooled polyclonal panspecific rabbit antisera against fibrin(ogen) [20] was added. After incubation for 30 minutes at room temperature, reactivity was assessed by adding 3,3',5,5'-tetramethyl benzidine (TMB) and H_2O_2 as the substrate mixture [21]. After 5 minutes, the reaction was stopped by adding 100 µl sulphuric acid (1 M) to the wells, and the absorbance at 450 nm was read using a munltichannel spectrophotometer. Reactivity with fibrin and fibrinogen of different species was tested using horseradish peroxidase conjugates of antisera against the corresponding antigens.

Cross-reactivity assay (CRA)

Localization of the epitope recognized by Y22 was carried out using the cross-

reactivity assay essentially according to Soria et al. [22]. The first step consisted of an EIA. Y22 was conjugated with horseradish peroxidase using N-succimidyl-3-(2-pyridyldithio) propionate (SPDP) as a coupling agent, according to the manufacturer's instructions. Dilutions of the Y22-horseradish peroxidase conjugate in PBS/Tween 20 were added to microtiter plates coated with fibrinogen degradation fragment Y. After conversion of the TMB substrate, the reactivity was assessed spectrophotometrically. The dilution giving 80% of the maximum response in the EIA was taken as working solution in the second step. In the second step, Y22-horseradish peroxidase conjugate working solution was preincubated (16 hours, 4°C) with several dilutions (in PBS) of D-dimer, fibrinogen degradation fragments X, Y, E and D-cate and separated Aα, Bβ and γ–chains. After preincubation, 100 μl samples of this incubation mixture were transferred to the wells of a fragment Y-coated microtiter plate for EIA. Reaction of the conjugated antibody with the antigen in the preincubation step would result in diminished reactivity with fragment Y, adsorbed to microtiter plates.

Preparation of artificial thrombi
Thrombi were formed in vitro from whole human blood in a loop of plastic tubing on a turntable as described by Chandler [23]. The thrombi were washed with saline and stored overnight at 4°C.

Visualization of binding of Y22 to artificial thrombi by immunofluorescence.
To visualize the binding of Y22 to thrombi, frozen sections of artificial thrombi were made and washed three times with PBS. The sections were incubated with 1:8 diluted normal goat serum to suppress possible background fluorescence. After incubation for 30 minutes at room temperature, the sections were washed with PBS and incubated with Y22 (0.15 μg/ml) in PBS for 30 minutes at room temperature. After washing with PBS, 1:40 diluted goat antimouse Ig conjugated with FITC was added and incubated for 30 minutes. Finally, the sections were washed and examined under an epi-fluorescence microscope

(Leitz Labolux D). A non-related IgG1 MoAb was used as a control.

Results and Discussion

Three weeks after fusion and selection, cell growth was observed in 34 of the 180 seeded wells. The media of 4 wells showed much higher reactivity with fibrin monomers than with fibrinogen in the double-sandwich EIA used for screening. After cloning and recloning, one clone was selected for its good growth and production properties. This clone, designated as Y22, has been injected into the peritoneal cavity of Balb/c mice for the production of ascites, where it has been productive for more than 6 months (9 passages). After two years of storage in liquid nitrogen, the clone could be thawed and grown. Subclass assessment showed that Y22 is an IgG1 monoclonal antibody with κ-light chains.

Figure II.3 shows that Y22 reacts strongly with fibrin monomers and only weakly with fibrinogen in the double-sandwich EIA. The figure also shows the reactivities with rabbit fibrin and rabbit fibrinogen. Rat material showed virtually the same profiles.

The observed small crossreactivity with fibrinogen may only be apparent, e.g. due to a low amount of fibrin present in the fibrinogen preparation. If, however, the weak cross-reactivity is actual and due to fibrinogen itself, the dissociation constant of the binding of Y22 with fibrin must be several orders of magnitude lower than for the binding with fibrinogen. We cannot discriminate between these two possibilities on the basis of our EIA results. The experiments on the binding of Y22 to thrombi in vitro (Chapters IV and V) and in vivo (Chapter VI) show that (whatever the reason for the observed weak crossreactivity is) Y22 will accumulate on thrombi in a plasma milieu, i.e. even in the presence of large excesses of fibrinogen.

It could be argued that fibrin monomers are much more reactive than fibrinogen in the EIA systems because the former have been dissolved in 0.02 M acetic acid, whereas fibrinogen has not. To check this, we exposed fibrinogen to

0.02 M acetic acid and assessed the reactivity of this acid-treated fibrinogen. After acid-treatment, the reactivity of fibrinogen was virtually equal to that of fibrin monomers. This would indicate that the higher reactivity of fibrin may be due to some acid-induced denaturation. However, when fibrin monomers were used, produced by adding thrombin (2 NIH units/mg fibrinogen) to Gly-Pro-Arg-Pro [16] containing fibrinogen solutions (in PBS) or plasma and further diluted in PBS/Tween (pH 7.4), the much higher affinity of Y22 for fibrin compared to fibrinogen was still observed. This indicates that fibrin polymerization is not a prerequisite for Y22 interaction, and that the Y22 epitope can be induced by the fibrinogen-to-fibrin conversion under physiologic conditions, but also (as an artifact) by acid treatment of fibrinogen. It also indicates that the binding of Y22 to fibrin is not blocked by binding of the polymerization inhibiting peptide Gly-Pro-Arg-Pro.
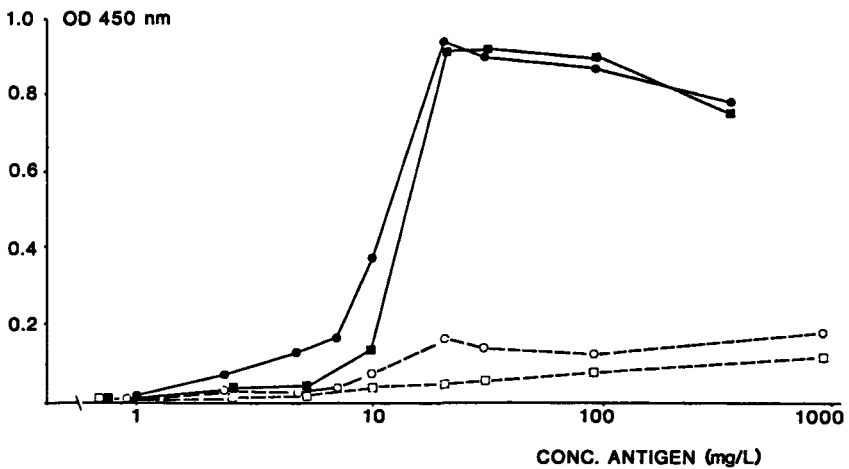

Fig. II.3   *Reactivity of Y22 in a double sandwich EIA expressed as optical density at 450 nm. Human (●) and rabbit (■) fibrin monomers were used as antigens and compared with human (○) and rabbit (□) fibrinogen*

We were not able to define the epitope of Y22 from the results of the cross-

reactivity assay to the level of amino acids or chain stretches involved. Figure II.4 shows that Y22 reacted well with fibrin(ogen) degradation products containing the D-domain, but not with fragment E. Y22 did not react with isolated Aα, Bβ or γ-chains in the CRA. However, it could be argued that the lack of reactivity of Y22 with the separate chains was due to their rather low solubility. This is probably not the case, since Y22 also did not react with isolated chains adsorbed to microtiter plates.
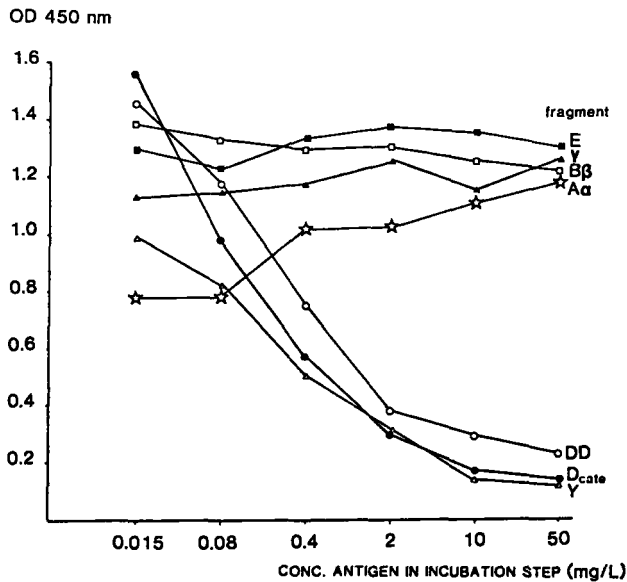

Fig. II.4   *Results of the crossreactivity assay (CRA). Reactivity of Y22 with fibrin(ogen) degradation fragments. High response in this assay indicates minimal binding of peroxidase labelled Y22 with the specific antigen in the preceding incubation step (see methods section)*

From these results it is conceivable that Y22 is directed against a conformation dependent epitope in the D-domain of fibrin. It seems to be a highly conserved epitope, since Y22 also reacts with fibrin of rabbits, rats, dogs and sheep adsorbed to microtiter plates (but not with murine or porcine fibrin). The

specificity of Y22 for fibrin of rats and rabbits, as compared to the corresponding fibrinogens, is similar to that for human fibrin(ogen).

To show that Y22 not only binds to fibrin monomers, but also to the polymerized and cross-linked fibrin of thrombi, immunofluorescence studies on frozen sections of artificial thrombi were performed.

Figure II.5 shows the immunofluorescence pattern of the fibrin network in these thrombi and also shows the resemblance of these artifical thrombi to in vivo thrombi with a white (Figure II.5A) and a red part (Figure II.5B). No fluorescence was observed after incubation with the control MoAb (Figure II.5C).
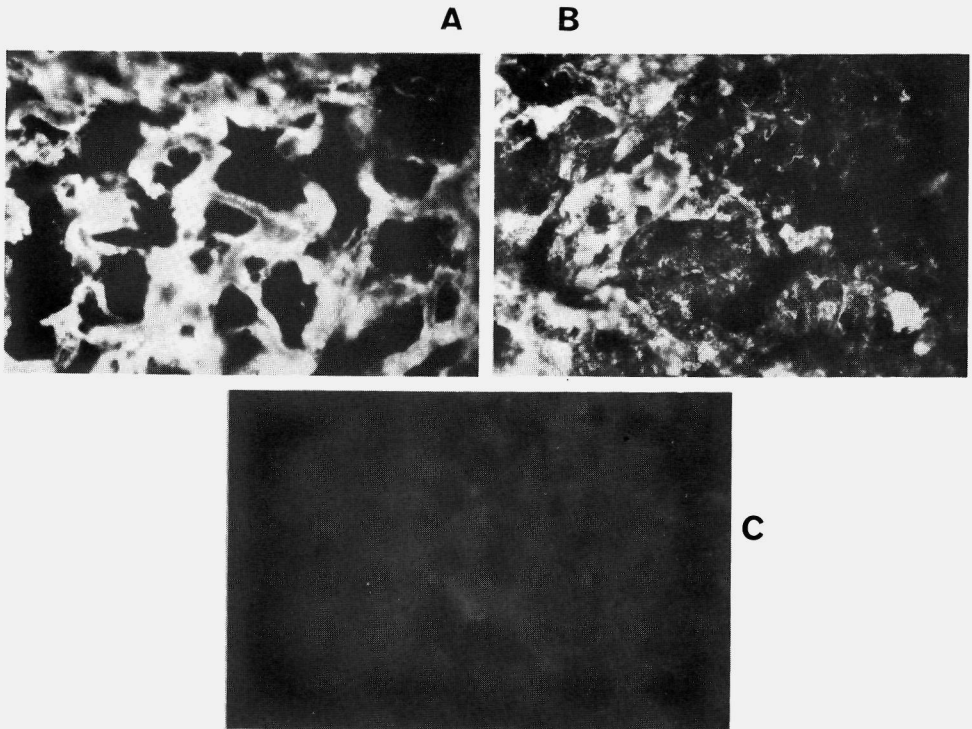

Fig. II.5.   *Immunofluorescence microscopy of thrombi with Y22 (A-B) and control MoAb anti-FITC (C); A: white part of thrombus; B: red part of thrombus.*

In conclusion, Y22 reacts with a conformation dependent epitope in the D-domain of fibrin. This epitope is present and available both in monomeric fibrin and in polymerized, crosslinked fibrin of thrombi, but not in fibrinogen.

References

1.   Edgington TS, Plow EF. Functional molecular anatomy of fibrinogen; antibodies as biological probes of structures. Contemp Top Mol Immunol 1973, 2: 237-271.

2.   Köhler G, Milstein C. Continuous cultures of fused cells secreting antibody of predefined specificity. Nature 1975, 256: 495-497.

3.   Larson SM. Radiolabeled monoclonal anti-tumor antibodies in diagnosis and therapy. J Nucl Med 1985; 26: 538-545.

4.   Hui KY, Haber E, Matsueda GR. Monoclonal antibodies to a synthetic fibrin-like peptide bind to human fibrin but not fibrinogen. Science 1983, 222: 1129-1132.

5.   Kudryk B, Rohoza A, Ahadi M, Chin J, Wiebe ME. Specificity of a monoclonal antibody for the NH2-terminal region of fibrin. Mol Immunol 1984, 21: 89-94.

6.   Hui KY, Haber E, Matsueda GR. Immunodetection of human fibrin using monoclonal antibody 64C5 in an extracorporeal chicken model.Thromb Haemost 1985, 54: 524-527.

7.   Rosebrough SF, Kudryk B, Grossman ZD, McAfee JG, Subramanian G, Ritter-Hrucirik CA, Witanowski LS, Tillapaugh-Fau G. Radioimmunoimaging of venous thrombi using Iodine-131 monoclonal antibody Radiology 1985, 156: 515-517.

8.   Scheefers-Borchel U, Muller-Berghaus G, Fuhge P, Eberle R, Heimburger N. Discrimination between fibrin and fibrinogen by a monoclonal antibody against a synthetic peptide. Proc Natl Acad Sci USA 1985, 82: 7091-7095.

9.   Verheyen JH, Nieuwenhuizen W, Wijngaards G. Activation of

plasminogen by tissue activator is increased specifically in the pre sence of certain soluble fibrin(ogen) fragments. Thromb Res 1982, 27: 377-385.

10. Van Ruijven-Vermeer IAM, Nieuwenhuizen W. Purification of rat fibrinogen and its constituent chains. Biochem J 1978, 169: 653-658.

11. Nieuwenhuizen W, Gravesen M. Anticoagulant and calcium-binding properties of high molecular weight derivatives of human fibrinogen, produced by plasmin (fragments X). Biochym Biophys Acta 1981, 668: 81-88.

12. Nieuwenhuizen W, Voskuilen M, Hermans J. Anticoagulant and cal cium-binding properties of high molecular weight derivatives of human fibrinogen (plasmin fragments Y). Biochim Biophys Acta 1982, 708: 313-316.

13. Van Ruijven-Vermeer IAM, Nieuwenhuizen W, Haverkate F, Timan G. A novel method for the rapid purification of human and rat fibrin(ogen) degradation products in high yields. Hoppe-Seyler's Z Physiol Chemie 1977, 360: 633-637.

14. Doolittle RF, Cassman KG, Cottrell BA, Friezner SJ, Hucko JT, Takagi T. Amino acid sequence studies on the alpha-chain of human fibrinogen. Characterization of 11 cyanogen bromide fragments. Biochemistry 1977, 16: 1703-1709.

15. Haverkate F, Timan G. Preparation of highly purified bovine fibrin plates in chemical fibrinolysis and thrombolysis, vol 2. New York, Raven Press 1976, p 67-71.

16. Laudano AP, Doolittle RF. Synthetic peptide derivatives that bind to fibrinogen and prevent the polymerization of fibrin monomers. Proc Natl Acad Sci USA 1978; 75:3085-3089.

17. Koppert PW, Huymans CMG, Nieuwenhuizen W. A monoclonal antibody, specific for human fibrinogen, fibrinopeptide A-containing fragments and not reacting with free fibrinopeptide A. Blood 1985, 66: 503-507.

18. Ey PL, Prowse SJ, Jenkin CR. Isolation of pure IgG1, IgG2a and IgG2b immunoglobulins from mouse serum using protein A-sepharose, Immunochem 1978, 15: 429-436.

19. Radl J. Immunoglobulin levels and abnormalities in aging humans and mice. In Adler WH, Nordin AA (eds): Immunological techniques applied to aging research. Boca Raton, Fla., CRC, 1981, p 122-139.

20. Koppert PW, Koopman J, Haverkate F, Nieuwenhuizen W. Production and characterization of a monoclonal antibody reactive with a specific neoantigenic determinant (comprising B-beta 54-118) in degradation products of fibrin and of fibrinogen. Blood 1986, 68: 437-441.

21. Bos ES, Van der Doelen AA, Van Rooy N, Schuurs AHWM. 3,3',5,5'-Tetramethylbenzidine as an Ames negative chromogen for horse-radish peroxidase in enzyme immunoassay. J Immunoassay 1981, 2: 187-204.

22. Soria J, Soria C, Boucheix C, Mirshahi M, Perrot JY, Bernadou A, Samama M. Immunochemical defferentiation of fibrinogen, fragment D or E, and cross-linked fibrin degradation products using monoclonal antibodies. In Haverkate F, Henschen A, Nieuwenhuizen W, Straub (eds): Fibrinogen- Structure, Functional Aspects, Metabolism, vol 2. Berlin, Walter de Gruyter, 1983, p 227-233.

CHAPTER III

EFFECTS OF ANTIFIBRIN MONOCLONAL ANTIBODY Y22 AND FRAGMENTS THEREOF ON SOME PROPERTIES OF FIBRIN

Introduction

In the final stage of the activation of the coagulation system, the soluble plasma protein fibrinogen is converted into insoluble fibrin by the action of thrombin. Thrombin cleaves the fibrinopeptides A (FPA) from the amino-terminal ends of the two fibrinogen Aα-chains [1]. The resulting new amino-terminal ends of the fibrin α-chains constitute polymerization sites by which fibrin monomers (fibrin I or desAA fibrin) aggregate to form so-called protofibrils, which are two stranded polymers [2]. This linear assembly continues until protofibrils of about 600 nm in length are formed. At that point lateral association between adjacent protofibrils occurs [2], which results in the formation of thicker fibres. Removal of fibrinopeptides B (FPB) by thrombin enhances the rate and extent of lateral association of protofibrils but is not required for polymerization [3]. Interfiber connections result in a three-dimensional network of fibrin, the fibrin gel, which is subsequently stabilized by formation of crosslinks (iso-peptide bonds) between fibrin subunits by the action of activated factor XIII, a transglutaminase.

Monoclonal antibody Y22, of IgG1 isotype with κ-light chains, is directed against a conformation dependent epitope in the D-domain of fibrin. Since a polymerization site is located in the D-domain of fibrin [4], we assessed the effect of Y22 and its F(ab)$_2$ and Fab-fragments on fibrin polymerization.

The D-domain of fibrin is also involved in the stimulation of plasminogen activation by tissue-type plasminogen activator (t-PA) [5]. Therefore, we also studied the effect of Y22 and its $F(ab)_2$- and Fab-fragments on this property of fibrin.

Materials

Papain was obtained from Sigma, St. Louis, USA; peroxidase labelled goat antimouse Fab (GAM-Fab/PO) was obtained from Nordic, Tilburg, The Netherlands. FITC labeled goat-antimouse antiserum was purchased from Taco Inc., Burlingame, USA. Anti-FITC IgG1 monoclonal antibody was a gift from Dr. J.J. Haaijman, Medical Biological Laboratory TNO, Rijswijk, The Netherlands.

Bovine thrombin was obtained from Leo, Ballerup, Denmark. The synthetic peptide H-Glycyl-L-Propyl-L-Arginyl-L-Proline (Gly-Pro-Arg-Pro) was kindly provided by Dr. G. Van Dedem, Diosynth, Oss, The Netherlands. The chromogenic substrate S-2251 (H-D-valyl-L-leucyl-L-lysine-p-nitroanilide dihydrochloride) was obtained from KabiVitrum Stockholm, Sweden; 3,3',5,5'-tetramethylbenzidine (TMB) from Aldrich Chemical Co., Milwaukee, USA. Plasminogen and two-chain t-PA were gifts from Drs. D. Traas and J. Verheijen respectively, Gaubius Institute TNO, Leiden, The Netherlands.

Fibrinogen was purified as described by Van Ruyven et al. [6]. Fibrin monomers were produced and purified as described by Haverkate et al. (7).

Methods

Preparation of $F(ab)_2$ and Fab-fragments of Y22

Digestion of antifibrin Y22 or of a control MoAb (anti-FITC IgG1) by papain was carried out by a method adapted from Parham et al. [8]. Y22 was dissolved in phosphate-buffered saline (PBS, pH 8.0) containing 10 mM cysteine and 2 mM EDTA. Papain (5% w/w) was added to the solution, the mixture was flushed

with nitrogen and incubated for 2 hours at 37°C. The amount of papain needed to obtain predominantly F(ab)$_2$-fragments had been determined empirically. Fab-fragments were obtained by a second addition of papain (5% w/w) and cysteine/EDTA-solution to the F(ab)$_2$-mixture and incubation for an additional 2 hours at 37°C. Digestion was stopped by addition of 50 mM Iodoacetamide. The mixture was passed over a protein-A-sepharose column to remove undigested Y22 and Fc-fragments. PBS (pH 8.0) was used as eluting buffer.

F(ab)$_2$ and Fab-fragments were separated by FPLC (Pharmacia, Uppsala, Sweden) on a Superose-12 column, using 0.15 M NaCl as eluent. Purity of the fragments was assessed by SDS-PAGE and FPLC.

Assessment of immunoreactivity of antibody fragments

The reactivity of the Fab and F(ab)$_2$-fragments of Y22 was assessed by enzyme immunoassay. Wells of microtiter plates were coated with fibrinogen (10 µg/ml in PBS, 120 µl/well) and incubated for 16 hours at 4°C. After washing with PBS containing 0.05% Tween 20 (PBS/Tween 20), the wells were treated with thrombin (0.01 NIH units/ml in 0.15 M NaCl, 100 µl/well). After incubation for 30 min at room temperature, the wells were washed with PBS/Tween 20. Ten-fold serial dilutions of Y22, Fab or F(ab)$_2$-fragments in PBS/Tween 20 were added and incubated for 30 min at room temperature. After washing with PBS/Tween 20, peroxidase conjugated goat antimouse anti-Fab Ig (7S) was added and incubated for 30 min at 37°C. After washing with PBS/Tween 20, a mixture of 3,3',5,5'-tetramethylbenzidine (TMB) and H_2O_2 was added [9]. After 5 min, the reaction was stopped by addition of 100 µl 1 M sulphuric acid and the absorbance at 450 nm was read using a multichannel spectrophotometer.

Thrombin time test

The effects of Y22 and its fragments on the clotting of human fibrinogen in plasma were determined using a modified thrombin time test, described by Haverkate et al. [4]. To 100 µl citrated plasma in plastic tubes, 300 µl of antibody (or fragment) solution of varying concentrations in 0.15 M NaCl was added.

After incubation for 5 min at 37°C, 100 µl of a thrombin solution in 0.15 M NaCl (6 NIH/ml, 0°C) was added. The tubes were placed in a coagulometer (Amelung GmbH, Lemgo, W. Germany) and the clotting time was recorded. In control experiments, non-related IgG1 MoAb (anti-FITC) and its fragments were used. The unbound fraction of antibody or fragments in the supernatant serum was determined by the enzyme immunoassay described above.

Transmission electronmicroscopy (TEM) studies

The effect of Y22 and its fragments on the assembly of fibrin fibres was studied by TEM. To 1 ml citrated plasma (fibrinogen concentration 2 mg/ml), 500 µg of Y22 or its fragments (in 300 µl 0.15 M NaCl) or a control antibody was added. The mixture was clotted by addition of thrombin (100 NIH units) and $CaCl_2$ (20 µl, 1 M) and incubated at 37°C for 30 min. Small fragments of the clots (approximately 1 mm³ in size) were fixed in formalin (2% in PBS). Post-fixation was done using formalin (4%) and glutaraldehyde (2%) in PBS. After dehydration with alcohol, the clots were embedded in epoxy resins and 100 nm thick sections were made on an ultramicrotome (LKB III). Contrast staining was obtained using uranyl-acetate (0.25% in 0.1 M acetate, pH 6.2) and lead-citrate (0.4% in distilled water). The sections were examined in a transmission electronmicroscope (JEOL, type 100 CX).

Scanning electronmicroscopy (SEM) studies

To 1 ml citrated whole blood, 500 µg of Y22, a control MoAb or their fragments (in 300 µl 0.15 M NaCl) was added. The mixture was clotted by addition of thrombin (100 NIH units) and $CaCl_2$ (20 µl, 1 M) and incubated at 37°C for 30 min. Small fragments of the clots (approximately 1 mm³ in size) were fixed in formalin (4%) and glutaraldehyde (2%) in PBS. After dehydration with alcohol, the fragments were dried to critical point (Polaron E 3000) using liquid CO_2. After evaporation (Polaron SEM coating unit E 5100), the fragments were examined in a scanning electronmicroscope (JEOL, T 200).

<u>Effects on the fibrin-induced rate-enhancement of the plasminogen activation
catalyzed by t-PA</u>

The effect of Y22 or its fragments on t-PA catalyzed activation of plasminogen
in the presence of fibrin was examined in a spectrophotometric assay, essentially
as described by Verheijen [10].

To wells of microtiter plates, 25 µl of a fibrin monomer solution (45 µg/ml in
20 mM acetic acid) was added. To this solution was added 225 µl of a mixture
composed of 25 µl plasminogen (1.1 µM), 100 µl S-2251 substrate (0.75 mM),
25 µl t-PA (1 U/ml), 50 µl Tris/Tween 20 (0.1 M, 0.1%) and 25 µl of Y22 or its
fragments in Tris/Tween. At different times, the optical density at 405 nm was
read using a multichannel spectrophotometer (Flow Laboratories). In control
experiments, Y22 was replaced by an anti-FITC MoAb or fragments thereof.

Results

F(ab)$_2$ and Fab-fragments of Y22 were produced by digestion of Y22 by papain
and purified by a combination of protein A Sepharose chromatography and
FPLC. The apparent molecular weights of Y22, F(ab)$_2$ and Fab were 158, 110
and 58 kD respectively. The immunoreactivity of the F(ab)$_2$ and Fab-fragments
as assessed by enzyme immunoassay (EIA) is depicted in Figure III.1. On a
molar basis F(ab)$_2$ appeared to be approximately as reactive as intact Y22. Fab-
fragments were at least one order of magnitude less reactive in this system.

Fab-fragments of Y22 bind to fibrin since no Fab-fragments were detectable
(with the EIA described above) in the supernatant serum of a clot formed in the
presence of Fab-fragments. They do not have an effect on the thrombin time.
F(ab)$_2$- fragments of Y22 interfere with clotting of plasma, but the strongest
effect is observed with intact Y22 (Fig. III.2). At concentrations exceeding those
depicted in Fig. 2, clotting was completely inhibited by Y22. At concentrations
of Y22 <1 µmol/l a slight acceleration of clotting was observed. A control
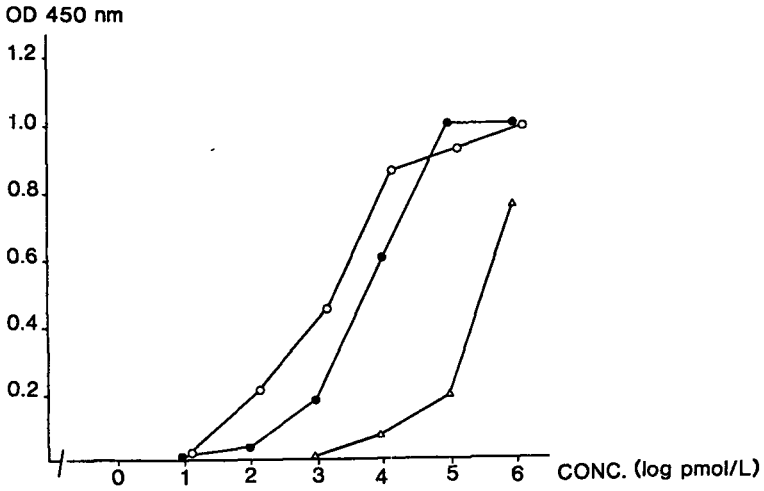MoAb (anti-FITC) and its F(ab)$_2$ and Fab-fragments had no effect.

Fig. III.1 *Immune reactivity of intact Y22 (●), F(ab)₂-fragments (○) and Fab-fragments (Δ) in an EIA (details in Materials and Methods section).*
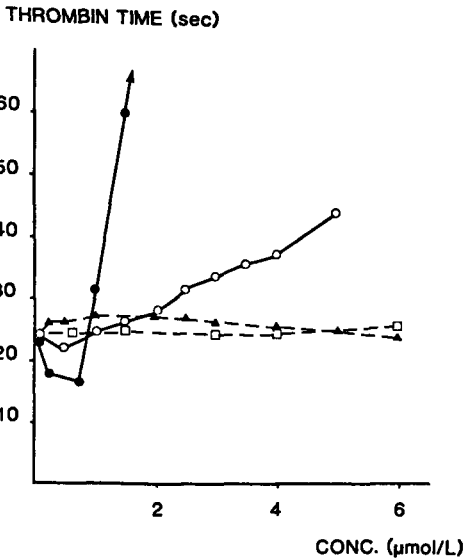

Fig. III.2 *Effects of Y22(●), F(ab)₂-fragments (○) and Fab-fragments (▲) on clotting of citrated plasma in a thrombin time test as compared with a control MoAb (□).*

The effect of Y22 on fibrin formation is evident from the transmission electronmicroscopy (TEM) studies (Figure III.3). In the control experiment (Fig. III.3A), clotting of plasma resulted in formation of long, thick fibrin fibres. However, when Y22 was added to the plasma (Fig. III.3B), only small and apparently thinner fibres were formed. In TEM no effect of Fab-fragments on fibrin structure was observed.
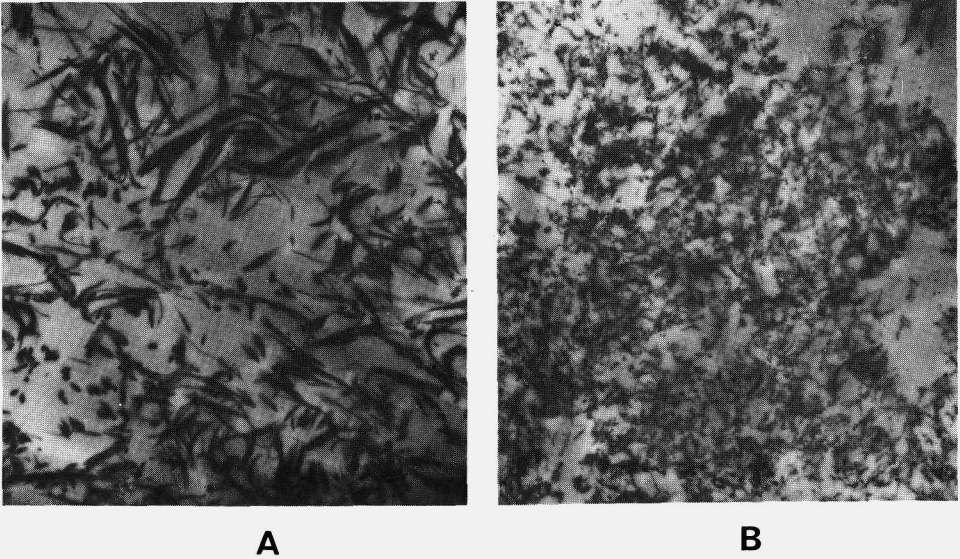

A   B

Fig. III.3. *Transmission electronmicroscopy studies of plasma clots, formed in the presence of a control antibody (A) and Y22 (B).*

The effect on fibrin formation in clotting whole blood was studied in scanning electronmicroscopic (SEM) images. In a control experiment (Fig. III.4A), a fibrin network appeared to be formed which consisted of thick interconnected fibrin fibres. Blood cells were trapped in the meshes of the network. In the presence of Y22 a loose, "foamy" fibrin structure resulted (Fig. III.4B). As in TEM, no effects of Fab-fragments on fibrin structure were observed in SEM.
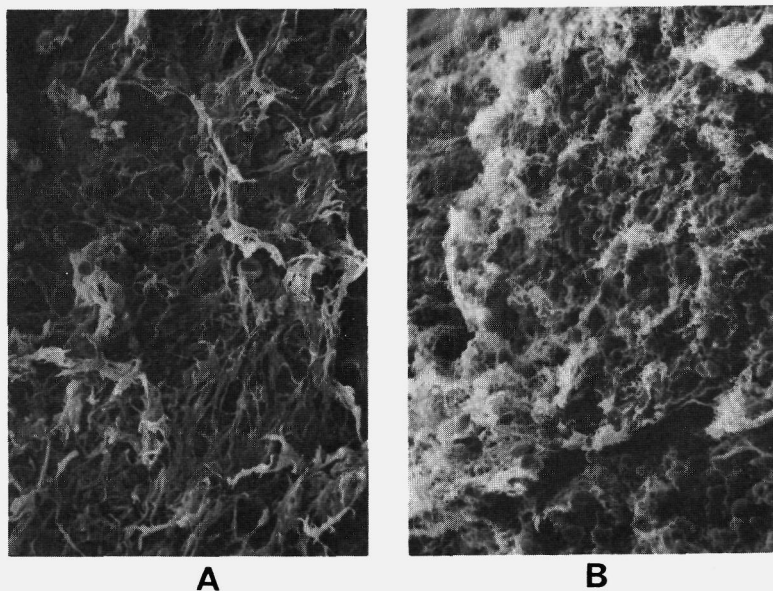
Fig. III.4. *Scanning electronmicroscopy of whole blood clots, formed in the presence of a control antibody (A) and Y22 (B).*

The effect of Y22 on the acceleration of t-PA-catalyzed plasminogen activation by fibrin was assessed using the parabolic rate assay as described by Verheijen et al. [10]. Both intact Y22 and a control MoAb had no significant effect on the stimulating capacity of fibrin (Figure III.5). Y22-F(ab)$_2$-fragments slightly and Fab-fragments strongly decreased the fibrin-induced stimulation of t-PA-catalyzed plasminogen activation at high concentrations. F(ab)$_2$ and Fab-fragments of the control antibody had no effect (not shown).

Discussion

In this study we investigated the effects of Y22 and its F(ab)$_2$ and Fab-fragments on the polymerization of fibrin, and on the rate-enhancing effect of fibrin in the
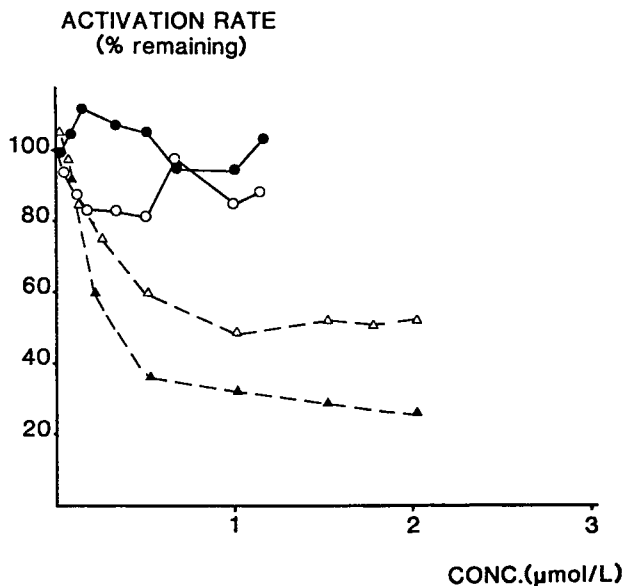
ACTIVATION RATE
(% remaining)

CONC.(μmol/L)

Fig. III.5. *Effects of Y22 (●), F(ab)₂-fragments (Δ) or Fab-fragments (▲) on t-PA catalyzed activation of plasminogen in the presence of fibrin. Activation rates are expressed as % of the system with fibrin but without Y22 or fragments. As a control, a non-related Moab (O) was used.*

t-PA catalyzed plasminogen activation. The rationale behind this was, that (as we had found before) Y22 has its epitope in the D-domain of fibrin, which comprises a polymerization site [4] and a site involved in the aforementioned rate-enhancing effect [5].

We found that Y22-Fab-fragments bind to forming and preformed fibrin. This binding, however, does not have any effect on the thrombin time of plasma. Y22-F(ab)₂- and especially intact Y22 have a strong effect on the thrombin time. This suggest that the more bulky appendages that resut from the binding of Y22 and F(ab)₂ cause steric hindrance of the aggregation of fibrin monomers, and that binding as such of the Y22-Fab moieties does not interfere with fibrin formation.

Alternatively, the bivalent Y22 and F(ab)$_2$-fragments may mask a binding site formed by two linearly aligned D-domains of adjacent fibrin molecules. The monovalent Fab-fragments may not be able to mask such a putative site, which does not seem to be directly related to the epitope.

It is interesting to note that an acceleration of clot formation occurs at Y22 concentrations <1 µmol/l, where the molar ratio of fibrin/Y22 is more than 1. The observed acceleration of clot formation could be due to bridging of fibrin monomers by (bivalent) Y22 molecules under those conditions. At higher Y22 concentrations this bridging action would be lost since only one binding site of Y22 could be saturated.

Our EM findings appear to confirm the above findings, i.e. Y22, when present in clotting plasma or blood, gives rise to shorter and apparently thinner fibrin fibrils, whereas Fab-fragments have no apparent effect on the fibrin structure. We found by EIA that Y22-Fab-fragments bind to fibrin. This indicates that, although the Fab-frments bind to fibrin, they are not bulky enough to interfere with fibrin polymerization. Y22-F(ab)$_2$-fragments take an intermediate position. A control antibody and its F(ab)$_2$- and Fab-fragments were without effect

In Chapter II is decribed that Y22 also binds to the polymerized, crosslinked fibrin of thrombi. Therefore, our findings suggest that the epitope of Y22 is not the polymerization site in the fibrin D-domain itself, but may be in the direct vicinity of the latter.

An apparently confusing observation was made when we studied the effect of Y22 and its fragments on the fibrin-induced acceleration of the t-PA catalyzed plasminogen activation. Y22 has no effect, whereas Fab-fragments suppress the enhancing effect dramatically.Fab-fragments of a control antibody had no effect (Fig. III.6) It has been reported in the literature [11] that polymerization contributes to the rate-enhancing effect of fibrin. This does not seem to be supported by our findings with Y22, which inhibits polymerization but has no effect on the enhancement. Fab-fragments on the other hand, which do not inhibit polymerization, strongly inhibit the rate-enhancement.

It seems from our results that the Y22 epitope is not in the site involved in the rate-enhancement, since even the Fab-fragments, which have the strongest effect, do not annihilate the rate-enhancement completely. The epitope may, however, be in the close vicinity of the rate-enhancing site. We cannot preclude that a limited extent of fibrin aggregation occurs in the used assay system. If this occurs, Y22-Fab-fragments may be incorporated in the partly polymerized fibrin whereas the more bulky Y22 molecules are not.

Further studies are needed to investigate these possibilities.

References

1.   Blombäck B. Studies on the action of thrombotic enzymes on bovine fibrinogen as measured by N-terminal analysis. Ark Kemi 1958, 12: 321-335.

2.   Hantgan RR, Hermans J. Assembly of fibrin: a light scattering study. J Biol Chem 1979, 254: 11272-11281.

3.   Shen LL, Hermans J, McDonagh J, McDonagh RP. Role of fibrinopeptide B release: comparison of fibrins produced by thrombin and ancrod. Am J Physiol 1977, 232: 629-633.

4.   Haverkate F, Timan G, Nieuwenhuizen W. Anticlotting properties of fragments D from human fibrinogen and fibrin. Eur J Clin Invest 1979, 9: 253-255.

5.   Voskuilen M, Vermond A, Veeneman GH, van Boom JH, Klasen EA, Zegers ND, Nieuwenhuizen W. Fibrinogen lysine residue A 157 plays a crucial role in the fibrin-induced acceleration of plasminogen activation catalyzed by tissue-type plasminogen activator. J Biol Chem 1987, 262: 5944-5946.

6.   Van Ruijven-Vermeer IAM, Nieuwenhuizen W. Purification of rat fibrinogen and its constituent chains. Biochem J 1978, 169: 653-658.

7   Haverkate F, Timan G. Preparation of highly purified bovine fibrin plates. In: Davidson JF, Samama MM, Desnoyers PC (eds). Progress in

Chemical Fibrinolysis and Thrombolysis, vol.2. New York, Raven Press 1976, p. 67-71.

8. Parham P, Androlewicz MJ, Brodsky FM, Holmes NJ, Ways JP. Monoclonal antibodies: purification, fragmentation and application to structural and functional studies of class I MHC antigens. J Immunol Methods 1982, 53: 133-173.

9. Bos ES, van der Doelen AA, van Rooy N, Schuurs AHWM. 3,3',5,5'-Tetramethylbenzidine as an Ames negative chromogen for horseradish peroxidase in enzyme immunoassay. J Immunoassay 1981, 2: 187-204.

10. Verheijen JH, Nieuwenhuizen W, Wijngaards G. Activation of plasminogen by tissue activator is increased specifically in the presence of certain soluble fibrin(ogen) fragments. Thromb Haemost 1982, 27: 377-385.

11. Suenson E, Peterson LC. Fibrin and plasminogen structures essential to stimulation of plasmin formation by tissue-type plasminogen activator. Biochim Biophys Acta 1986, 870: 510-519.

CHAPTER IV

LABELLING OF Y22 WITH Tc-99m: METHOD AND QUALITY

Introduction

For immunoscintigraphic purposes, the decision concerning which radionuclide is to be used for radiolabelling of a given monoclonal antibody is based upon the following criteria [1,2]: 1) physical characteristics of the radionuclide: half-life ($T_{1/2}$), photon-energy; 2) chemical reactions to be used for incorporating the radionuclide into the antibody, the effects of labelling on the immunoreactivity of the antibody and stability of label attachment in vivo; 3) target and kinetics of biodistribution of the antibody; 4) radiation dose expected to be delivered to the target and other tissues of the patient.

It is desirable that the radionuclide emits photons of adequate energy for achieving the resolution needed for the imaging studies, while giving as small a radiation burden as possible. The half-life of the photon emitter should be as short as possible, but has to be compatible with the biodistribution patterns of the monoclonal antibody and its accumulation in the target tissue. Table IV.1 shows some characteristics of the radionuclides most commonly used for immunoscintigraphic purposes.

Of these radionuclides, Tc-99m has the best decay characteristics, given its short half-life and its photon-energy (ideally detectable with an Anger gamma camera). Moreover, it is a Mo-99m-generator product and is readily available and essentially carrier-free.

Table IV.1 *Lederers' Table of Isotopes [3]*

Nuclide	$T_{1/2}$ (hours)	photon energy (keV)
I-131	193	364
I-123	13	159
In-111	68	171/247
Tc-99m	6	140

However, an important issue to be considered in immunoscintigraphy, is the time required to obtain suitable target-to-background ratios after injection of the antibody. In other words, a short $T_{1/2}$ of the radiolabel may be disadvantageous if a long time is required for the antibody to accumulate in the target tissue. In several studies using labelled MoAb's for the detection of primary and metastatic tumor sites, it took at least 20 hours (and even days) to localize the final target [4]. Avidity of the labelled antibody is an important parameter for the rate of binding to the antigen in the target tissue. But biodistribution patterns and kinetics are also critical in this sense. In case of tumour imaging, the labelled antibody has to be transferred via the vascular space in order to reach the cells of the target tissue. The rate-limiting step appears to be the transport of the radiolabelled, lipid-insoluble antibody from the blood via the endothelial lining of the vessel into the extracellular fluid of the target tissue. On the one hand, this transport process may be enhanced in inflamed or cancerous areas as compared with normal tissue. On the other hand, the centre of many tumours is necrotic and avascular, and accumulation of antibody is often limited to the surface of the tumour.

Finally, the rate of clearance of the radiolabelled antibody from the circulation is important for visualization of accumulated antibody, since it determines the background activity. Anyhow, the radionuclide to be selected must retain a sufficient activity at the time an image is to be taken. Therefore, I-131 and In-111 are most frequently used in radiolabelling antibodies for tumour detection, although good results have also been reported with Tc-99m labelled MoAb's [5]. In the case of thrombus imaging, however, the target object is already present in the blood stream and, in theory, readily accessible to the antibody. High target-to-background ratios should be feasible within a short time after injection of the labelled antibody, and visualization of the thrombus is theoretically only dependent on the avidity of the antibody and its clearance from the circulation. We therefore decided to label our monoclonal antifibrin antibody with the radionuclide Tc-99m according to a method developed at the Division of Nuclear Medicine (Department of Diagnostic Radiology) of the University Hospital Leiden. In this chapter, this labelling procedure is briefly described and experiments are presented which show the quality of the labelling procedure and its effects on immunoreactivity of the antifibrin monoclonal antibody Y22.

Methods

Tc-99m labelling procedure
This labelling method consists of two steps. Briefly, in the first step N,N-dimethylformamide (DMF) was reacted with Technetium-99m pertechnetate under acidic conditions for 4 hours at 140°C to form a reactive intermediate Tc-99m-compound. In the second step, this intermediate compound and the MoAb were reacted at pH7, for one hour at 37°C to produce the Tc-99m labelled antibody. Non-bound low molecular weight radioactive contaminants were removed by size exclusion chromatography on a 5x1 cm Sephadex G50 (Pharmacia, Uppsala, Sweden) column. The labelling yield was assessed by precipitation of the labelled protein with 20% trichloroacetic acid (TCA).

Assessment of integrity of antibody Y22 after labelling with Tc-99m

a) *Paper electrophoresis of labelled antibody*
The behavior of labelled Y22 on paper electrophoresis was assessed before and after molecular sieving on a 5x1 cm Sephadex G50 column. Samples were applied on Whatman paper no. 1 and electrophoresed in 0.1 M acetate buffer of pH 4.8 for 40 min. at 4°C with 300 V. Thereafter, an autoradiogram was made of the Whatman paper.

b) *HPLC-analysis of labelled antibody*
Determination of protein-bound and non-protein-bound radioactivity before and after gelpermeation chromatography on a Sephadex G50 column (see above) was done, using a HPLC system (LKB) with a Superose-12 column (Pharmacia, Uppsala, Sweden) and an on-line NaI(Tl)-crystal gamma detection system.

Assessment of stability of label attachment in vitro.
Stability of the Tc-99m binding to Y22 was assessed by incubation of the labelled proteins with excess HSA for 24 hours at 37°C. At different times of incubation, samples were taken and analysed on the HPLC to determine possible transfer of the label from Y22 to HSA.

Effect of Tc-99m labelling on immunoreactivity of Y22
To assess a possible effect of labelling technique on the functional activity of the monoclonal antibody, two assays were performed:

a) *Double-sandwich Immuno Assay (EIA)*
In this assay we examined the antigen binding capacity of the labelled antibody compared to that of the unlabelled antibody. This assay is an adapted version of the assay, described in Chapter II. Briefly, wells of microtiter plates were coated with rabbit antimouse Ig. Dilutions of labelled or unlabelled Y22 or its F(ab)$_2$

and Fab-fragments were added and fibrin monomers were used as antigens. Finally, a horseradish peroxidase conjugate of a mix of IgG's from polyclonal rabbit antisera against fibrin, fibrinogen and degradation products was added. Reactivity of the antibody was demonstrated by spectrophotometric assessment of the conversion of a TMB-substrate by the horseradish peroxidase catalyzed reaction.

b) *Binding of labelled antibody at antigen excess*

To assess whether the small fraction of antibody that actually carries a label is still capable of binding the antigen, another assay was developed. In this assay we measured the fraction of labelled antibody that could be incorporated into fibrin clots at various antigen concentrations. To aliquots of 1 ml of various fibrinogen dilutions in a 1% bovine serum albumin (BSA) solution in PBS, 2-5 μg of labelled Y22 was added. After incubation for 1 hour at 37°C, thrombin was added at a ratio of 1 NIH units thrombin per mg fibrinogen. After incubation for 1 hour at 37°C, the clots were washed twice with 1% BSA/PBS. The percentage of clot-bound radioactivity was measured in an auto-gamma wellcounter.

We compared the reactivity of Y22 after labelling with Tc-99m according to our technique with that after labelling with established procedures such as radio-iodination, direct Tc-99m labelling after pretinning, and In-111 labelling via chelation with diethylenetriaminepentaacetic acid (DTPA).

- Radioiodination was carried out according to Fraker and Speck [5]. To a vial, pre-coated with 100 μg tetra-chlorodiphenylglycouril (Iodogen, Pierce, Rockford, Ill., USA), 4 MBq I-123 and 100 μg of Y22 in 1 ml of 0.1 M borate buffer (pH 8.0) were added and incubated for 30 minutes at room temperature.

- The direct labelling with Tc-99m was performed as described by Rhodes et al. [6]. Y22 (600 μg/ml) was pretinned for 24 hours in a

phtalate/tartrate buffer of pH 5.6 with 2 mM $SnCl_2$ and labelled by addition of TcO_4^- .

In-111 labelling was performed as described by Hnatowich et al. [8] after introduction in Y22 of a diethyleneaminepenta-acetic acid (DTPA) group by means of the bicyclic anhydride of DTPA at a molar ratio of 1:1. The DTPA-coupled protein was then complexed with In-111-chloride in a 0.5 M acetate buffer (pH 6).

In all labelling procedures, free label was removed by gelchromatography on a 5 x 1 cm Sephadex G50 column.

<u>In vitro binding of Tc-99m labelled Y22 to clots</u>

a) *Binding to preformed plasma clots*
To aliquots of 1 ml plasma or serum containing 1000 KIU aprotinin (Trasylol, a protease inhibitor), 10 µg of Tc-99m labelled Y22 was added. In control experiments 10 µg of Tc-99m-HSA, Tc-99m-fibrinogen or Tc-99m-non-related MoAb (anti-FITC) was used. Plasma clots (formed by clotting 1 ml citrated plasma with 2 NIH units of thrombin) were added to the plasma or serum and incubated at 37°C. After 24 hours the clots were removed, washed and counted in an auto-gamma wellcounter.

b) *Binding to aggregating fibrin monomers*
To assess the binding of the labelled antibody to aggregating fibrin, an assay was developed, based on the pH dependence of the solubility of fibrin monomers. To aliquots of 1 ml plasma or serum, containing 1000 KIU aprotinin, 5 µg of Tc-99m-Y22, 5 µg of Tc-99m control MoAb or 10 µg of Tc-99m-fibrinogen was added. After incubation for 30 minutes at room temperature, 250 µl of a solution containing 500 µg fibrin monomers in 0.02 M acetic acid (pH 3.5) was added. The resulting pH neutralisation of the fibrin monomer solution, caused

by the mixing with plasma or serum, induced polymerization of the monomers and after incubation for 30 minutes at 37°C a clot had formed. After centrifugation at 10.000 g for 10 minutes, the total radioactivity was measured in a gamma counter. A 200 µl sample of the supernatant was then taken and counted separately. Total radioactivity bound to the clot was calculated from the activity in the 200 µl sample and the known total volume.

Results

Under standard conditions of the Tc-99m labelling procedure, Y22 could be labelled with a yield of approximately 60%, as was measured after precipitation with 20% trichloroacetic acid. Distribution of radioactivity after paper electrophoresis of the Tc-99m labelled Y22 is shown in Fig. IV.1. Three spots of radioactivity can be distinguished (lane A): one large spot representing the antibody-bound Tc-99m, another spot at the other end representing free pertechnetate, and one between these two, possibly of the intermediate compound. Gelchromatography on a Sephadex G50 column effectively removed radioactivity that was not incorporated into the antibody (lane B).

$^{99m}TcO_4^-$ $^{99m}Tc-Y22$

A

B
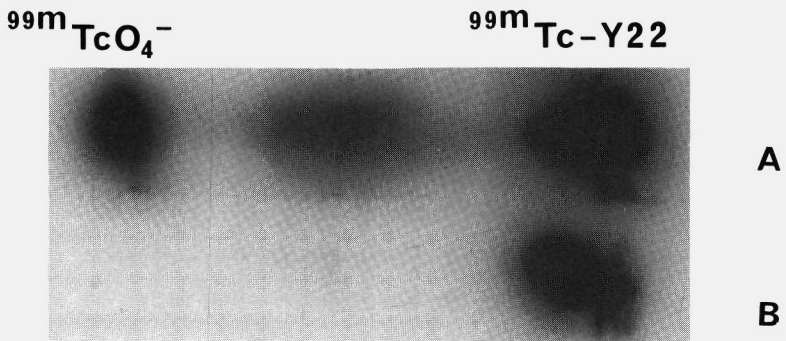
Fig. IV.1. *Paper electrophoresis of Tc-labelled Y22 before (A) and after (B) purification over a Sephadex G-50 column*

HPLC-radiochromatography also showed that, after passage of Tc-99m-Y22 over a G50 column, only Y22-bound radioactivity remained and that no extra activity peak could be observed (Fig. IV.2). In a control experiment, unlabelled Y22 eluted from the column at the same position as Tc-99m labelled Y22 (not shown).
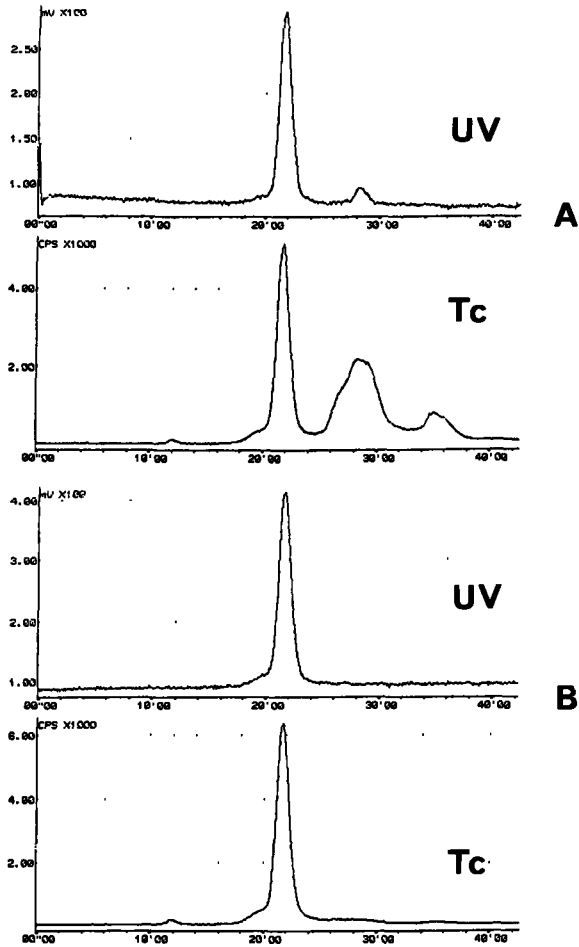

Fig IV.2. *HPLC-pattern of Tc-99m labelled Y22 before (a) and after (b) gelchromatography. The upper figures represent the protein distribution as asessed by UV-absorbance (UV), the lower figures show the distribution of radioactivity (Tc)*

Fig. IV.3 shows the distribution of radioactivity after HPLC-chromatography over a Superose 12 column of a mixture of Tc-99m-Y22 with HSA at the start of incubation (A) and after incubation for 24 hours (B). No transfer of label could be seen in these experiments.
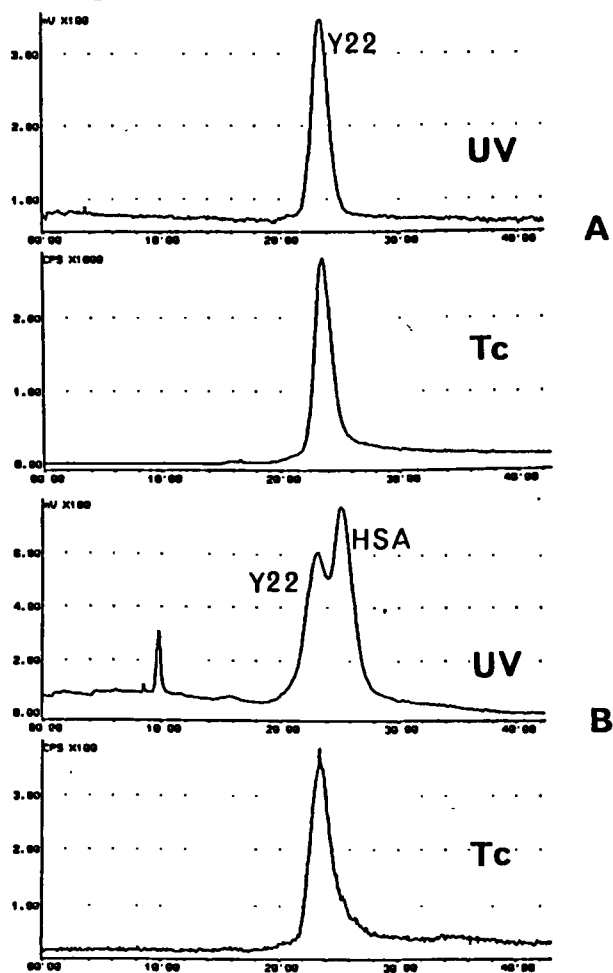
Fig. IV.3. *HPLC-analysis of Tc-99m labelled Y22 before (A) and after incubation with HSA for 24 hours. The upper figures represent the protein distribution as assessed by UV-absorbance (UV), the lower figures show the distribution of radioactivity (Tc)*

The effect of the labelling procedure on the immunoreactivity of Y22 was assessed by double sandwich EIA (Fig. IV.4). The functional activity of the total amount of intact antibody was not significantly diminished after labelling with Tc-99m. The same result was true for F(ab)$_2$ and Fab-fragments of Y22 (not shown).
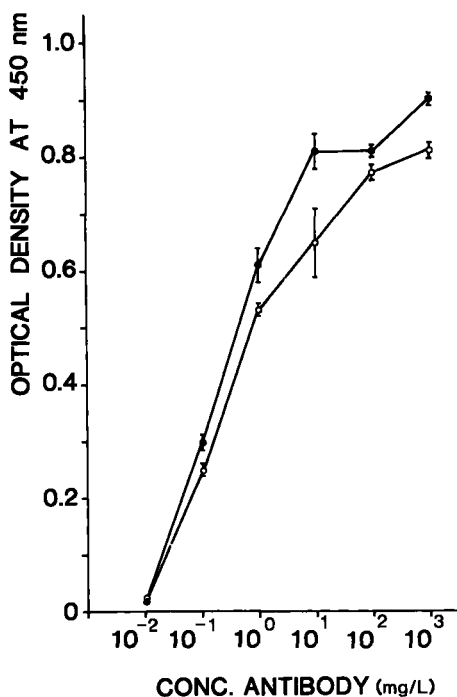
Fig. IV.4 *Double sandwich enzyme immunoassay of Y22. Absorbance of various Y22 dilutions at a fixed antigen (fibrin) concentration. The non-labelled antibody (●) in comparison with Tc-99m labelled Y22 (○). Absorbance is a measure for the antigen-antibody reactivity*

At large antigen excess, 99% of Y22 labelled with Tc-99m by the DMF-method was incorporated into fibrin clots (Fig. IV.5). This result was at least as good as the results obtained after radiolabelling with I-123, In-111 or Tc-99m after pretinning. Direct labelling of Y22 after pretinning resulted in 85%

incorporation of the labelled antibody into the clots. However, when the antibody preparation was allowed to stand for 24 hours after labelling and G50-gelchromatography, only 50% of radioactivity was recovered in the clot. This time dependent decrease in binding capacity was not observed after Tc-99m labelling using the DMF method (not shown).
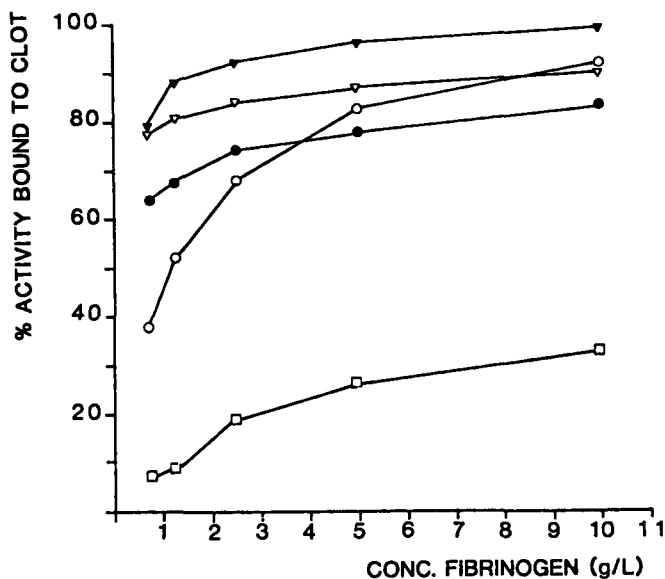

Fig. IV.5 *Immunoreactivity of labelled Y22 as tested by incorporation percentages of radioactivity in fibrin clots formed from fibrinogen solutions with increasing concentrations. Results of our Tc-99m method (▼), the I-123-Iodogen labelling (○), the Tc-99m-pretinning (▽) and the In-111-DTPA chelation (●). As control, anti-FITC MoAb was used, labelled with Tc-99m according to our method (□)*

Table IV.1 shows a 3-4 times higher binding of Tc-99m Y22 (DMF method) to preformed, 24 hours old plasma clots than of Tc-99m-HSA, Tc-99m-fibrinogen

or Tc-99m-control MoAb, after incubation for 24 hours in plasma. After incubation in serum, approximately the same amount of Tc-99m-Y22 was bound to the clots.

When soluble fibrin monomers were allowed to polymerise in a plasma milieu in the presence of Tc-99m-Y22, 70% of the antibody was bound to the aggregated fibrin. Less than 10% of Tc-99m-fibrinogen, Tc-99m-HSA or Tc-99m control MoAb was bound under the same conditions. When serum was used instead of plasma, the same amount of Y22 was bound to the aggregated fibrin. In serum, 40% of Tc-99m-fibrinogen was bound to the clots as opposed to less than 10% of the other control proteins (not shown).

Table IV.2 *Binding of Tc-99m-Y22, Tc-99m-fibrinogen, Tc-99m-control MoAb and Tc-99m-HSA to clotting purified fibrin monomers (after 30 minutes) and preformed plasma clots (after 24 hours) in plasma milieu (average of two experiments, and individual observations in parenthesis)*

Protein added	% bound to	
	Aggregating fibrin	Preformed clots
	mean	mean
Tc-99m-Y22	68.3 (69.9, 66.8)	22.2 (19.6, 24.8)
Tc-99m-contr. MoAb	7.5 (8.5, 6.6)	6.7 (8.5, 4.9)
Tc-99m-fibrinogen	1.4 (0.7, 2.1)	6.3 (6.6, 6.0)
Tc-99m-HSA	0.1 (0.1, 0.2)	4.1 (5.3, 2.9)

Discussion

Because of its short half-life (6 hours) and its photon energy (140 keV), Tc-99m is a frequently used radionuclide in nuclear medicine. For immunoscintigraphic detection of tumours, however, it is not always possible to use Tc-99m as a radiolabel, since in several studies tumour uptake of the monoclonal antibody was quite slow in comparison to the half-life of Tc-99m [4]. The rate-limiting step in the targeting of tumour tissue appeared to be the permeation of the labelled antibody from the blood stream into the extravascular compartment [2]. Thrombi, however, are present in the bloodstream and should therefore be more readily accessible to monoclonal antibodies such as antifibrin antibody Y22. For that reason we decided on using Tc-99m as radiolabel in our studies on the feasibility of Y22 for thrombus imaging (Chapters V and VI).

For protein-labelling with Tc-99m some methods have been described, but they have not been widely accepted. They all suffer from the inability to keep the radiolabel firmly attached to the antibody without deminishing the functional activity of the latter [9-14]. Therefore, we labelled Y22 with Tc-99m according to a newly developed two-step method using N,N-dimethylformamide. Under standard conditions, Y22 could be labelled with an efficiency of approximately 60% as assessed by TCA-precipitation. The remaining unbound radioactivity could be effectively removed by gelchromatography on a small Sephadex G50 column, as was shown by paperelectrophoresis and HPLC-analysis. It is essential to remove the radiolabel not attached to the antibody, since it may cause an elevated background upon scintigraphy (as will be shown in Chapter VI).

In vitro, no transfer of Tc-99m label could be observed when Tc-99m-Y22 was incubated with HSA for 24 hours. As will be shown in Chapter VI, experiments in rabbits indicated that binding of the Tc-99m label to Y22 is stable even in vivo, since no thyroid uptake or stomach activity was observed. Moreover, experiments in rabbits showed that Tc-99m labelled Y22 was cleared from the circulation at the same rate as Y22 labelled with I-125 according to the Iodogen method, a widely accepted technique. This observation also shows that no

detectable effects were caused to the protein by our Tc-99m labelling as compared with labelling with I-125 using the Iodogen method. Damaged antibody would have been cleared at a much higher rate.

Enzyme immunoassays showed that the immunoreactivity of Y22 and its Fab or F(ab)$_2$-fragments was not significantly affected by our labelling procedure. However, only a small fraction of the antibody is actually labelled and may be missed in the double-sandwich EIA. To test whether the immunoreactivity of the actually labelled antibody was diminished, the binding of Tc-99m-Y22 at antigen excess was assessed. Tc-99m labelling according to the DMF method resulted in 99% recovery of radiolabel in the fibrin clots. This result was at least as good as the figure obtained following I-125 labelling using the Iodogen method. Tc-99m labelling after pretinning resulted in a maximum of approximately 85% incorporation of label into the clots.

However, when the antibody labelled via the pretinning method was kept at 4°C for 24 hours and tested in this assay, only 50% of label was bound to the clots. This may either be due to loss of immunoreactivity of the antibody or to release of label. This phenomenon was not observed after Tc-99m labelling according to our DMF method, which is another indication of the stability of the Tc-99m coupling using DMF.

When preformed plasma clots were added to Tc-99m-Y22 containing plasma, about 25% of the label was bound after 24 hours of incubation, whereas only 5-10% of the labelled control proteins was bound.

When fibrin monomers were added to plasma containing Tc-99m labelled Y22, 70% of the labelled Moab's was bound to the aggregating fibrin. Less than 10% of labelled control proteins (including fibrinogen) was bound under the same conditions. This indicates a higher rate of binding of Y22 to forming, polymerising fibrin than to polymerized fibrin, in which the epitopes may be less easily accessible to Y22.

The binding of Tc-99m-Y22 must have occurred extremely rapidly, since aggregation of the fibrin monomers at neutral pH takes place within a few minutes. In serum, approximately the same amount of Tc-99m-Y22 was bound

to the fibrin. The finding that binding of Tc-99m-Y22 to clots in serum is not different from that in plasma milieu, indicates that fibrinogen, present in plasma, does not hamper the binding of Y22 to fibrin. The observed increase in binding of Tc-99m-fibrinogen in serum may be explained by the presence of residual thrombin activity in the serum.

In conclusion, the newly developed labelling method using DMF couples the radionuclide Tc-99m tightly to antifibrin Y22 without diminishing the functional activity of the antibody. Binding experiments with clots indicate that Tc-99m-Y22 binds both to preformed and forming clots and that it reacts more rapidly with forming clots.

References

1. Eckelman WC, Paik CH. Comparison of Tc-99m and In-111 labelling of conjugated antibodies. Nucl Med Biol 1986, 13: 335-343.

2. Wolf W, Sham J. Criteria for the selection of the most desirable radionuclide for radiolabelling monoclonal antibodies. Nucl Med Biol 1986, 13: 319-324.

3. Lederer CM, Shirley VS. Table of Isotopes. Wiley, New York, 1978.

4. Goodwin DA. Pharmacokinetics and antibodies (editorial). J Nucl Med 1985, 26: 1358-1362.

5. Buraggi GL, Callegaro L, Mariani G, Turrin A, Cascinelli N, Attili A, Bombardieri E, Ferno G, Plassio G, Dovis M. Imaging with 131I-labeled monoclonal antibodies to a high molecular weight melanoma-associated antigen in patients with melanoma: efficacy of whole immunoglobulin and its F(ab')$_2$ fragments. Cancer Res 1985, 45: 3378-3387.

6. Fraker PJ, Speck JC. Protein and cell membrane iodinations with a sparingly soluble chloroamide, 1,3,4,6,tetrachloro-3a,6a, diphenylglycouril. Biochem Biophys Res Commun 1987, 80: 849-857

7. Rhodes BA, Zamora PO, Newell KD, Valdez EF. Technetium-99m labelling of murine monoclonal antibody fragments. J Nucl Med 1986,

27: 685-693.

8.	Hnatowich DJ, Layne WW, Childs RL. The production and labeling of DTPA-coupled albumin. Int J Appl Radiat Isot 1982, 33: 327-332.

9.	Wong DW, Huang JT. Labeling of human immune gamma globulin with Tc-99m. Int J Appl Radiat Isot 1977, 28: 719-722.

10.	Khaw BA, Strauss HW, Carvalho A, Locke E, Gold HK, Haber E. Technetium-99m labeling of antibodies to cardiac myosin Fab and to human fibrinogen. J Nucl Med 1982, 23: 1011-1019.

11.	Wong DW, Dhawan VK, Tanaka T, Mishkin FS, Reese IC, Thadepalli H. Imaging endocarditis with Tc-99m-labeled antibody-an experimental study: concise communication. J Nucl Med 1982, 23: 229-234.

12.	Harwig SSL, Harwig JF, Coleman RE, Welch MJ. In vivo behavior of Tc-99m-fibrinogen and its potential as a thrombus imaging agent. J Nucl Med 1976, 17: 40-46.

13.	Hill PM. A rapid method for the preparation of stable Tc-99m-urokinase. Br J Radiol 1977, 50: 518-520.

14.	Kanellos J, Pietersz GA, McKenzie IFC, Bonnyman J, Baldas J. Coupling of the Technetium-99m-nitrido group to monoclonal antibody and use of the complexes for the detection of tumours in mice. J Natl Cancer Inst 1986, 77: 431.

CHAPTER V

SCINTIGRAPHIC DETECTION OF CLOTS IN VITRO

Introduction

In the previous chapter it was shown that Tc-99m labelled Y22 binds to plasma clots in a stationary system (i.e. in test tubes). To determine the scintigraphic implications of this clot-binding capacity of Tc-99m-Y22 and the effects of various environmental conditions of the clots on the up- take of Tc-99m-Y22 by the clots, we developed an in vitro circulation model. This model also enabled us to determine the kinetics of accumulation of antibody in the clots in a flow system: directly, by dynamic uptake studies on a gammacamera, and indirectly, by immunofluorescence microscopy of the clots after exposure to the circulating antibody.

Materials

Heparin was obtained from Leo, Pharmaceutical Products, Weesp, The Netherlands; hirudin from Sigma Chemical Company, St. Louis, USA. The synthetic peptide Gly-Pro-Arg-Pro was a gift from Dr. G. van Dedem at Diosynth, Oss, The Netherlands. Aprotinin (Trasylol) was purchased from Bayer, Mijdrecht, The Netherlands. Fluorescein-iso-thiocyanate (FITC) labelled goat-antimouse Ig was obtained from Tago Inc., Burlingame, USA. Fibrinogen was purified from human plasma as described by Van Ruijven et al.

[1]. Non-related MoAb anti-FITC IgG1 was kindly provided by Dr. J.J. Haaijman, Medical Biological Laboratory TNO, Rijswijk, The Netherlands.

Methods

Preparation of plasma

Human blood was collected in plastic tubes, containing 0.11 mol/l sodium citrate solution (1 vol per 9 vol blood), and centrifuged at 2300 g for 20 minutes at room temperature. The plasma was stored at -20°C.

Preparation of serum ("defibrinated plasma")

Serum was prepared by addition of thrombin (2 NIH/ml plasma) and calcium chloride (2 mM) to citrated plasma in plastic tubes. After incubation for 1 hour at 37°C and 1 hour at 4°C, the tubes were centrifuged at 2300 g for 20 minutes. The serum was stored at -20°C.

Preparation of clots

Clots were formed by adding 2 NIH units of thrombin to 1 ml aliquots of plasma in plastic tubes, containing a thin woollen thread. After incubation for 1 hour at 37°C, the tubes were centrifuged at 2300 g for 20 minutes at room temperature. The clots, formed around the woollen thread, were washed with phosphate buffered saline (PBS) and stored at 4°C until use.

Circulation model

Uptake of Tc-99m labelled antifibrin Y22 by clots was visualized using an in vitro circulation model as shown in Fig. V.1. A plasma clot, formed around a woollen thread as described above, was placed in a glass chamber (5x1 cm) on a gamma camera (Toshiba GCA 102S), connected to a computer (MDS-A^2). The clot was fixed in the glass chamber by its woollen thread. Using a peristaltic pump with plastic tubing (inner diameter 2 mm), 10 ml of citrated plasma was circulated over the clot at a flow rate of 10 ml/min. After 1 hour of circulation,

1-5 µg Tc-99m-Y22 (1.1-2.6 MBq) was added to the plasma and dynamic studies of the uptake of Tc-99m label by the clots were made with the gamma camera for 15 hours (5 minutes per image). To assess the total amount of Tc-99m that was actually bound, the clots were removed at the end of perfusion, washed with saline, and counted in an autogamma counter (Packard 5110). In control experiments, Tc-99m labelled fibrinogen or a non-related MoAb was used. Four clots could be perfused and studied simultaneously using separate glass chambers and separate plasma reservoirs.
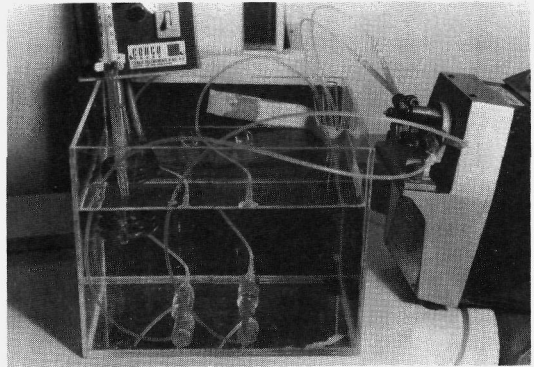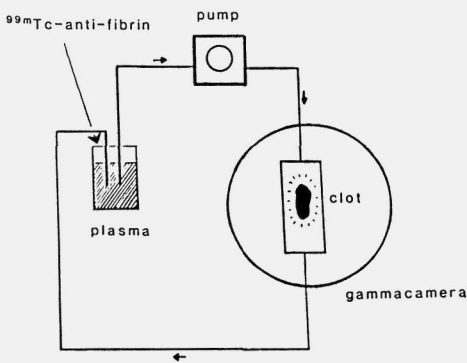
A   B

Fig. V.1   *Schematic (Fig. 1A) and photographic (Fig. 1B) representation of the in vitro circulation model. A plasma clot is placed in a glass chamber and plasma is circulated over the clot using a peristaltic pump. After 1 hour, Tc-99m-Y22 is added to the plasma and accumulation of antibody in the clot is assessed by use of the gamma camera*

Determination of detection limit of uptake of Tc-99m-Y22 by clots

As a measure for the rate of accumulation of Tc-99m-Y22 in clots, we determined the time required to obtain positive images of the clots from the start

of circulation of Tc-99m-Y22 containing plasma. With the aid of the computer connected to the gamma camera, clot-to-plasma ratios were calculated for the various experiments and the ratio at which a hotspot became visible on the scintigrams was determined.

For objective assessment of this ratio, the following experiment was performed. With the computer, hotspots, comparable to the size of a clot in the circulation model, were generated on predetermined positions in a background. Poisson-distributed noise was applied to both background and hotspots. Six persons were asked to localize the hotspots on these computerized scintigrams with target-to-background ratios ranging from 1.0 to 2.0. On the scintigrams with target-to-background ratios of 1.1 or more, all six persons localized the hotspots correctly. The ratio of 1.1 was therefore taken as the ratio at which a hotspot would also become visible in the circulation experiments (Fig. V.2). The time required to obtain a target-non-target ratio of 1.1 was then used as a measure for the rate of accumulation of Tc-99m-Y22 in the clots.
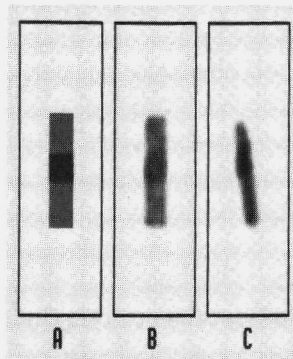

Fig. V.2   *Images of computer-generated hotspots without (A) and with (B) Poisson-distributed noise at a target-to-background ratio of 1.1. Fig C shows the image of a clot in the circulation model at a clot-to-plasma ratio of 1.1*

Effect of experimental conditions on scintigraphic detection of clots in vitro

The effect of various experimental parameters on the rate of uptake of Tc-99m-Y22 by the clots was assessed by determining the time at which a ratio of 1.1 was reached in the various experiments.

1   Using a waterbath, the temperature of clots and plasma was varied and the temperature-dependence of the accumulation of Tc-99m-Y22 in the clots was determined.

2   In other experiments, the effects of addition of different anticoagulants on the binding of Tc-99m-Y22 to clots was determined by addition of heparin (500 IU/ml), hirudin (0.6 U/ml) or Gly-Pro-Arg-Pro (10 mM) to the citrated plasma. (Hirudin is an inhibitor of thrombin and the synthetic peptide Gly-Pro-Arg-Pro inhibits polymerization of fibrin [1]).

3   Experiments in circulating serum were compared with those in plasma to assess the effect of circulating fibrinogen on accumulation of Tc-99m-Y22 in clots.

4   Since Y22 was elicited by immunizing mice with fibrin(ogen) degradation product Y, we evaluated the possibility that accumulation of Tc-99m-Y22 in clots was caused by activation of the fibrinolytic cascade in our system and, as a consequence, by generation of fibrin-degradation products within the clots. Therefore, we assessed the effect of inhibition of fibrinolysis by addition of the plasmin inhibitor aprotinin (Trasylol) to the circulating plasma to a concentration of 1000 KIU/ml.

5   The effect of variation of antibody dose on uptake by the clots was determined by adding different amounts of a Tc-99m-Y22 solution (conc. 50 μg/ml) with specific activity of 1 MBq/μg to the circulating citrated plasma.

6   Finally, the circulation model was used to visualize the binding of Tc-99m-Y22 to polymerising fibrin. To this end a woollen thread, soaked in a thrombin solution (10 NIH units/ml), was placed in a glass chamber and

perfused with citrated plasma to which Tc-99m-Y22 was added.

Visualization of penetration of Y22 into clots by immunofluorescence studies
In Chapter II it was shown that Y22 binds to frozen sections of thrombi. In the experiments in this chapter the penetration of Y22 into a thrombus is visualized at different times of circulation in the circulation model. Plasma clots (formed as described above, but without woollen thread) were placed in the circulation model. Y22 (non labelled) was added to the circulating plasma to a concentration of 0.2 µg/ml.
At different times of circulation (2,6 and 19 hours), clots were removed, washed with saline and frozen sections were made. After washing with PBS, 1:8 diluted normal goat serum was added and incubated for 30 minutes. After washing, 1:40 diluted fluorescein-isothiocyanate (FITC) labeled goat-antimouse Ig was added and incubated for 30 minutes. Finally, the sections were examined under an epi-fluorescence microscope (Leitz Labolux D). A non-related MoAb was used as a control.

Results

With the use of a gamma camera and a dedicated computer system, the uptake of Tc-99m labelled antifibrin Y22 by plasma clots was recorded. Figure V.3A shows images of a plasma clot after 10 minutes, 2 hours and 15 hours of circulation with Tc-99m-Y22 containing citrated plasma at 37°C (corrected for decay of Tc-99m). Initially, a filling defect was observed caused by the presence of the clot. This defect disappeared rapidly and the clot was visible as a clearcut hotspot after 2 hours of circulation, and was even more prominent after 15 hours.
In Fig. V.3B the distribution of activity is depicted in a longitudinal section through the chamber at different times of circulation (corrected for decay). It shows that the activity in the plasma surrounding the clot remained relatively constant. There was no difference in plasma activity on either side of the clot.

The radiolabel was selectively taken up by the clot with time, as is apparent from the single peak at the site of the clot, increasing in height with increasing circulation time.
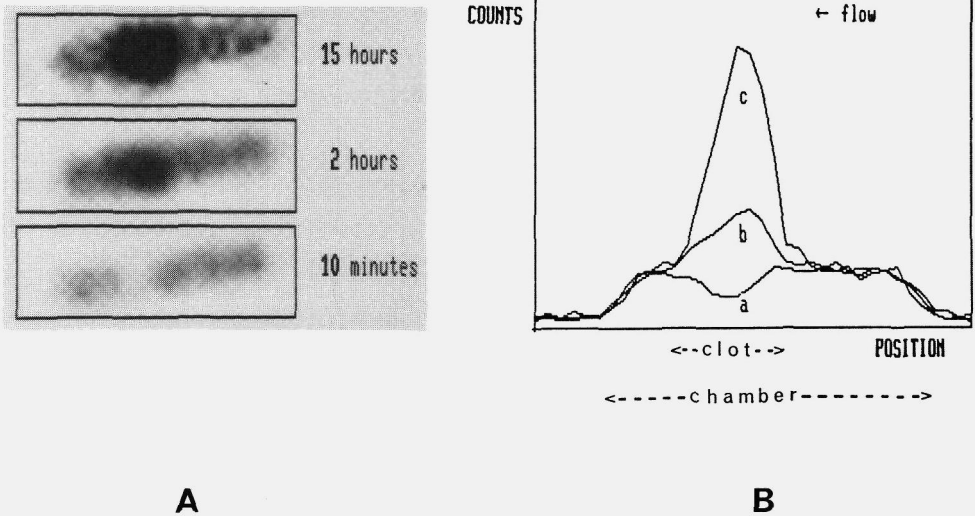

A   B

Fig. V.3   *Gamma camera images of a clot after 10 minutes, 2 hours and 15 hours of circulation with Tc-99m-Y22 containing plasma (A).*
Figure B shows the activity distribution at different positions in a longitudinal section through the chamber (a = after 10 minutes, b = after 2 hours, c = after 15 hours of circulation)

Regions of interest were drawn over clot and background on the basis of Fig. V.3B and accumulation curves were generated. Figure V.4 shows a graphic representation of the time-dependence of Tc-99m activity in clot and plasma after correction for Tc-99m decay. In the beginning, activity in the clot was less than that in plasma, due to the filling defect observed on the images. Thereafter, activity accumulated in the clot (corrected for decay), while the activity in

plasma remained approximately constant. Counting of the clots in a gamma counter showed that only between 5 and 10% of initially applied Tc-99m activity was eventually bound to the clots after 15 hours of circulation (not shown).
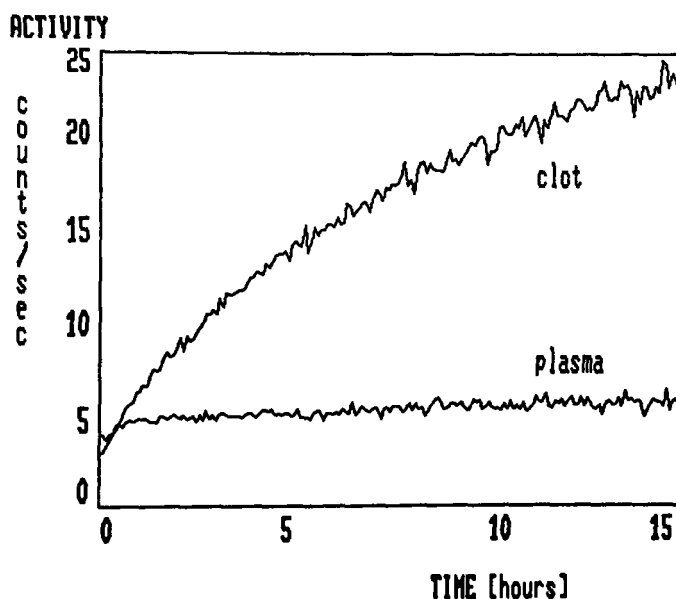

Fig. V.4   *Activity curves of clot and plasma (equal regions of interest) during circulation of Tc-99m-Y22 containing citrated plasma at 37°C (corrected for Tc-99m-decay)*

We determined the time dependence of the absolute amount of antibody molecules that was taken up by the clots by calculating the amount of accumulated radioactivity (arrived at by dose calibration). This was converted to the amount of protein using the known specific activity. The resulting curve is shown in Fig. V.5. The rate of uptake of antibody molecules dropped rapidly within one hour, following a gamma-fitted curve. Using this curve, we calculated the amount of Y22 bound to the clot after 15 hours to be 8% of initially applied Y22.

UPTAKE RATE
[fmol/sec]

TIME [hours]
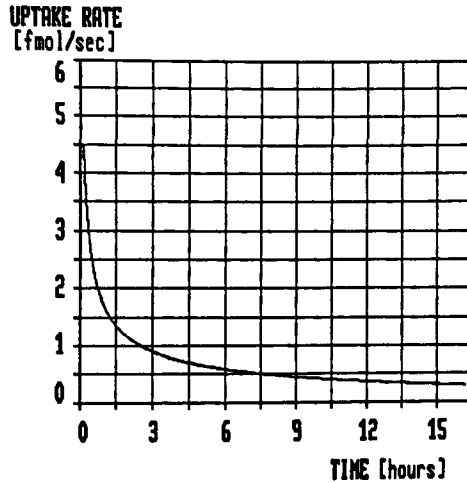
Fig. V.5   *Time-dependence of rate of accumulation of Y22-molecules in a*
plasma clot. This curve is the first derivative of that in Fig. V.4
(after smoothing by a gamma fit). The amount of antibody was
calculated from the amount of Tc-99m-activity using the known
specific activity

During circulation with Tc-99m-Y22 in citrated plasma at 37°C, a target-non-
target ratio of 1.1 was obtained after 73 ± 59 min (n=8, Table V.1). Upon
circulation with Tc-99m labelled fibrinogen or a non-related MoAb this ratio
was not attained even after 15 hours of circulation (not shown).
Table V.1 shows the times of circulation at which a target-non-target ratio of 1.1
was reached after addition of Tc-99m-Y22 to citrated plasma, and citrated
plasma to which various anticoagulants were added. There was no significant
difference in the time required to reach this ratio for the various anticoagulants
added to the circulating plasma. A remarkable effect of temperature was
observed: the time needed to obtain a clot-to-plasma ratio of 1.1 was
approximately 4 times shorter at 37°C than at 20°C, which indicates an
approximately 4 times higher binding rate.
In the presence of aprotinin at 37°C, the standard deviation in the binding rates
of Tc-99m-Y22 to clots was much smaller. This phenomenon was less prominant

upon circulation at 20°C.

In serum, the binding rate of Tc-99m-Y22 to clots was comparable to the results obtained with plasma (ratio 1.1 reached after 85 min).

Table V.I. *Effect of various variables on rate of uptake of Tc-99m-Y22 by clots (expressed as time required to obtain a clot-to-plasma ratio of 1.1.)*

Tc-99m-Y22 in	Ratio 1.1 reached after (min)	
	at	
	20°C	37°C
citrated plasma	280 ± 152 (*n=11*)	73 ± 50 (*n=8*)
citrated plasma + heparin	340 ± 101 (*n=4*)	85 ± 60 (*n=4*)
citrated plasma + hirudin	n.d	112 ± 58 (*n=3*)
citrated plasma + Gly-Pro-Arg-Pro	n.d.	73 ± 37 (*n=6*)
citrated plasma + aprotinin	277 ± 51 (*n=3*)	43 ± 6 (*n=3*)
serum	n.d.	85 ± 56 (*n=3*)

Figure V.6 shows the activity curves of clots after addition of different amounts of Tc-99m-Y22 to the circulating plasma at 37°C, corrected for decay. There was a direct correlation (r=0.998) between antibody dose and absolute amount of counts present in the clot after 15 hours of circulation (Fig. V.7).
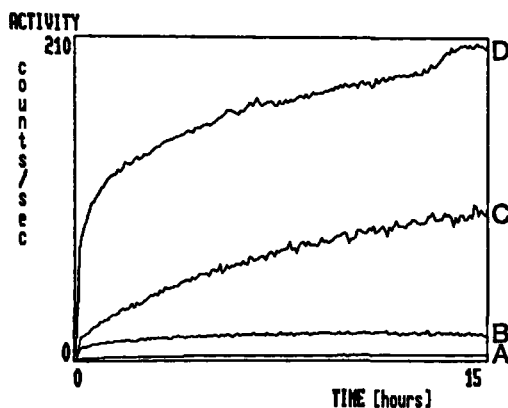

Figure V.6 *Dose-dependent accumulation of Tc-99m-Y22 in clots after addition of 1.5 (A), 6.5 (B), 33 (C) and 66 μg (D) labelled Y22 with a constant specific activity (1 MBq/μg)*
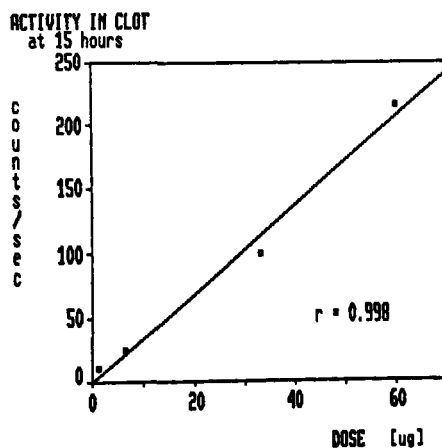
Figure V.7 *Relationship between antibody dose and accumulated activity in the clots after 15 hours of circulation of Tc-99m-Y22 containing plasma*

Clot-to-plasma ratios after 15 hours, however, did not differ significantly for the different doses of Tc-99m-Y22 (Table V.2). Also, the rate of uptake of Tc-99m-Y22 by the clots expressed as time required to obtain a clot to plasma ratio of 1.1 did not differ much for the various amounts of antibody.

Table V.2 *Effect of antibody dose on rate of uptake by the clots (expressed as time required to obtain a clot-to-plasma ratio of 1.1) and on clot-to-plasma ratios (after 15 hours of circulation at 37°C). Different amounts of Tc-99m-labelled Y22 with constant specific activity (1 MBq/μg) were added to the circulating plasma*

Dose Tc-99m-Y22	time at which ratio 1.1 is reached	clot-to-plasma ratio (after 15 hours)
1.3 μg / 1.3 MBq	90 min	2.2
6.5 μg / 6.5 MBq	130 min	2.5
33.0 μg / 33.0 MBq	115 min	2.0
66.0 μg / 66.0 MBq	85 min	2.2

When a thrombin-soaked woollen thread was used instead of a preformed clot, accumulation of radiolabel was already visible after a few minutes of circulation of Tc-99m-Y22 containing citrated plasma (Fig. V.8A). As expected, perfusion of a thrombin-soaked woollen thread with Tc-99m-fibrinogen containing plasma also showed rapid uptake of this agent (not shown). Figure V.8B depicts the accumulation of Tc-99m-Y22 in the forming and preformed clot with increasing circulation time. The curve of the thrombin thread showed a rapid initial increment in counts and levelled off thereafter, whereas the preformed clot showed a more gradual accumulation of radioactivity.
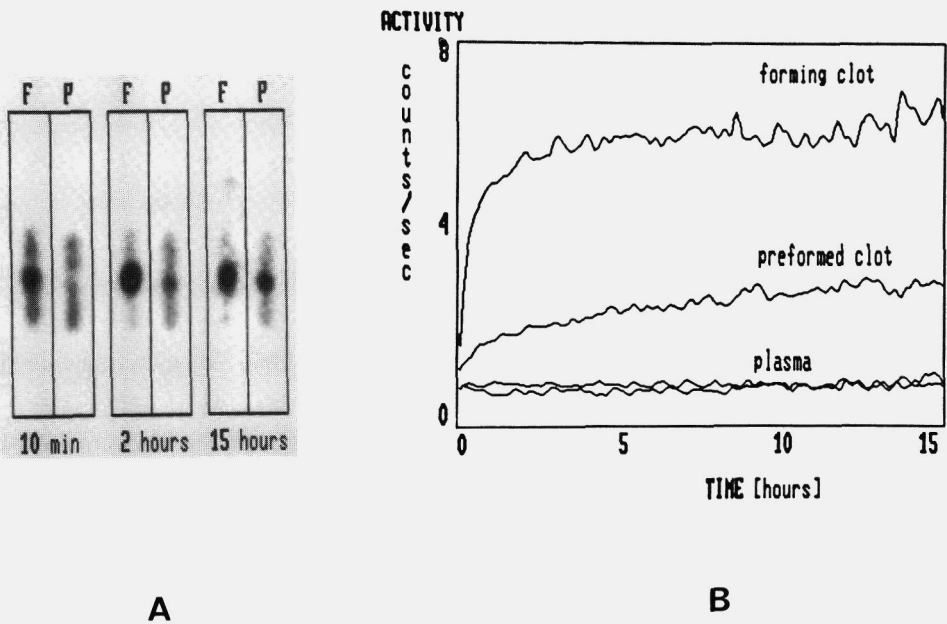
Fig. V.8   *Images of the binding of Tc-99m-Y22 to a thrombin-soaked woollen thread (forming clot, "F") and a preformed plasma clot ("P") after perfusion on a gamma camera for 10 minutes, 2 hours and 15 hours (A). Fig. B shows the radioactivity curves as assessed by dynamic uptake studies on the gamma camera (5 minutes/image) of the preformed and the forming clot compared to background activity in equal volumes of plasma (corrected for decay)*

We were able to visualize the localization of anti-fibrin Y22 within plasma clots by immunofluorescence microscopy at different times of circulation. A time-dependent penetration of Y22 into the thrombi was seen, as is shown in Fig. V.9. Almost the entire thrombus showed fluorescence after 19 hours of circulation, as is shown in fig. C. No fluorescence was observed after circulation with a non-related MoAb (Fig. D).
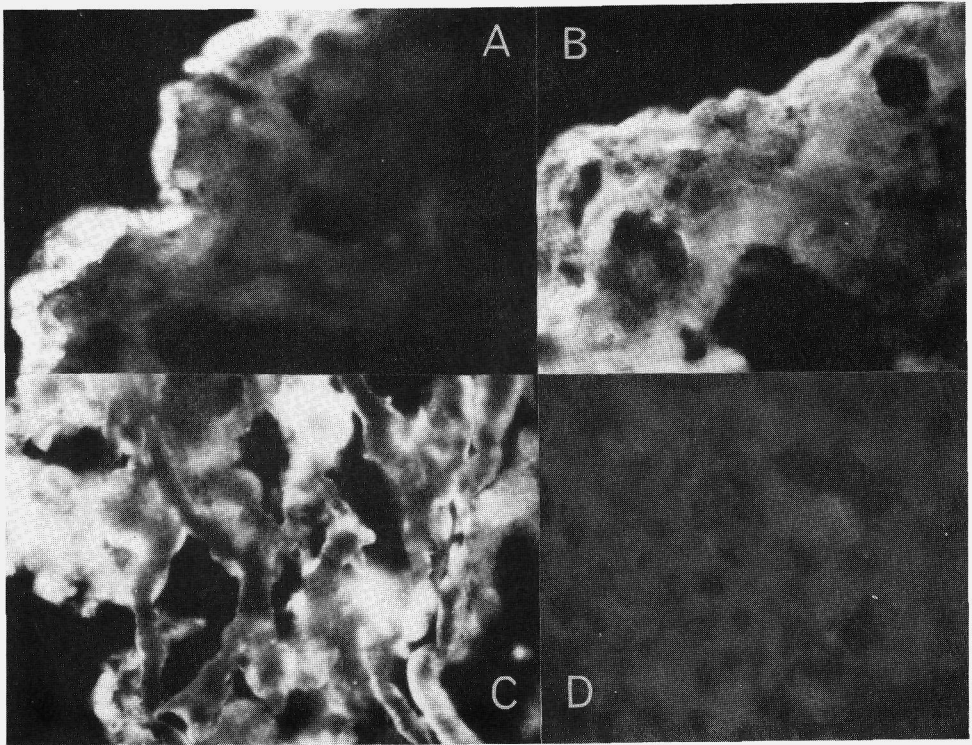
Fig. V.9   *Immunofluorescence microscopy of clots after 2 hours (A), 6 hours (B) and 19 hours (C) of circulation of Y22 in the circulation model. No fluorescence is seen after circulation of a control MoAb for 19 hours (D)*

Discussion

A circulation model was developed for the immunoscintigraphic detection of clots in vitro. In this model, plasma clots were placed in a glass chamber on a

gamma camera, and Tc-99m labelled Y22 was added to plasma which circulated over the clots. In citrated plasma, clots were visible as hotspots after about 1 hour of circulation at 37°C. The clots did not become visible upon circulation with Tc-99m labelled fibrinogen or non-related MoAb. There was a time-dependent accumulation of Tc-99m-Y22 in the clots (corrected for decay). The activity in the plasma remained approximately constant (corrected for Tc-99m-decay), which indicates that only a small fraction of total applied Tc-99m-Y22 was actually bound to the clots. This was confirmed by counting of the clots in a gamma counter at the end of circulation. Only 5-10% of total applied Y22 was bound to the clots. Apparently, this was sufficient to visualize the clots, due to the difference in local concentration of Tc-99m-Y22 in clots and circulating plasma as expressed in the target-to-background ratio. When the rate of uptake of Tc-99m-Y22 was plotted against the time of circulation, a gamma fitting curve resulted, which shows a rapid drop in accumulation rate within the first hour of circulation.

The accumulation of radiolabel quantitatively reflects the amount of antibody in the clot, since our labelling method ensures stable attachment of Tc-99m to the antibody, as was shown in the previous chapter.

The time-dependence of the uptake of Tc-99m-Y22 by the clots, as observed in the scintigraphic experiments, was confirmed by immufluorescence studies on frozen sections of the clots. They showed a time-dependent penetration of Y22 into the clots. Almost the entire clot showed fluorescense after 19 hours of circulation. This clearly demonstrated that binding of Y22 is not limited to the surface of a clot.

Combining the results of the fluorescence experiments and the calculations of the uptake rate curve (Fig. 4), we postulate that the initial rapid accumulation of label in the clot is due to coating of the surface of the clot by Tc-99m-Y22. Thereafter, the antibody has to penetrate the clot by diffusion, which apparently is a much slower process, probably due to the compact structure of the clot or the fibrin fibres in the clot.

It was observed that a clot became visible as a hotspot when a target-to-

background ratio of at least 1.1 was obtained. The time required to obtain this ratio was then taken as measure to compare the effects of various experimental conditions on the rate of uptake of Tc-99m-Y22 by the clots.

A remarkable effect of temperature on the binding of Tc-99m-Y22 to the clots was observed. At 37°C clots became visible as hotspots 4 times faster than at room temperature. This may result from a temperature dependence of the physico-chemical properties of the interaction between fibrin and the antibody.

Various anticoagulants did not affect the rate of binding of Tc-99m-Y22 to the clots. The results with heparin, in particular, are of the utmost clinical importance, since it would mean that heparin therapy in patients can be started before application of Tc-99m-Y22 for thrombus imaging. In these experiments, heparin was added to a concentration of 500 IU/ml. Extrapolated to a total plasma volume of ± 3 l, this would imply a dosage of 1.500.000 IU for an individual patient, which is much higher than the dose normally given (20.000 - 30.000 IU/24 hours). Even this extremely high heparin dose did not affect the binding of Tc-99m-Y22 to clots.

In the various experiments there was a large standard deviation in times required to obtain target-non-target ratios of 1.1. When, however, the plasmin inhibitor aprotinin was added to the plasma, the standard deviation was much smaller. Possibly, part of the uptake of antibody by the clot is counterbalanced by lysis of the clot, when fibrinolysis is not inhibited by aprotinin. The variability of times required to obtain a ratio of 1.1 in the experiments without aprotinin, is therefore possibly due to interindividual differences in fibrinolytic activity in the used plasma (plasmas were prepared from blood of different donors and at different times of the day: fibrinolytic activity has a diurnal rhythm [2]). These experiments also show that generation of fibrin degradation products within the clots is not responsible for accumulation of Tc-99m-Y22, since it was not affected by addition of aprotinin.

There was no difference in the binding rate of Tc-99m-Y22 to the clots during circulation in plasma compared to serum. This indicates that fibrinogen, present in plasma, does not hamper the binding of Tc-99m-Y22 to fibrin.

We also assessed the effect of antibody dose on rate of accumulation in the clots. In this experiment we added different amounts of Tc-99m-Y22 with a constant specific activity to the circulating plasma. The absolute radioactivity dose added was varied in this setting with samples of Tc-99m-Y22 of identical quality. The results would not have been comparable if the activity used was kept constant and the antibody dose was increased, thus changing the specific activity of the preparations. There was an approximately linear relationship between labelled antibody dose and the amount of activity present in the clot at the end of circulation. The time required to reach a clot-to-plasma ratio of 1.1, however, was not dependent on the antibody dose. The absolute increase in clot-bound activity at higher Tc-99m-Y22 dose was not reflected in an increased clot-to-background ratio. This can be explained by the finding that only a small fraction of the applied Tc-99m-Y22 is eventually bound to the clots and, in the absence of clearance, an increased antibody dose will therefore result in a concomittant elevated background.

Yet, circulation with higher doses of labelled antibody resulted in better images as a result of lower "noise" in clots and plasma.

We observed that forming clots already became visible already after a few minutes of perfusion with Tc-99m-Y22 containing citrated plasma. In these experiments, clotting was induced by a woollen thread, soaked in a thrombin solution. This result is in full agreement with that of the experiments with aggregating fibrin monomers, described in the previous chapter.

Since fibrin is a large (MW 340 KD) and complicated molecule, different antifibrin monoclonal antibodies may be directed against different epitopes on fibrin. Various physiological and clinical conditions may affect the accessibility of the epitope to the antibody, depending on its location in the fibrin molecule. Using our model it seems possible to predict the effects of these environmental conditions on the clot binding capacity of a certain antifibrin antibody without the use of animal models. Because it is a dynamic system, the model resembles more closely the in vivo situation than static test tube experiments.

References

1. Laudano AP, Doolittle RF. Synthetic peptide derivatives that bind to fibrinogen and prevent the polymerization of fibrin monomers. Proc Natl Acad Sci USA 1978, 73: 3085-3089.

2. Kluft C, Jie AFH, Allen RA. Behaviour and quantitation of extrinsic (tissue-type) plasminogen activator in human blood. Thromb Haemost 1983, 50: 518-523.

CHAPTER VI

IN VIVO EXPERIMENTS

---

1 THROMBUS IMAGING IN ANIMALS

Introduction

In the previous chapters it was shown that Tc-99m-labelled antifibrin antibody Y22 binds to human fibrin (and virtually not to fibrinogen) in an enzyme immunoassay (Chapter II), to human plasma clots in test tubes (Chapter IV) and to plasma clots in a circulation model (Chapter V). In this chapter the experiments are described which were performed to assess the feasibility of immunoscintigraphic imaging of thrombi in vivo.

We found by enzyme immunoassay (Chapter II) that Y22 reacts not only with human fibrin, but also with fibrin of rabbits, rats, dogs and sheep (but not with porcine or murine fibrin). This enabled us to perform imaging studies with autologous thrombi in animal models.

For practical reasons we decided to use rabbits and rats for the in vivo experiments.

Materials

Vetamine hydroxide (Vetalar) was obtained from Parke Davis, Morris Plains, USA, and acepromazine (Vetranquil) from Algin, Maassluis, The Netherlands. Pentobarbital (Nembutal) was obtained from Ceva, Paris, France. Control MoAb anti-FITC IgG, was kindly provided by Dr. J.J. Haaijman, Medical Biological Laboratory TNO, Rijswijk, The Netherlands. Heparin was purchased

from Leo Pharmaceutical Products, Weesp, The Netherlands. Cephotest reagent was obtained from Nyegaard Diagnostics Division, Oslo, Norway. Microtiter plates (Immulon) were purchased from Greiner, Alphen a/d Rijn, The Netherlands. Rabbit antimouse Ig(7S) and goat antirabbit Ig(7S) were obtained from Nordic, Tilburg, The Netherlands; 3,3',5,5'-tetramethylbenzidine (TMB) from Aldrich Chemical Co., Milwaukee, USA. Fibrinogen was purified as described by Van Ruijven et al (1).

Methods

ANIMAL MODELS

1. *Rabbits*

Jugular Vein Thrombosis Model

Male New Zealand White rabbits, weighing from 2.5 to 4 kg, were anaesthetized by intramuscular injection of a 10:1 mixture (0.5 ml/kg body weight) of ketamine hydroxide (Vetalar, 100 mg/ml) and acepromazine (Vetranquil, 10 mg/ml). Anaesthesia was maintained by intermittent intravenous injections of pentobartital (Nembutal) at a dose of 5 mg/kg body weight in a marginal ear vein. A clot was made in the right jugular vein, using a modification of the method of Collen et al. [2]. An incision of about 5 cm in the neck of the rabbit was made and the right jugular vein was exposed. All branches were ligated. The jugular vein was clamped proximally and distally. A thin woollen thread (length 3-4 cm) was inserted in the clamped segment, using a needle (diameter 0.5 mm). A clot was allowed to form on the woollen thread for 30 minutes and the clamps were released. The blood volume of the clamped segment was approximately 1 ml. Finally, the wound was closed.

Two to three hours after the end of the operation, Tc-99m labelled Y22 (1.0 mg, 37 MBq), Tc-99m labelled fibrinogen (2.0 mg, 37 MBq), control Moab anti-FITC (1.0 mg, 40 MBq) or I-123 labelled fibrinogen (2.0 mg, 24 MBq) was

injected into a marginal ear vein of the rabbits. In another control experiment, 190 MBq of the intermediate compound used in the Tc-99m labelling procedure (see chapter IV) was injected into a rabbit. At timed intervals, images of the rabbits were made with a gamma camera (Toshiba, GCA 102S), connected to a computer (MDS-A^2).

Independent confirmation for the clot-specific binding of Tc-99m-Y22 was obtained by determination of the blood clot radioactivity ratios after removal of the clots, 20 hours after injection of the antibody.

The extent of occlusion of the jugular vein by the thrombus was assessed by contrastvenography, 20 hours after thrombus induction.

Clots in the peritoneal cavity

The abdomen of anaesthetized New Zealand White rabbits was opened by medial incision and two cylindrical cotton pads (0.5 x 2 cm), each soaked in 1 ml human plasma to which 2 NIH thrombin had been added, were adhered to the abdominal wall. Finally, the peritoneum and the skin were closed.

Two to three hours after the end of operation, Tc-99m labelled Y22 (1.0 mg, 37 MBq), Tc-99m labelled fibrinogen (2.0 mg, 37 MBq) or anti-FITC monoclonal antibody (1.0 mg, 40 MBq) was injected in a marginal ear vein and images were made with the gamma camera.

2. Rats

Inferior Vena Cava Thrombosis Model

Male Wistar rats (weighing 300-600 g) were anaesthetized by intraperitoneal injection of 0.1 ml pentobarbital (6 mg) and the abdomen and peritoneum were opened by medial incision. The inferior vena cava was exposed, clamped and a thin woollen thread (length 2 cm) was inserted in the clamped segment using a needle. A clot was allowed to form for 30 min and the clamps were released. Finally, the peritoneum and skin were closed. One hour after the end of operation, Tc-99m-Y22 (250 μg, 24 MBq) was injected into a penis vein and

images of the rats were made with the gamma camera. As a control, Tc-99m labelled anti-FITC monoclonal antibody (250 µg, 30 MBq) was injected. In another control experiment, Tc-99m-Y22 (250 µg, 24 MBq) was injected in a non-operated rat.

Clots in the peritoneal cavity

The abdomen of anaesthetized Wistar rats was opened by medial incision and two cylindrical cotton pads (0.5 x 0.5 cm), each soaked in 1 ml human plasma to which 2 NIH thrombin had been added, were adhered to the inside of the abdominal wall. One hour after the end of operation, Tc-99m-Y22 (250 µg, 24 MBq) was injected into a penis vein and images of the rats were made with the gamma camera. As a control, Tc-99m-anti-FITC monoclonal antibody (250 µg, 30 MBq) was used.

Extracorporeal Thrombosis Model

An extracorporeal thrombus model was used, as described by Umetsu and Sanai [2]. An incision of about 2 cm in the neck of an anaesthetized rat was made and the left jugular vein and right carotid artery were exposed. An extracorporeal shunt was made between the vessels with plastic tubing (inner diameter approximately 1 mm). A segment of the shunt was clamped and a thin woollen thread was inserted. A clot was allowed to form around the woollen thread for 5 minutes and the clamps were released. Heparin (20 IU) was injected in the extracorporeal circuit every hour.

Thirty minutes after induction of the thrombus, Tc-99m labelled Y22 (200 µg, 55.5 MBq) was injected into a penis vein of the rat. At timed intervals, images were made with the gamma camera.

EXPERIMENTAL VARIABLES

Effect of heparinization on thrombus detection

The jugular vein thrombosis model in rabbits was used to assess the effect of

heparin on binding of Tc-99m-Y22 to thrombi in vivo. Heparin was administered intravenously (700 IU/kg) at 2, 4 and 6 hours after thrombus formation and then intraperitoneally (a bolus injection of 1400 IU/kg). The efficiency of anticoagulation was determined by activated partial thromboplastin time test (using Cephotest reagent according to the manufacturers' instructions). Tc-99m labelled Y22 (1 mg, 37 MBq) was injected in a marginal ear vein two hours after induction of the thrombus and images were made with the gamma camera.

Imaging with F(ab)$_2$ and Fab-fragments of Y22

Fab- and F(ab)$_2$-fragments of Y22 were produced as described in Chapter III. Tc-99m labelled F(ab)$_2$ (1.0 mg, 37 MBq) or Fab-fragments (1.0 mg, 37 MBq) were injected into rabbits with a thrombus in the jugular vein. At timed intervals, images of the rabbits were made with the gamma camera. Twenty hours after injection of the labelled fragments, the animals were sacrificed. The clots were removed and counted in an autogamma counter to determine thrombus-to-blood radioactivity ratios.

Blood clearance studies

The rate of clearance from the circulation of Tc-99m labelled Y22, F(ab)$_2$ and Fab was determined in rabbits. After injection of the radioactive material, blood samples of 0.9 ml in syringes (containing 0.1 ml of a 0.11 mol/l sodium citrate solution in saline) were collected from an indwelling catheter in a femoral artery, which was kept patent by regular flushing with a heparin solution (100 IU/ml saline). The samples were counted in an autogammacounter together with a sample of the injected material and the clearance rate was determined.

Assessment of immunogenicity of Y22

Three weeks after intravenous injection of Tc-99m-Y22 (1.0 mg, 37 MBq), rabbits were boosted intravenously with 1.0 mg Tc-99m-Y22 and gamma camera images were made.

The presence of rabbit-antimouse antibodies in the rabbits was assessed by a newly developed enzyme immunoassay. Wells of microtiter plates were coated with Y22 in PBS (10 μg/ml), 110 μl/well). After incubation overnight at 4°C, the plates were washed with PBS containing 0.05% Tween 20 (PBS/Tween). Serum of the boosted rabbits, control rabbits or rabbit antimouse Ig (7S) was pipetted into the wells. After incubation for 30 min at room temperature, the plates were washed with PBS/Tween. Horseradish peroxidase labelled goat antirabbit Ig (7S) was added to the wells and incubated for 30 min at room temperature. After washing with PBS/Tween, reactivity was assessed by adding 3,3',5,5'-tetramethylbenzidine (TMB) and H_2O_2 as the substrate mixture (3). The reaction was stopped by addition of 100 μl sulphuric acid (1M) and the optical density at 450 nm was measured with a multichannel spectrophotometer (Flow Laboratories).

Results

To assess the feasibility of immunoscintigraphy of thrombi in vivo we injected Tc-99m-Y22 into rabbits, in which thrombi had been introduced. Figure VI.1A shows the clearcut image of a thrombus in the jugular vein, obtained 18 hours after injection of the labelled antibody. Figure VI.1B shows the image of a rabbit after injection of Tc-99m labelled fibrinogen. The clot was only faintly visible.

After injection of I-123 labeled fibrinogen (Fig. VI.1C), there was considerable accumulation of radiolabel in the thyroid glands, but the clot was not visible. After injection of Tc-99m labelled control monoclonal antibody anti-FITC IgG, the thrombus was not visualized.

This shows the specific targeting properties of Tc-99m-Y22 of autologous thrombi in rabbits.
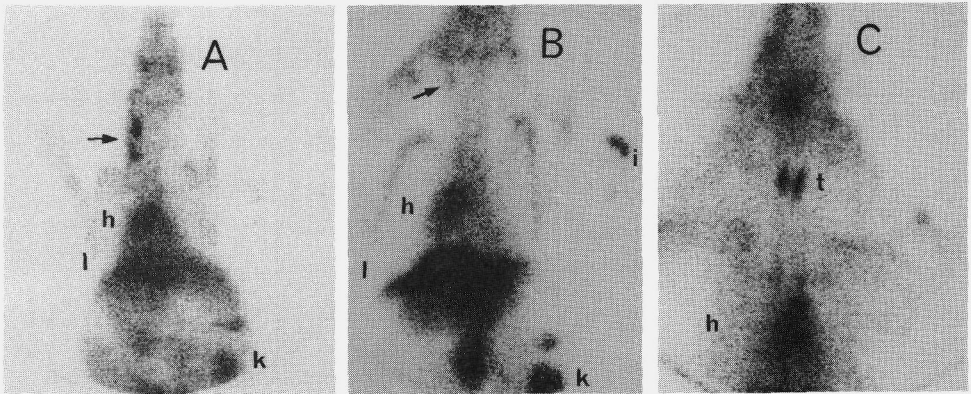
Fig. VI.1 *Images of thrombi in the jugular vein of rabbits (→); h = heart; l = liver; k = kidney; i = site of injection; t = thyroid gland. Images made at 18 hours after injection of Tc-99m-Y22 (A), Tc-99m-fibrinogen (B), and I-123-fibrinogen (C)*

With the computer system dedicated to the gamma camera, target-to-background ratios were calculated. The clot-to-blood ratios of the rabbit in Fig. VI.1A (i.e. activity in the clot compared to the contralateral vein) were 1.2, 4.9 and 7.7 at 45 min, 4 hours and 18 hours after injection of Tc-99m-Y22, respectively. Injection of Tc-99m fibrinogen resulted in a ratio of 1.5 (after 18 hours). After injection of Tc-99m labelled control monoclonal antibody (anti-FITC IgG), the clot-to-blood ratio was only 1.2. These findings are in agreement with the results of experiments in which the thrombi were removed from the jugular veins (after 20 hours) and counted in an autogammacounter. Average clot/blood ratios were 6.1 ± 0.57 (n=3), and 0.9 ± 0.06 (n=3) for the Tc-99m-Y22 and the Tc-99m control antibody injected animals, respectively.

Figure VI.2 shows the macroscopic appearance of a thrombus in the jugular vein, 20 hours after formation.
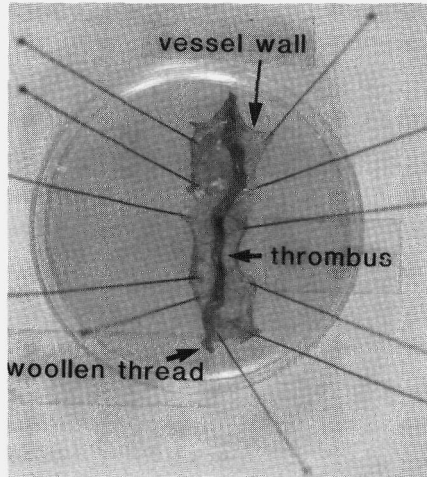
Fig. VI.2 *Jugular vein thrombus, 20 hours old*

When we injected the intermediate compound of the Tc-99m-labelling method into rabbits, a large amount of radioactivity was still present in the bloodstream of the animals 20 hours after injection (Fig. VI.3), but the clot was not visible.
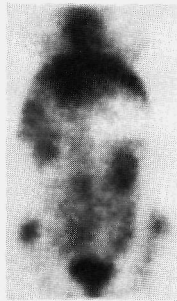

Fig. VI.3 *Image of a rabbit, 17 hours after injection of intermediate compound of the Tc-99m-labelling*

To assess the extent of occlusion of the jugular vein by the thrombus, venography was performed by injection of contrast material in a marginal ear

vein.

Figure VI.4 shows the images of the occluded jugular vein (Fig. VI.4A) and the contralateral, normal side (Fig. VI.4B). As can be seen, the vessel is not completely occluded by the thrombus, but blood flow is severely impaired.
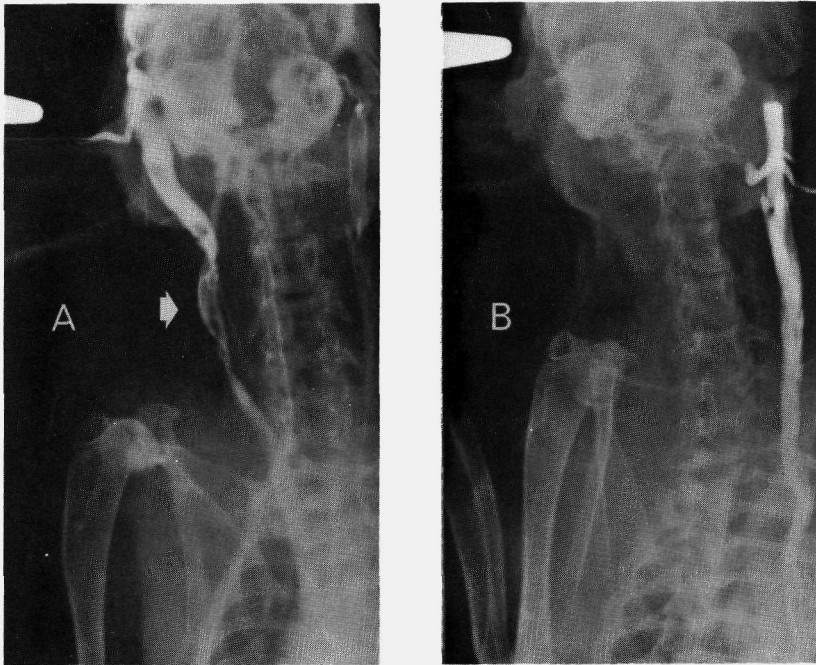
Fig. VI.4   *Contrastvenography of a rabbit with a thrombus (→) in the jugular vein (A) as compared with the contralateral, normal side (B). The venography was performed by Dr.J. van Unnik, Dept. of Diagnostic Radiology, University Hospital Leiden*

Figure VI.5A shows the image of clots in the abdomen of a rabbit, obtained 18 hours after injection of Tc-99m-Y22. After injection of Tc-99m-fibrinogen, the clots were only faintly visible (Fig. VI.5B). The clots were not visualized after

injection of Tc-99m labelled control monoclonal antibody (anti-FITC). The ratio of the radioactivity of the clots in the abdomen and that in surrounding soft tissues (clot-to-soft tissue ratio) were 5.8 for Tc-99m-Y22, 1.4 for Tc-99m-fibrinogen and 1.2 for Tc-99m-control monoclonal antibody.
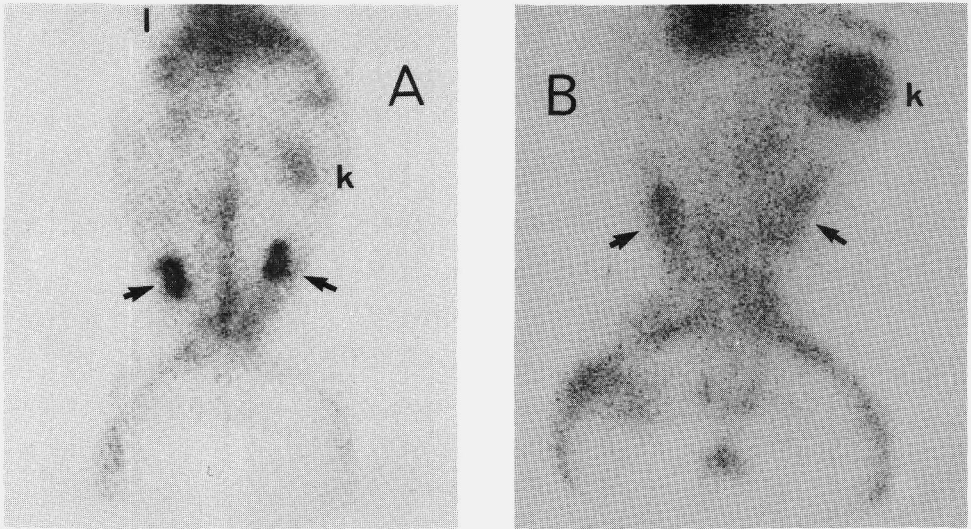

Fig. VI.5   *Images of thrombi in the abdomen of rabbits (→); l = liver; k = kidney. Images obtained 18 hours after injection of Tc-99m-Y22 (A) and Tc-99m-fibrinogen (B)*

Besides the aforementioned experiments in rabbits, we also performed experiments in rats to determine the potential of Tc-99m-Y22 for thrombus imaging.

Figure VI.6A shows the images of a thrombus in the inferior vena cava of a rat 4 hours after injection of Tc-99m-Y22. The lateral view, in particular, clearly shows the presence of a hotspot as compared with the bloodpool of a control rat (Fig. VI.6B). After injection of a Tc-99m-control antibody, the thrombus was not visible. Thrombus-to-blood ratios were 4.4 for Tc-99m-Y22, and 1.2 for Tc-99m-control antibody (representing only the bloodpool).
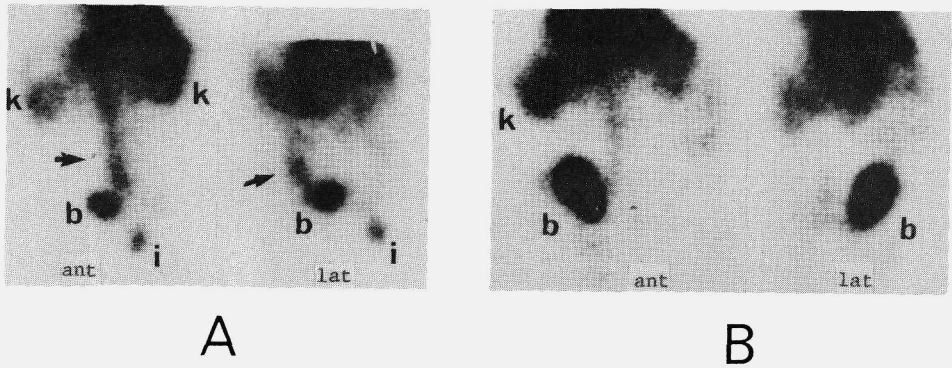
Fig. VI.6 *Images of a rat with a thrombus in the inferior vena cava (→), 4 hours after injection of Tc-99m-Y22: anterior (ant) and right lateral (lat) view (A). Fig B shows the images of a control rat after injection of a Tc-99m labelled control MoAb; b = bladder; i = site of injection*

Figure VI.7 shows the image of a rat in which human plasma-soaked cotton pads were introduced in the peritoneal cavity.
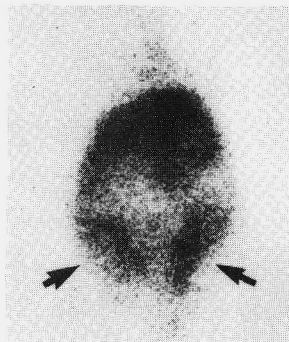

Fig. VI.7 *Image of a rat with clots in the peritoneal cavity (ϸ), 17 hours after injection of Tc-99m-Y22; l = liver; k = kidney*

As a variant of the in vitro circulation model, described in Chapter V, an extracorporeal shunt model in rats was produced, as described by Umetsu and Sanai [3]. Binding of Tc-99m-Y22 to the thrombus was visible one hour after injection of the labelled antifibrin (Fig. VI.8A) and, more clearly, after three hours (Fig. VI.8B). The diameter of the extracorporeal loop was 1 mm, allowing only a small volume of blood to pass through the loop. This necessitated a long exposure time, as can be seen from the large amount of activity present in the body of the rat, compared to that in the loop.
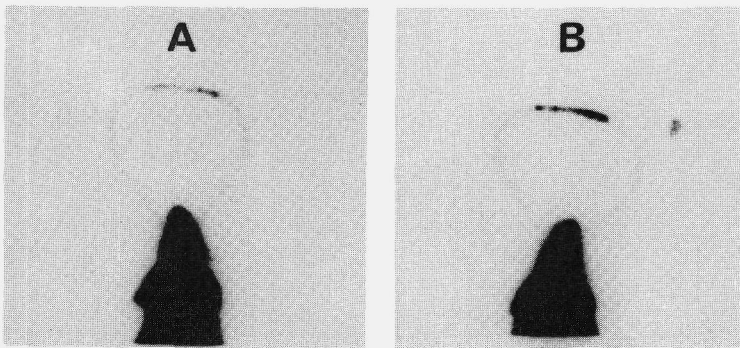

Fig. VI.8 *Images of a thrombus in an extracorporeal circuit in a rat at 1 (A) and 3 hours (B) after injection of Tc-99m-Y22*

We observed no effect of heparin on the binding of Tc-99m-Y22 to thrombi in vivo. Thrombi in the jugular vein of heparinized rabbits were visualized with clot-to-blood ratios of 5.5, as measured 20 hours after injection of Tc-99m-Y22. Our heparinization scheme was adequate, as was assessed by activated partial thromboplastin time test (APTT). Control experiments in rabbits showed that a twofold elongation of the APTT is obtained at a heparin dose of 350 IU/kg ($T_{1/2}$ approximately 2 hours).

After injection of Tc-99m-F(ab)$_2$, thrombi in the jugular vein of rabbits could be visualized (see Fig. 9 A) with thrombus-to-blood ratios (after

20 hours) of 3.3 - 4.0 (n=2). After injection of Tc-99m-Fab, however, thrombi were only faintly visible with thrombus-to-blood ratios of 1.2-1.4.

In Fig. VI.9 the clearance rates of Tc-99m-labelled Y22, F(ab)$_2$ and Fab are depicted. The estimated halflives (β-phase) of Tc-99m-Y22, -F(ab)$_2$ and -Fab were 28.3, 18.4 and 12.4 hours, respectively.
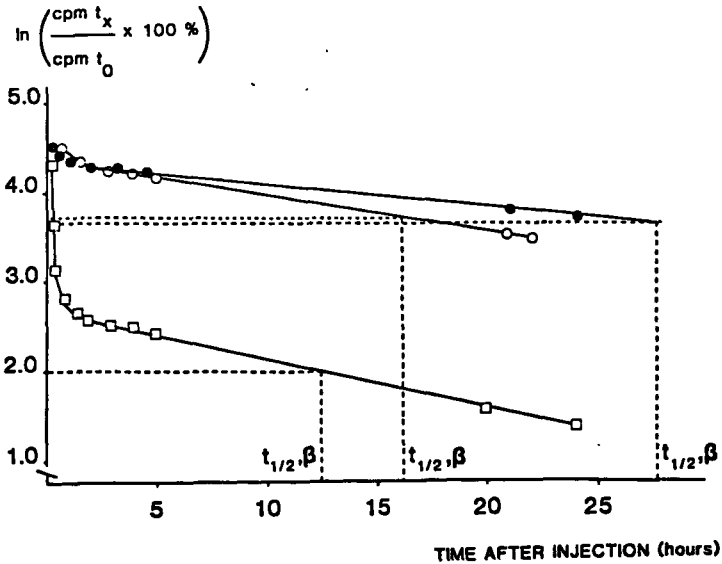

Fig. VI.9   *Clearance curves of Tc-99m-Y22 (●), Tc-99m-F(ab)$_2$ (O) and Tc-99m-Fab (□) in rabbits as percentage of the injected dose*

The biodistribution patterns of Tc-99m-Y22, Tc-99m-F(ab)$_2$ and Tc-99m-Fab were assessed in rabbbits and in rats. With Tc-99m-Y22, there was still high background activity in the circulation of the rabbit after 17 hours and considerable accumulation in the liver (Fig. VI.10A), whereas the kidneys showed higher uptake after injection of Tc-99m-F(ab)$_2$. Tc-99m-Fab was largely excreted from the circulation after 17 hours, due to rapid clearance by the kidneys (Fig. VI.10B).
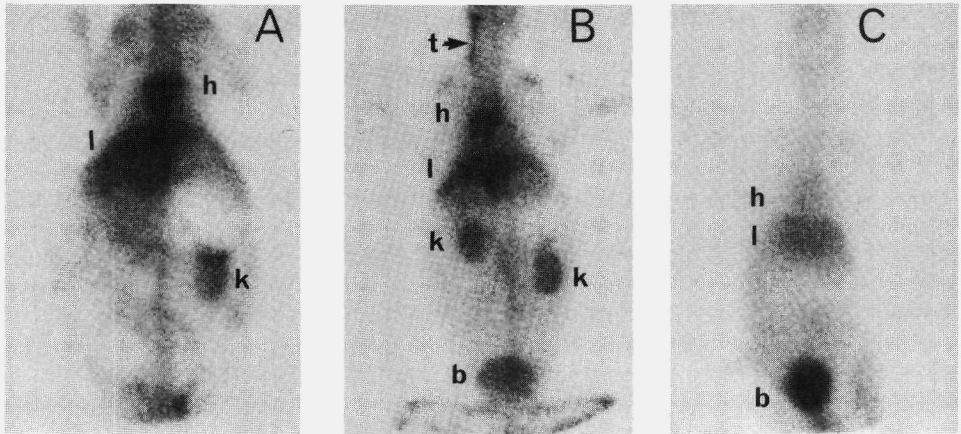
Fig. VI.10 *Biodistribution in rabbits of Tc-99m-Y22 (A), Tc-99m-F(ab)₂ (B)*
and Tc-99m-Fab (C); h = heart; l = liver; k = kidney; b = bladder; t
= thrombus. Images obtained 18 hours after injection

Fig. VI.11 shows images of rats, 17 hours after injection of Tc-99m-Y22, Tc-99m-F(ab)₂ and Tc-99m-Fab. The same biodistribution pattern as that obtained in the rabbits was observed.
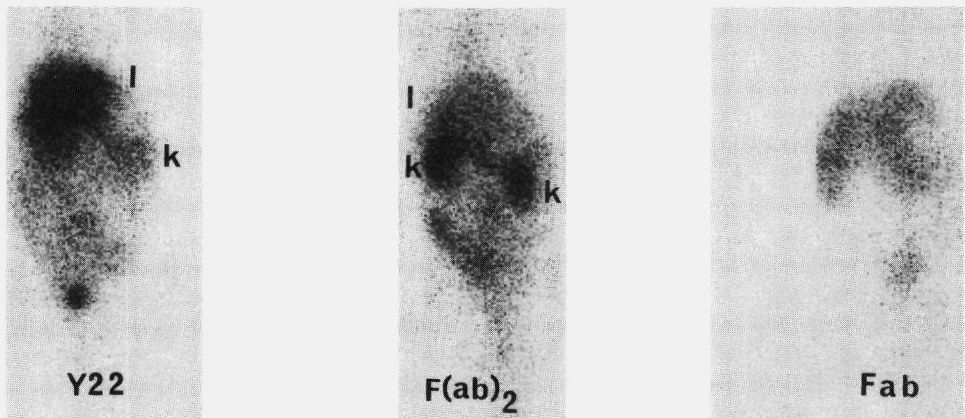

Fig. VI.11 *Images of rats, 17 hours after injection of Tc-99m-Fab, Tc-99m-*
F(ab)₂ and Tc-99m-Y22; l = liver; k = kidney

Repeated injection of Tc-99m-Y22 caused a more rapid clearance from the circulation and a rapid accumulation in the liver (Fig. VI.12A) as compared with primary injection (fig.VI.12B). Fig. VI.12C shows that serum of the boosted rabbits gave a higher response in the EIA compared with normal rabbit serum, indicating the presence of rabbit antimouse antibodies in the circulation of the boosted rabbits.
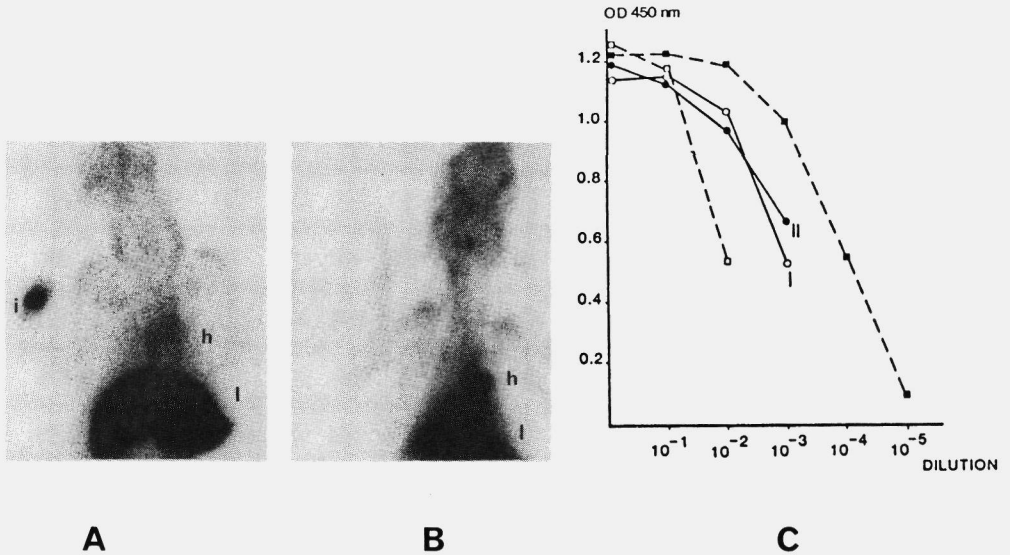

Fig. VI.12 *Image of a rabbit 3 hours after repeated injection of Tc-99m-Y22 (A); h = heart; l = liver. Fig. B: image of a rabbit 3 hours after primary injection of Tc-99m-Y22. Fig.C shows the response in the EIA of serum of the boosted rabbits (I and II), as compared with normal rabbit serum (□) and rabbit-anti-mouse serum (■)*

Discussion

To assess the feasibility of thrombus imaging with Tc-99m-Y22 in vivo, various thrombus models in rabbits and rats were employed. Excellent images of the

thrombi were obtained with high target-non-target ratios. In contrast, when Tc-99m-fibrinogen was used instead of Tc-99m-Y22, the clots were only faintly visible. Using a Tc-99m-control monoclonal antibody, the thrombi were not visible. This shows that the images obtained with Tc-99m-Y22 were not due to extravasation caused by the operation procedure.

When we injected I-123 labelled fibrinogen into a rabbit, a high accumulation of radiolabel was observed in the thyroid glands, due to dehalogenation of the labelled antibody in the liver, followed by sequestration of free iodine by the thyroid. Upon injection of the Tc-99m labelled proteins, no accumulation of label was seen in thyroid glands or stomach. This indicates that the binding of Tc-99m to proteins is stable not only in vitro, as was demonstrated in chapter IV, but also in vivo. After injection of the Tc-99m intermediate compound (which is used in the labelling prodedure) in rabbits, a large amount of activity was still present in the animals 20 hours after injection. It is conceivable that the active intermediate compound reacted with plasma proteins (predominantly albumin) upon injection, and circulated in the body. This stresses the need for adequate purification of the antibody after labelling from the active intermediate compound.

Heparin did not affect the binding of Tc-99m-Y22 to the thrombi. This may be advantageous in the clinical situation when imaging with Tc-99m-Y22 is considered, since it would mean that heparin therapy in patients can be started before application of Tc-99m-Y22 for thrombus imaging.

After 18 hours, there was still much Tc-99m-Y22 present in the circulation of the animals. We observed that the clearance behaviour of Y22 and of a control antibody (both Tc-99m labelled) was very similar. This is another indication for the fibrin specificity of Y22, since, if Y22 crossreacted with fibrinogen in the circulation and formed immune complexes, a much more rapid clearance would have been expected.

The relatively long lifetime of Tc-99m-Y22 in the circulation results in high background activity. Therefore we investigated the possibility of thrombus imaging with Fab and $F(ab)_2$ fragments of Y22, which have a shorter plasma

lifetime ($T_{1/2}$ 18.4 and 12.4 hours respectively). It has been found that the Fc-fragment determines the lifetime of IgG antibodies in the circulation (4-6).

Thrombi in the jugular vein of rabbits could also be clearly visualized with Tc-99m-F(ab)$_2$. Tc-99m-Fab, however, gave disappointing results, possibly due to a combination of the higher clearance rate and the lower immunoreactivity of Fab compared with Y22 and F(ab)$_2$.

The biodistribution pattern of Tc-99m-Y22 differs from that of Tc-99m-Fab and Tc-99m-F(ab)$_2$. Tc-99m-Y22 is predominantly cleared by the liver, while Tc-99m-F(ab)$_2$ shows an increased accumulation in the kidneys. Tc-99m-Fab is rapidly taken up by the kidneys and excreted in the urine.

The Fc-part not only determines the lifetime of IgG antibodies in the circulation, but is also considered to be largely responsible for the elicitation of antimouse antibodies (7). Upon repeated injection of Tc-99m-Y22 in rabbits, we observed an increased blood clearance and accumulation of antibody in the liver. In an enzyme immunoassay, serum of these boosted animals gave a much higher response than that of control rabbits, indicating the presence of antimouse antibodies. The slight reaction of normal rabbit serum in this assay may be due to suboptimal test conditions, or it may be considered as "background response". In conclusion, Tc-99m labelled antifibrin monoclonal antibody Y22 and its F(ab)$_2$-fragments have great potential for the in vivo detection of thrombi with various localizations. Because of their higher clearance rate (resulting in lower background activity) and presumably lower immunogenicity, together with their retained immunoreactivity, Tc-99m labelled F(ab)$_2$ fragments of Y22 may be preferable for use in humans.

2 PROVISIONAL ASSESSMENT OF OTHER APPLICATIONS

A *Monitoring of thrombolytic therapy*

The recent developments in thrombolytic therapies have increased the need for

reliable means to monitor the efficacy of these therapies. Since fibrin is the target of these thrombolytic therapies, it was believed that fibrin degradation products would be specific blood markers for assessment of success of the treatment. However, it has been demonstrated that this assumption is not correct, since fibrin degradation products also increase when thrombolytic agents are given to normal healthy volunteers (8). Tc-99m labelled Y22 scintigraphy may be a good alternative to follow directly the course of lysis of thrombi induced by thrombolytics.

Preliminary results of experiments to assess the feasibility of thrombolysis monitoring are outlined below.

Two models were used:

- **Circulation model in vitro**

    After circulation of Tc-99m-Y22 containing plasma over plasma clots in the in vitro circulation model (see Chapter V), two chain t-PA (2000 IU/ml) was added to the plasma and dynamic studies of the clots were made with the gamma camera.

- **Vena Cava Thrombosis model in the rat**

    Four hours after injection of Tc-99m labelled Y22 in a rat with a thrombus in the inferior vena cava, 245.000 IU of two chain t-PA was injected in a penis vein. At timed intervals, images of the rat were made with the gamma camera.

Results and Discussion

When, after circulation for 15 hours in the circulation model with Tc-99m-Y22 containing citrated plasma, t-PA was added to the plasma, the radioactivity in the clot declined rapidly (Fig. VI.13). Macroscopic inspection of the chamber showed that the clot had indeed disappeared. Apparently, the presence of Tc-99m-Y22 in the clot does not prevent thrombolysis by t-PA.
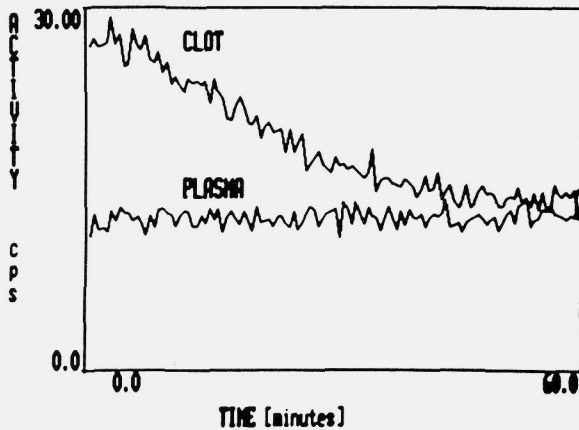
Fig. VI.13 *Activity curves of clot and plasma after addition of 20000 IU t-PA/ml to plasma in the circulation model*

In Figure VI.14A, an image of a rat is shown, taken 4 hours after injection of Tc-99m-Y22. The thrombus in the inferior vena cava is clearly visible. There is also a considerable accumulation of radiolabel in the left kidney, possibly caused by obstruction of the left renal vein by the thrombus. Two hours after injection of t-PA, the size of the hotspot in the vena cava had decreased significantly (Fig. VI.14B). Moreover, the radioactivity in the left kidney was reduced, possibly due to improvement in renal blood flow by dissolution of the thrombus.
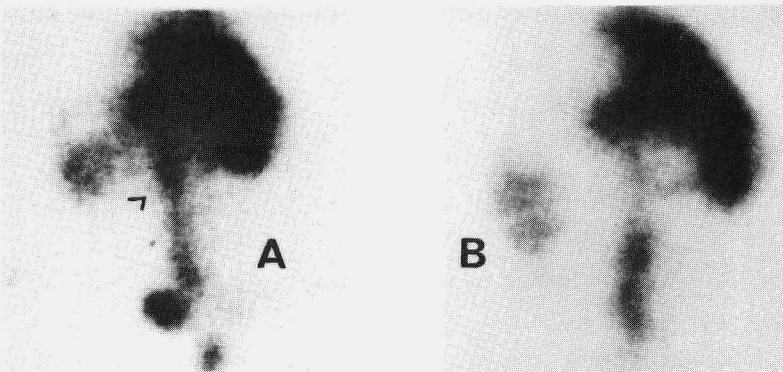

Fig. VI.14 *Effect of i.v. injection of 245.000 IU t-PA on a thrombus in the inferior vena cava of a rat*

These preliminary results suggest that Tc-99m-Y22 imaging of thrombi may also be used to monitor thrombolytic therapy with t-PA.

B *Detection of pulmonary emboli*

We assessed the feasibility of embolism detection with Tc-99m-Y22 in rabbits. The jugular vein of rabbits was exposed and a catheter was inserted (inner diameter 0.5 mm). Small fragments of rabbit blood clots (approximately 0.3 mm^3) in saline were injected via the catheter. We observed a change in the respiration pattern of the rabbits as an indication that the clots had lodged in the pulmonary circulation. The rabbits were ventilated with pure oxygen by a nasal tube. One hour after the operation, Tc-99m-Y22 (1 mg, 37 MBq) was injected in a marginal ear vein and images of the rabbits were made with the gamma camera at timed intervals. Twenty hours after injection of Tc-99m-Y22, the animals were sacrificed. The lungs were excised, the clots were removed from the pulmonary vessels and counted in an autogammacounter.

Results and Discussion

Figure VI.15 shows a macroscopic view of the lungs of the experimental rabbits with a dark area representing an area of infarction.
Unfortunately, the emboli were not observed on the scintigrams. Embolus-to-blood ratios, however, were as high as 5.5, 20 hours after injection of Tc-99m-Y22. After injection of Tc-99m labelled control monoclonal antibody (anti-FITC IgG1), embolus-to-blood ratios were only 0.9 - 1.1.
The fact that we were unable to image pulmonary emboli in the rabbits, although a strong accumulation of Y22 in the emboli could be demonstrated, may be explained by the high background activity in heart and liver, which blurrs the images of the emboli. Experiments to lower the background activity e.g. by use of F(ab)$_2$-fragments are needed to assess the feasibility of

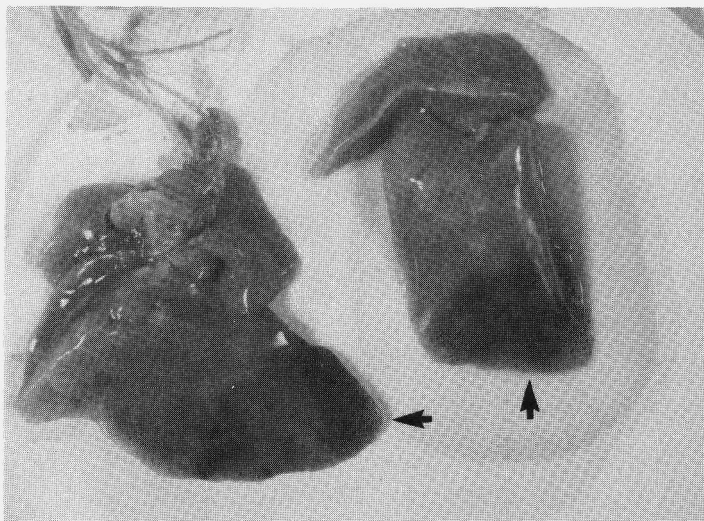immunoscintigraphic detection of pulmonary embolism.

Fig. VI.15 *Macroscopic aspect of the lungs of a rabbit in which pulmonary emboli were introduced; → = site of infarction*

References

1   Van Ruijven-Vermeer IAM, Nieuwenhuizen W. Purification of rat fibrinogen and its constituent chains. Biochem J 1978, 169: 653-658.

2   Collen D, Stassen JM, Verstraete M. Thrombolysis with human extrinsic (tissue-type) plasminogen activator in rabbits with experimental jugular vein thrombosis. Effect of molecular form and dose of activator, age of the thrombus, and route of administration. J Clin Invest 1983, 71: 368-376.

3   Umetsu T, Sanai K. Effect of 1-methyl-2-mercapto-5-(3-pyridyl)-imidazol (KC-6141), an anti-aggregating compound, on experimental thrombosis in rats. Thromb Haemost 1978, 39: 74-83.

4   Spiegelberg HL, Weigle WO. The catabolism of homologous and

heterologous 7S gamma globulin fragments. J Exp Med 1965, 121: 323-338.

5   Dorrington K, Painter R. Functional domains of immunoglobulin G. Prog Immunol II 1974; 1: 75-84.

6   Walmann TA, Strober w. Transport and catabolism of immunoglobulins. Prog Immunol II 1974, 1: 230-233.

7   Moldofsky Ph J, Powe J, Hammond ND. Monoclonal antibodies for radioimmunoimaging: current perspectives. In: Freeman LM, Weissman HS (eds.). Nuclear Medicine Annual 1986. Raven Press, New York, 1986: pp 57-103.

9   Seifried E, Tauswell P, Rijken DC, Kluft C, Hoegee E, Nieuwenhuizen W. Fibrin degradation product are not specific markers for thrombolysis in myocardial infarction (letter). The Lancet 1987; 2:333-334.

General discussion and summary

This thesis describes a study on the development of a new detection method of thrombosis. Patients with deep venous thrombosis are at high risk for the development of potentially fatal pulmonary embolism. For that reason, it is essential to recognize the condition in an early stage and to start anticoagulant therapy as soon as possible. However, because of its possible haemorrhagic side effects, this therapy should be reserved for patients in whom the diagnosis is certain.

It has become generally accepted that the diagnosis deep venous thrombosis is not made on the basis of clinical signs and symptoms alone. Many tests have been developed for objective confirmation of the diagnosis, but most of them suffer from lack of sensitivity and/or specificity. Contrast venography is considered the gold standard with which other tests have to be compared. However, this test also has its limitations, some of them due to the use of contrast media. Of the non-invasive tests, impedance plethysmography and real time ultrasonography have been evaluated most extensively. They have been found to be highly sensitive and specific for proximal deep vein thrombosis, but relatively insensitive for thrombosis of the calf veins, from which most thrombi originate. Since fibrin is an essential constituent of thrombi, methods to detect fibrin deposits are in theory powerful tools for the detection of thrombi. This thesis describes experiments which were performed to develop a new method for the detection of fibrin deposits (i.e. thrombi) using a mouse monoclonal antibody directed against fibrin.

This antifibrin monoclonal antibody (designated as Y22) was labelled with the

radionuclide Tc-99m, which has excellent characteristics for imaging with a gamma camera.

In chapters II and III of this thesis, antifibrin antibody Y22 is characterized and its specificity defined. Y22 (of IgG1 isotype with kappa light chains) is directed against a conformation dependent epitope in the D-domain of fibrin of humans, dogs, rabbits, rats and sheep (but not of porcine or murine fibrin). In an enzyme immunoassay, Y22 reacts strongly with fibrin monomers, and only weakly with fibrinogen. Y22 not only reacts with monomeric fibrin, but also with the polymerized and crosslinked fibrin of blood clots as was assessed by immunofluorescence microscopy.

Since the D-domain of fibrin contains a site, which is involved in the polymerization of fibrin, the effects of Y22 and its $F(ab)_2$ and Fab fragments on fibrin assembly were assessed. Intact Y22 prolongs the thrombin time of citrated plasma much stronger than $F(ab)_2$ fragments. Fab fragments have hardly any effect on clotting of plasma. This apparent correlation with the size of the immunoreactive material suggests that the anticlotting effect of intact Y22 is due to steric hindrance. A control monoclonal antibody has no effect on clotting of plasma. Transmission and scanning electronmicroscopic studies show that Y22 interferes with fibrin polymerization. Clotting of citrated plasma or blood in the presence of intact Y22 results in formation of shorter, thinner fibres as compared with fibrin formed in the absence of Y22. This is less pronounced with $F(ab)_2$ fragments, whereas Fab fragments have no effect on fibrin structure.

The D-domain of fibrin is also involved in the stimulation of plasminogen activation, catalyzed by tissue plasminogen activator (t-PA). Therefore, we also assessed the effects of Y22 and its $F(ab)_2$/Fab fragments on this property of fibrin. Intact Y22 has no effect on the stimulating capacity of fibrin in plasminogen activation by t-PA in a parabolic rate assay. $F(ab)_2$ fragments slightly and Fab fragments strongly inhibit the stimulating capacity of fibrin. As in the formation of fibrin, the different behaviour of Y22 and its fragments in this stimulation assay seems to be related to their molecular size and may be due

to differences in the effectiveness in hindrance of the binding of plasminogen or t-PA to fibrin. These findings indicate that Y22 and its fragments may be useful tools in the study of the topography of sites involved in polymerization and in the fibrin-induced rate enhancement of the t-PA catalyzed plasminogen activation.

An other interesting potential application of Y22 may involve its use in the development of new thrombolytic drugs. At present, hemorrhage is a prominent adverse effect of thrombolytic therapies and is thought to be related to systemic effects of the thrombolytic agents. Fibrin specificity of a lytic agent may circumvent this problem of systemic fibrinogen consumption. Therefore, Y22 with its fibrin selectivity may serve as a vehicle for plasminogen activators, thus concentrating the conversion of plasminogen at the clot surface. This may then result in increased thrombolysis and in less systemic fibrinogenolysis.

Chapter IV describes the method and quality assessment of labelling Y22 with the radionuclide Tc-99m. In vitro experiments showed that the labelling method couples Tc-99m tightly to Y22, since no transfer of label could be observed when Tc-99m-Y22 was incubated with albumin for 24 hours at 37°C. Experiments in rabbits indicated that the binding of Tc-99m to Y22 is also stable in vivo, since no thyroid uptake or stomach activity was observed after injection of Tc-99m-Y22. Functional assays showed that the Tc-99m labelling method does not affect the immunologic activity of the antibody.

Binding experiments with clots indicated that Tc-99m-Y22 binds both to preformed and forming clots and that it reacts more rapidly with forming clots. The reason for the lower rate of reaction of Y22 with preformed plasma clots as compared with forming fibrin is not clear. Possibly the epitope for Y22 is more readily accessible in non-aggregated than in aggregated fibrin. The high reactivity of Y22 with forming clots suggests that Y22 will especially accumulate in active, extending thrombi. However, also preformed, aged thrombi will bind Tc-99m-Y22.

In chapter V, an in vitro circulation model is described, which was developed to assess the scintigraphic implications of the clot-binding capacity of Tc-99m-Y22

and the effects of various environmental conditions of the clots on the uptake of Tc-99m-Y22 by the clots. In this model, there was a time dependent accumulation of Tc-99m-Y22 in the clots, and the clots could be visualized with a gamma camera after approximately 1 hour of cirulation at 37°C. After 15 hours of circulation of Tc-99m-Y22, only a small fraction (5-10%) of total applied Tc-99m-Y22 was bound to the clots. However, this was sufficient to visualize the clots due to the difference in local concentration of Tc-99m-Y22 in clots and circulating plasma. Immunofluorescence microscopy experiments indicated that binding of Y22 to clots is not limited to the surface, but that Y22 penetrates the clots.

Various anticoagulants, including heparin, did not affect the rate of binding of Tc-99m-Y22 to the clots. This finding may be of clinical importance, since it would mean that heparin therapy in patients can be started before application of Tc-99m-Y22 for thrombus imaging.

In serum, there was no difference in binding rate of Tc-99m-Y22 to clots compared to experiments in plasma. This observation indicates that fibrinogen, present in plasma, does not hamper the binding of Tc-99m-Y22 to fibrin, and it shows the fibrin specificity of Y22. The small crossreactivity of Y22 with fibrinogen in an enzyme immunoassay, as is described in chapter II, is therefore probably due to artifacts, caused by the used test system.

Using the circulation model, described in this chapter, it may be possible to predict the effects of various environmental conditions on the clot binding capacity of an antifibrin antibody without the use of animal models. Because it is a dynamic system, the model resembles more closely the in vivo situation than static test tube experiments.

Since Y22 not only reacts with human fibrin, but also with fibrin of rats and rabbits, these animals were used to assess the feasibility of thrombus imaging in vivo with autologous thrombi (chapter VI).

Thrombi in the jugular vein and abdomen of rabbits, and in the inferior vena cava and abdomen of rats could be visualized with high clot-to-background ratios. Some of the thrombi were already visible 3 to 4 hours after injection of

Tc-99m-Y22, but results were better after 18 hours. Heparinization (in a dose that doubles the APTT) did not affect the visualization of thrombi in the jugular vein of rabbits. This finding is in accord with the results obtained with the circulation model (chapter V).

Thrombi could not be visualized with Tc-99m labelled fibrinogen or a control monoclonal antibody.

Intact Y22 has a relatively long lifetime in the circulation, resulting in considerable background activity. $F(ab)_2$ and (especially) Fab fragments are cleared more rapidly as compared with intact Y22. After injection of Tc-99m-$F(ab)_2$ fragments, thrombi in the jugular vein could also be visualized. Injection of Tc-99m-Fab fragments did not result in positive images of the thrombi, probably due to the lower immunologic activity of Fab compared with $F(ab)_2$ or Y22. The results show that antifibrin Y22 and its $F(ab)_2$ fragments may have potential in the detection of thrombi with various localizations.

Because of their enhanced clearance, their possibly lower immunogenicity and their retained immunoreactivity, $F(ab)_2$ fragments of Y22 may be preferable for use in humans.

Preliminary experiments indicate that immunoscintigraphy of thrombi may also be useful to monitor the efficacy of thrombolytic therapies e.g. with tissue-type plasminogen activator (t-PA). When, after imaging of clots, t-PA was added to the circulating plasma in vitro or was injected into a rat with a thrombus in the inferior vena cava, the radioactivity in the clots decreased significantly.

Finally, experiments were performed in rabbits to determine the feasibility of imaging pulmonary embolism with Tc-99m-Y22. Although high embolus-to-blood ratios were obtained 18 hours after injection of Tc-99m-Y22, visualization of the emboli was severely hampered by the high background activity in heart and liver. Therefore, experiments to lower the background activity are needed to determine a possible role of immunoscintigraphy in the diagnosis of pulmonary embolism.

SAMENVATTING

Algemeen wordt erkend dat de klinische diagnostiek van diepe veneuze trombose niet erg betrouwbaar is. Slechts ongeveer 50% van de patienten bij wie de diagnose vermoed wordt heeft ook werkelijk trombose. De diagnose moet dan ook altijd met objectieve middelen bevestigd of uitgesloten worden. Als "gouden standaard" voor de objectieve diagnostiek van diepe veneuze trombose geldt de röntgencontrastflebografie. Deze methode is echter invasief, niet altijd makkelijk uitvoerbaar en kan bijwerkingen hebben, veroorzaakt door het gebruikte contrastmiddel.

Van de huidige niet-invasieve diagnostische methoden zijn impedantie-plethysmografie (IPG) en real-time echografie zeer sensitief en specifiek voor het opsporen van proximale diepe veneuze trombose, maar weinig gevoelig voor de detectie van kuitvenetrombose.

Dit proefschrift beschrijft de ontwikkeling van een nieuwe diagnostische methode, die mogelijk ook de aanwezigheid van kuitvenetrombose zal kunnen aantonen. De methode is gebaseerd op het gegeven dat het fibrine-netwerk een essentieel bestanddeel vormt van een trombus. Een methode om specifiek fibrine-neerslagen te detecteren is daarom in theorie zeer geschikt om trombose op te sporen. Antilichamen, gericht tegen fibrine, zijn hiervoor goede kandidaten.

Er werd daarom een monoclonale antistof ontwikkeld, die specifiek gericht is tegen fibrine en niet reageert met de in het bloed circulerende voorloper van fibrine, fibrinogeen. Deze antistof (Y22 genoemd) werd gemerkt met het radioaktieve isotoop technetium-99m (Tc-99m) met behulp van een nieuw ontwikkelde methode. Tc-99m heeft een korte halfwaardetijd (6 uur), resulterend in een lage stralenbelasting voor de patient. Bovendien is de foton-energie van de gammastraling van Tc-99m ideaal voor detectie met een

gammacamera.

Tc-99m-Y22 bleek zich in vitro specifiek aan stolsels te binden, in tegenstelling tot gemerkte controle-eiwitten als fibrinogeen, albumine of een willekeurige andere monoclonale antistof, niet gericht tegen fibrine.

Tevens bleek dat Y22 een stollingsremmende werking heeft door remming van de aggregatie van fibrine. Dit is een gunstig neveneffekt van de toepassing van Tc-99m-Y22 voor diagnostiek in vivo, daar bij toediening van Y22 verdere aangroei van een trombus zal worden vertraagd.

De experimenten in vitro toonden bovendien dat diverse antistollingsmiddelen (waaronder heparine) geen invloed hebben op de binding van Tc-99m-Y22 aan de stolsels. In de praktijk betekent dit dat direkt met heparine-therapie begonnen kan worden bij het vermoeden van de diagnose, zonder dat dit invloed heeft op de in tweede instantie uit te voeren diagnostiek.

Enkele modellen in ratten en konijnen werden ontworpen om de mogelijkheid van trombosediagnostiek in vivo te onderzoeken. Trombi in de vena jugularis van konijnen en in de vena cava inferior van ratten konden uitstekend zichtbaar gemaakt worden met behulp van een gammacamera na injektie van Tc-99m-Y22, hetgeen niet lukte met de eerder genoemde controle-eiwitten. Ook hierbij bleek dat heparine geen invloed heeft op de diagnostiek met Tc-99m-Y22.

Onderzoek in patienten zal uit moeten wijzen of deze veelbelovende resultaten in vitro en in proefdieren ook gelden voor de mens.

Fibrine is eveneens een belangrijk onderdeel van een embolus, dat immers een losgeslagen en versleept stuk trombus is. Daarom werd ook geprobeerd longembolieën te detecteren met Tc-99m-Y22, waarvoor een konijnemodel werd ontworpen. Tc-99m-Y22 bleek zich inderdaad ook specifiek op te hopen in embolieën, maar dit kon niet zichtbaar gemaakt worden met de gammacamera. De oorzaak is waarschijnlijk gelegen in de hoge achtergrond-radioaktiviteit in hart en longen, die de ophoping van Tc-99m-Y22 in de zeer nabij gelegen longembolieën maskeerde. Er werden daarom fagmenten van Y22 gemaakt (Fab en $F(ab)_2$ genaamd), die sneller uit de circulatie worden verwijderd

(halfwaardetijd resp. 12 en 18 uur, vergeleken met 28 uur voor intact Y22) en daardoor resulteren in een snellere daling van de achtergrond-aktiviteit. Fab-fragmenten van Y22 zijn echter minder immunologisch aktief dan intact Y22 en niet erg bruikbaar voor diagnostiek. De (grotere) $F(ab)_2$-fragmenten, daarentegen, zijn even reaktief als intact Y22 en wel goed bruikbaar voor detectie van trombi in de vena jugularis van konijnen.

Nader en meer gedetailleerd onderzoek zal uit moeten wijzen of het mogelijk is ook longembolieën immunoscintigrafisch aan te tonen met een combinatie van goede immunoreaktiviteit en relatief hoge verwijderingsnelheid uit het bloed (bijvoorbeeld met $F(ab)_2$-fragmenten van Y22).

LIST OF PUBLICATIONS

Parts of this study have appeared elsewhere:

Wasser MNJM, Koppert PW, Arndt JW, Emeis JJ, Feitsma RIJ, Pauwels EKJ, Nieuwenhuizen W. An anti-fibrin monoclonal antibody, useful in immunoscintigraphic detection of thrombi. Blood, 1989; 74: 708-714

Wasser MNJM, Welling M, Lamers G, Pauwels EKJ, Nieuwenhuizen W. Effects of antifibrin monoclonal antibody Y22 and fragments thereof on some properties of fibrin. Thromb Haemost, accepted for publication

Wasser MNJM, Cleyndert P, Feitsma RIJ, Camps JAJ, Nieuwenhuizen W, Pauwels EKJ. An in vitro model for the scintigraphic detection of thrombi using a Tc-99m labeled antifibrin monoclonal antibody. Nucl Med Commun 1989; 10: 653-659

Wasser MNJM, Pauwels EKJ, Nieuwenhuizen W. Thrombus detection using a Tc-99m labeled anrifibrin monoclonal antibody (MoAb): experiments in vitro and in animals. Thromb Res, in press

Feitsma RIJ, Blok D, Wasser MNJM, Nieuwenhuizen W, Pauwels EKJ. A new method for Tc-99m labelling of proteins with an application to clot detection with an antifibrin monoclonal antibody. Nucl Med Commun 1987; 8: 771-777

Blok D, Feitsma RIJ, Wasser MNJM, Nieuwenhuizen W, Pauwels EKJ. A new method for protein labeling with Tc-99m. Nucl Med Biol 1989; 16: 11-16

Wasser MNJM, Feitsma RIJ, Pauwels EKJ, Nieuwenhuizen W. Thrombus imaging with an antifibrin monoclonal antibody (MoAb). Int Congress on Fibrinolysis, Amsterdam 1988; Fibrinolysis 1988; 5: 86 (abstr)

Wasser MNJM, Nieuwenhuizen W, Pauwels EKJ. Scintigraphic detection of thrombi using a Tc-99m labelled antifibrin monoclonal antibody: experiments in vitro and in animals. Proc. symposium Clinical use of monoclonal antibodies, Amsterdam 1988; 122 (abstr)

Wasser MNJM, Welling M, Lamers G, Koppert P, Pauwels EKJ, Nieuwenhuizen W. Effects of antifibrin monoclonal antibody Y22 and its F(ab)2/Fab-fragments on some properties of fibrin. Int Congress on Haemostasis and Thrombosis, Tokyo 1989; Thromb Haemost 1989; 62: 201 (abstr)

Wasser MNJM, Welling M, Pauwels EKJ, Nieuwenhuizen W. Feasibility studies on antifibrin monoclonal antibody Y22 for thrombus imaging: experiments in animals. Int. Congress on Haemostasis and Thrombosis, Tokyo, 1989; Thromb Haemost 1989; 62: 335 (abstr)

ACKNOWLEDGEMENTS

CURRICULUM VITAE

De auteur van dit proefschrift werd geboren op 26 november 1958 te Eindhoven. In 1977 behaalde hij het einddiploma Gymnasium β aan het Lyceum Augustinianum te Eindhoven. In hetzelfde jaar begon hij met de studie Geneeskunde aan de Rijksuniversiteit Leiden. In 1984 werd het artsexamen afgelegd. Van 1984 tot 1986 was hij gedetacheerd als militair bloedbankarts op de afd. Immunohaematologie en Bloedbank van het Academisch Ziekenhuis Leiden. Van 1986 tot 1987 was hij gedurende 1 jaar werkzaam als algemeen wachtassistent in het Reinier de Graaff Gasthuis, lokatie Bethel, te Delft. Van 1986 tot 1989 verrichtte hij het onderzoek, beschreven in dit proefschrift, in het kader van een samenwerkingsverband tussen het Gaubius Instituut TNO en de onderafdeling Isotopendiagnostiek van het Academisch Ziekenhuis Leiden. Sinds april 1988 is hij in opleiding tot radiodiagnost bij de afdeling Radiodiagnostiek van het Academisch Ziekenhuis Leiden (opleider: Prof.dr. A.E. van Voorthuisen).